Improving the detection of carbonylated peptides by mass spectrometry via solid-phase hydrazide enrichment and selective labeling with Oxygen-18 (^{18}O)

A DISSERTATION
SUBMITTED TO THE FACULTY OF THE GRADUATE SCHOOL
OF THE UNIVERSITY OF MINNESOTA
BY

Mikel Robert Roe

IN PARTIAL FULFILLMENT OF THE REQUIREMENTS
FOR THE DEGREE OF
DOCTOR OF PHILOSOPHY

Timothy J. Griffin

January 2010

Acknowledgements

I would like to thank my mentor and thesis advisor Dr. Timothy Griffin for introducing me to the field of biological mass spectrometry, and for patiently guiding me through the ups and downs of my thesis research. His sensitivity towards several of my life changes along the way proved critical to my maturation as a research scientist, for which I cannot thank him enough.

I also need to acknowledge Dr. Sri Bandakhavi, Dr. Ebbing DeJong, Dr. Matt Stone, and Joel Kooren for making the Griffin lab such an enjoyable place to work. I've thoroughly enjoyed our many conversations and I will forever treasure the friendship forged with each of them. I am eternally thankful for the assistance and support they provided me as I concluded my thesis.

Finally, I thank my thesis committee members Drs. Arriaga, Bernlohr, LaPorte, and Walters for all their guidance and support throughout my graduate studies.

Dedication

This dissertation is dedicated to my wife Jenny and our children Nathan and Aubrey for reminding me that life is so much more than academic achievement. Jenny and Nathan especially have sacrificed greatly over the last three years in support of my studies and I owe my success to them. I am forever grateful for their unwavering love and for always believing in me.

I further dedicate this dissertation to my parents Mikel and Carolyn Roe for always encouraging me to reach for the stars and for supporting me in all my endeavors, scholastic and otherwise.

Abstract

Protein carbonylation is a post-translational oxidative protein modification known to alter protein function and impair cellular mechanisms. It is a relatively complex modification, characterized by a variety of structurally distinct reactive carbonyls that target a number of amino acid residues and originate via several different oxidative mechanisms. While identification of specific carbonylated proteins by mass spectrometry has provided insight regarding the protein pathways and complexes affected, the specific sites of carbonyl modification, necessary for determining the oxidative mechanisms involved as well as for explaining any associated functional consequences, are not routinely identified due to the relatively low abundance of carbonylated proteins. To address this issue, a number of methods for enriching carbonylated peptides have been developed, all of which involve derivatization with bulky reagents that often complicate the identification of peptides by tandem mass spectrometry. As an alternative to these label-based approaches, I have developed a label-free method for enriching carbonylated peptides that is based on their selective capture and controlled release from a novel solid-phase hydrazide reagent (SPH). The value of the SPH reagent method is demonstrated using a yeast lysate treated with the reactive lipid carbonyl 4-hydroxynonenal (HNE), where the use of pulsed-Q-dissociation (PQD) and neutral-loss triggered MS/MS/MS was employed for the first time to assist the identification of HNE-modified peptides by mass spectrometry. To further improve the confidence by which carbonylated peptides are identified via mass spectrometry, a novel ^{18}O-labeling method that selectively introduces an ^{18}O molecule

into the carbonyl oxygen of carbonylated peptides was developed. The resulting ^{18}O isotope signature enables carbonylated peptide precursor ions and carbonylated MS/MS fragment ions to be tracked in the full-scan MS and MS/MS spectra, respectively, thus providing an independent validation of the MS/MS spectra matched to carbonylated peptides by proteomic database searching. The value of ^{18}O-labeling for both improving the accuracy and measuring the efficiency of database-based identification of carbonylated peptides is demonstrated in an HNE-treated lysate from rat skeletal muscle homogenate. In conclusion, the development of the SPH reagent and the ^{18}O-labeling method are useful tools for identifying carbonylated peptides in complex biological mixtures and represent important steps forward in the field of redox proteomics.

Table of Contents

LIST OF TABLES

LIST OF FIGURES

Chapter 1

Introduction to protein carbonylation

Introduction

The reduction of molecular oxygen (O_2) to water is an essential and ubiquitous event in the lifecycle of aerobic organisms. When impaired, the incomplete reduction of O_2 generates the free-radical superoxide, whose metabolism leads to the production of additional reactive oxygen species (ROS). These ROS, both free-radicals and non-free-radicals alike, readily react with and alter the function of various biological macromolecules including nucleic acids, lipids, and proteins (Richter, Park et al. 1988; Esterbauer, Schaur et al. 1991; Chakravarti and Chakravarti 2007; Catala 2009). To minimize ROS-induced damage, aerobic organisms have evolved a complex anti-oxidant system that establishes and maintains a redox balance under steady state conditions (Sies 1997; Schafer and Buettner 2001; Siems and Grune 2003; Lin and Beal 2006). This delicate balance is perturbed in age-associated cellular and tissue degeneration, either as a result of increased ROS, decreased anti-oxidant capacity, or both (Sies 1997; Beckman and Ames 1998; Andreyev, Kushnareva et al. 2005). The correlation between this condition, known as oxidative stress, and aging has lead to the oxidative stress theory of age-associated degeneration (Harman 1956; Sohal and Weindruch 1996; Beckman and Ames 1998).

Proteins appear to be among the most susceptible biological macromolecules oxidized by ROS, accounting for as much as 75% of ROS adducts (Davies, Fu et al. 1999; Stadtman and Levine 2003). Since proteins are functional gene products involved in effecting all cellular processes, their structural and consequential functional modification by ROS adduction often leads to organellar, cellular, and tissue dysfunction (Oxidative damage to

proteins: Structural modifications and consequences in cell function. In Dalle Donne I, Scaloni A, Butterfield DA, editors. Redox Proteomics: From Protein Modifications to Cellular Dysfunction and Disease. Hoboken: John Wiley & Sons, Inc.; 2006. P399-471). Protein carbonylation, or the post-translational introduction of aldehyde and ketone moieties into amino acid residues, is one class of ROS directed modifications known to alter protein function, and strongly correlates with the onset and progression of various age-associated phenotypes, including type II diabetes, cancer, neurodegenerative disorders, as well as the ageing process itself (Picklo, Montine et al. 2002; Dalle-Donne, Giustarini et al. 2003; Dalle-Donne, Aldini et al. 2006). Indeed, protein carbonylation has been, and continues to be used as a hallmark indicator of oxidative stress.

In addition to tracking global protein carbonylation, numerous relatively recent studies have also sought to elucidate the very proteins and pathways damaged by this oxidative protein modification (Dalle-Donne, Giustarini et al. 2003; Grimsrud, Picklo et al. 2007; Grimsrud, Xie et al. 2008). Largely dependent on mass spectrometry-based protein identification technologies, these studies have provided the identification of numerous proteins in various biological contexts whose function is compromised upon carbonylation. While certainly useful, the information gained from these studies is limited, as both the specific site of carbonylation and the chemical identity of the modifying carbonyl remain undefined. To this end, novel front-end enrichment strategies have been devised in an effort to improve the mass-spectrometric identification of the specific carbonylated peptide within these oxidized proteins (Chavez, Wu et al. 2006;

Mirzaei and Regnier 2006; Han, Stevens et al. 2007). My contributions towards this effort are the focus of this doctoral thesis, which will cover the following aspects of protein carbonylation biology: endogenous sources and mechanisms, prevention and metabolism, mitochondrial targets, and the mass spectrometry technologies used for their detection.

Endogenous sources of reactive oxygen species (ROS)

The most common means of protein carbonylation involve ROS mediated mechanisms. Here, commentary is provided on the primary endogenous sources of ROS, the superoxide radical specifically, while a discussion of the mechanisms of ROS-derived protein carbonylation will be addressed in the subsequent section.

Superoxide radicals are endogenously produced by a class of redox sensitive protein complexes known as oxidoreductases, which transfer electrons from one molecule to another (Babcock and Wikstrom 1992). When this reaction is stalled or prematurely terminated, free radicals are generated. The enzyme complexes that generate superoxide radicals can be separated by those that directly use O_2 in their reaction mechanisms and those that do not. Examples of the former include lipoxygenase, cyclooxygenase, cytochrome P450, NADPH oxidase, and Xanthine oxidase. The best examples from the latter group include the mitochondrial transport chain complexes I (NADH dehydrogenase) and III (Cytochrome c reductase).

In addition to their oxidative and non-oxidative categories, the oxidoreductase complexes that generate superoxide radicals are further loosely defined by their subcellular-localization , either mitochondrial or extra-mitochondrial. The basis for this distinction comes from the fact that roughly 90% of cellular O_2 supplies are consumed by mitochondria, presumably for respiration (Harper, Bevilacqua et al. 2004). In addition, while mitochondrial respiration occurs in all cell types, the activity for many of the extra-mitochondrial ROS generating protein complexes is largely restricted to specific cell types (Lacy, Gough et al. 1998; Paravicini and Touyz 2008). Still, concerns of extra-mitochondrial sources are legitimized by the substantial number of studies implicating extra-mitochondrial sources of ROS in the pathology of various mammalian disease phenotypes (Rajagopalan, Kurz et al. 1996; Fukui, Ishizaka et al. 1997; Suzuki, DeLano et al. 1998; Mervaala, Cheng et al. 2001; Laakso, Teravainen et al. 2004; Pawlak, Naumnik et al. 2004; Virdis, Neves et al. 2004; San Martin, Du et al. 2007; Kim, Kim et al. 2008). However, for the sake of brevity I will concentrate on the mechanisms through which mitochondria, and specifically the electron transport complexes, generate the superoxide radical, as they are generally viewed as the primary source of endogenous ROS (Trifunovic and Larsson 2008).

Mitochondrial production of ROS

The mitochondrial electron transport chain (ETC) is composed of five multiprotein complexes integrated into the inner membrane of the organelle (Figure 1A). In general, these complexes work in series to establish an electrochemical gradient across the innermembrane by pumping protons from the matrix to the intermembrane space. The

Figure 1.

Generation of reactive oxygen species (ROS) by the electron transport chain promotes protein carbonylation of various mitochondrial proteins involved in energy production and antioxidant defense.

A. Generation of superoxide radicals ($O_2^{\cdot-}$) by electron transport chain (ETC) complexes I and III (C-1 & C-III) is associated with either an elevated level of NADH (NADH/NAD^+), or with a high proton motive force (Δp) across the mitochondrial inner membrane. (CI-CV), ETC complexes I-V; designate targets of protein carbonylation Green diamonds, vitamin E; Red diamonds, vitamin C;. ADP, adenosine diphosphate; ATP, adenosine triphosphate; NAD^+, nicotinamide adenine dinucleotide (oxidized); NADH, nicotinamide adenine dinucleotide (reduced), $O_2^{\cdot-}$, superoxide radical. **B**. Hydoxyl radical ($OH^{\cdot}$) induced lipid-peroxidation of free and membrane-bound polyunsaturated fatty-acids generates a pool of reactive lipid carbonyls that modify and impair proteins throughout the mitochondria, including enzymes involved in their metabolism. ALR, aldehyde reductase; ALDH-2, mitochondrial isoform of aldehyde dehydrogenase, GST, glutathione transferase; GSH, glutathione (reduced); chemical structures in oval represent reactive lipid carbonyls. **C**. Protein carbonylation of select mitochondrial antioxidant proteins involved in metabolizing reactive oxygen species (ROS) and maintaining redox-balance further propagates oxidative stress. MnSOD, manganese superoxide dismutase; GPX, glutathione peroxidase; IDH, NADP-isocitrate dehyrogenase, GR, glutathione reductase, TXR2, mitochondrial isoform of thioredoxin reductase, PRX3(r)/(o), reduced or oxidized form of the peroxiredoxin mitochondrial isoform; TRX2(r)/(o) reduced or oxidized form of the thioredoxin mitochondrial isoform; GRX2(r)/(o), reduced or oxidized form of the glutathione reductase mitochondrial isoform. **D**. Protein carbonylation of select enzymes in the citric acid cycle likely reduces NADH pools, slowing ATP production and increasing proton motive force. PDH, pyruvate dehydrogenase; ACO, aconitase; ICDH, isocitrate dehydrogenase; KGDH, α-ketoglutarate dehydrogenase.

A.

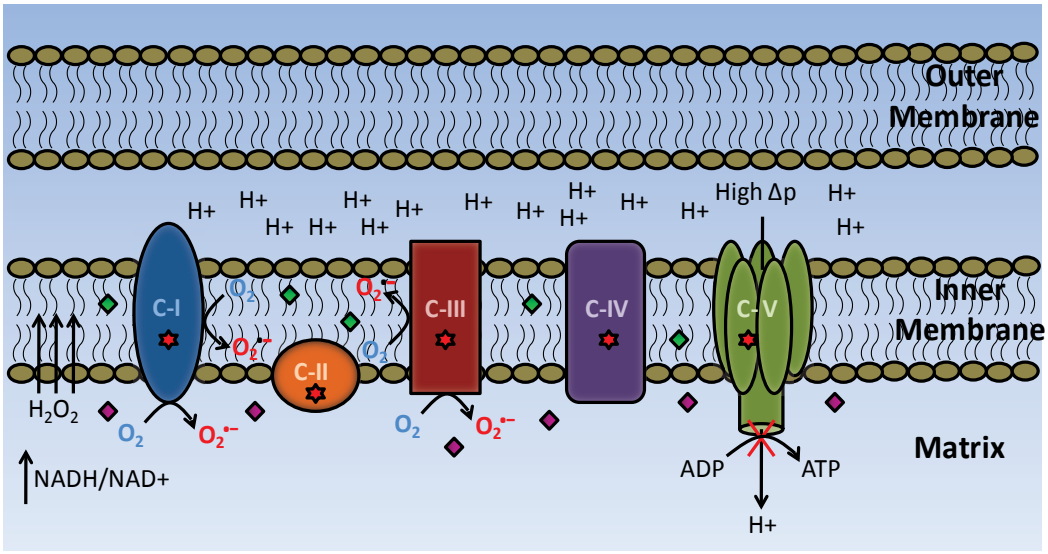
Outer
Membrane
Inner
Membrane
Matrix
C-I
C-II
C-III
C-IV
C-V
High Δp
H+
H_2O_2
O_2
$O_2^{\bullet-}$
NADH/NAD+
ADP
ATP

B.

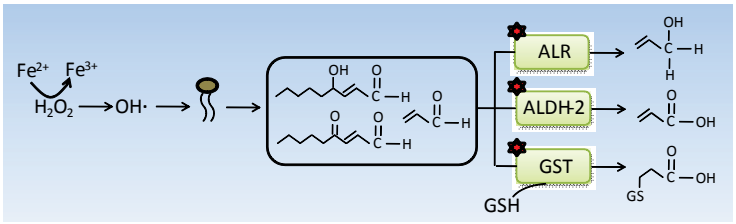
Fe^{2+} Fe^{3+}
H_2O_2
OH·
ALR
ALDH-2
GST
GSH
GS

C.

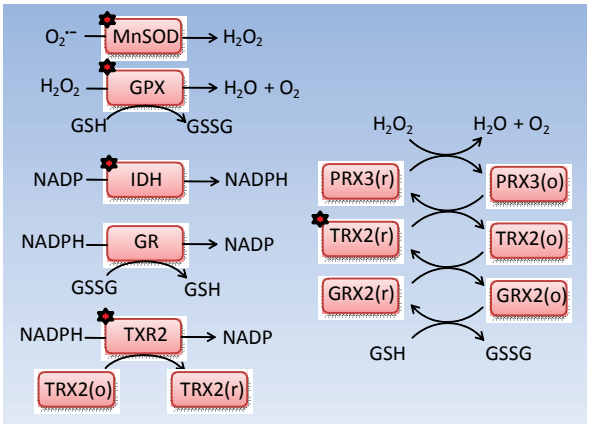
$O_2^{\bullet-}$
MnSOD
H_2O_2
GPX
$H_2O + O_2$
GSH
GSSG
NADP
IDH
NADPH
GR
TXR2
TRX2(o)
TRX2(r)
PRX3(r)
PRX3(o)
GRX2(r)
GRX2(o)

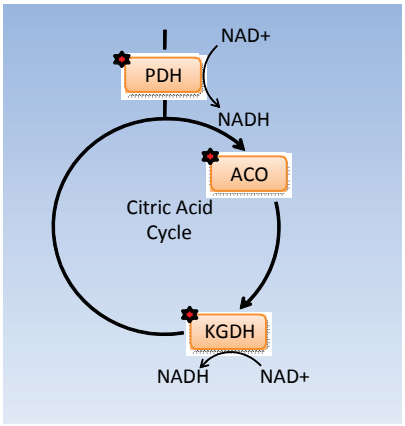
NAD+
PDH
NADH
ACO
Citric Acid
Cycle
KGDH

resulting energy created by the disequilibrium (i.e. proton motive force) is subsequently harnessed to drive ATP synthesis. The energy required for this process is provided by the citric acid cycle as reducing equivalents in the form of NADH and $FADH_2$. In turn, the substantial negative change in free energy associated with transferring the electrons from these molecules down the electron transport chain powers the translocation of protons across the innermembrane. When active (state 3), respiring ETC have lower proton gradients, steady production of ATP, and produce low levels of superoxide radicals (Kushnareva, Murphy et al. 2002). However, when resting (state 4) or impaired, ETCs are not respiring which produces a large proton gradient, stymied ATP production, and a significant increase in superoxide production (Kushnareva, Murphy et al. 2002; Turrens 2003; Trifunovic and Larsson 2008). The details of superoxide production by various complexes within the ETC have been the subject of numerous reviews which significantly informed the discussion provided below (Turrens 2003; Murphy 2009).

NADH dehydrogenase (Complex I), an approximately 1MDa complex comprised of 45 polypeptides, is the ETC entry site for NADH electrons and a significant generator of superoxide radicals (Cadenas, Boveris et al. 1977; Barja and Herrero 1998; Hirst, Carroll et al. 2003; Sazanov 2007). Superoxide radicals are produced when electrons are haphazardly transferred from the fully reduced FMN prosthetic group of the matrix exposed flavoprotein within Complex I to proximal molecular oxygen (Kussmaul and Hirst 2006). One condition that favors increased numbers of fully reduced FMN cofactors, and thus superoxide production, is increased NADH / NAD+ ratio in the

mitochondrial matrix (Votyakova and Reynolds 2001; Seo, Marella et al. 2006). This ratio is heightened when respiration is inhibited by either loss of critical electron transporters such as cytochrome c, or when the ETC is damaged by mutation or chemical modification (Kushnareva, Murphy et al. 2002; Kudin, Bimpong-Buta et al. 2004; Kussmaul and Hirst 2006). Decreased respiration resulting from low ATP demand has also been linked to accumulation of NADH (Hansford, Hogue et al. 1997). A second condition favoring superoxide radical production by Complex I is the combination of a high proton gradient across the innermembrane, and the build-up of ubiquinol (QH_2), the fully reduced form of the hydrophobic electron transporter ubiquinone (Q) (Votyakova and Reynolds 2001; Liu, Fiskum et al. 2002; Kudin, Bimpong-Buta et al. 2004; Adam-Vizi and Chinopoulos 2006). The back-pressure applied by the unused proton pool in the intermembrane space drives the transfer of the QH_2 electrons back to the FMN prosthetic group (reverse electron transport, or RET) where they are used to reduce NAD+ and elevate NADH pools. Although yet to be definitively defined, it appears that the FMN, and the ubiquinol cofactors via the ubisemiquinone intermediate (Q.), are the sources of electron leakage that produce superoxide radicals under these conditions (Murphy 2009).

Cytochrome c reductase (Complex III) is an 11 polypeptide integral protein complex that uses a combination of sulfer-iron clusters and heme groups to transfer electrons from QH_2 to the water-soluble electron carrier cytochrome c, and has long been considered a source of superoxide radicals (Turrens, Alexandre et al. 1985; Iwata, Lee et al. 1998). Briefly, QH_2 binds the Qo site of the complex and the electrons are separately processed

by parallel pathways. One electron is passed from the Qo site to an iron-sulfur cluster in the Rieske subunit of the complex, where it is further transferred to cytrochrome c1, a membrane encapsulated protein, and ultimately captured by cytochrome c just outside the innermembrane in the intermembrane space (Turrens 2003). The second electron on what has now become a Qo site ubisemiquinone (Q.) is transferred sequentially to cytochrome Bl, cytochrome Bh, and ultimately to the Qi site of the complex (Turrens 2003). Using various Complex III inhibitors (i.e Antimycin A) to force superoxide production, it was determined that autooxidation of the Qo ubisemiquinone is the primary mechanism by which Complex III leaks electrons, generating superoxide radicals at both sides of the innermembrane (Cadenas, Boveris et al. 1977; Turrens, Alexandre et al. 1985; Trumpower 1990; Liu, Fiskum et al. 2002; St-Pierre, Buckingham et al. 2002; Kudin, Bimpong-Buta et al. 2004; Muller, Liu et al. 2004). Although Antimycin A is not present in native mitochondria, respiratory conditions expected to recapitulate the drugs stabilizing effects on Q. bound at the Qo site are consistent with those observed during increased mitochondrial production of superoxide, namely increased proton motive force, and increased levels of reduced cytochrome c and QH_2 (Murphy 2009) . However, it has been shown under these conditions that, in the absence of Antimycin A, the major source of mitochondrial $O_2^{\cdot-}$ production is Complex I by way of RET (Votyakova and Reynolds 2001; Lambert and Brand 2004). Still, it has been suggested that Complex III may contribute more significantly to superoxide radical production during active respiration when Complex I is unperturbed, perhaps by local conditions that stabilize the Qo site ubisemiquinone (Murphy 2009).

Mechanisms of protein carbonylation by reactive carbonyls

Although superoxide radicals ($O_2^{\cdot -}$) have been associated with elevated levels of oxidative stress in various systems, they are themselves relatively innocuous to biological macromolecules. This is likely due to their rapid enzymatic conversion to hydrogen peroxide (H_2O_2), and to their hydrophilic properties which prevent $O_2^{\cdot -}$ from permeating membrane bilayers and freely diffusing throughout the cell (Fridovich 1995). Even so, $O_2^{\cdot -}$ is the precursor for a number of more toxic ROS largely responsible for the oxidative damage associated with ageing phenotypes (Berlett and Stadtman 1997). Reactive carbonyls are a particularly abundant and reactive class of ROS largely resulting from $O_2^{\cdot -}$ metabolism, and their adduction to proteins is considered one of the contributing factors involved in oxidative phenotypes (Dalle-Donne, Aldini et al. 2006; Ellis 2007; Grimsrud, Xie et al. 2008). The primary mechanisms through which reactive carbonyls are formed and adducted to proteins are described herein (Table I).

Metal-catalyzed formation of reactive carbonyls.

The Fenton reaction involves the metal-catalyzed partial oxidation of hydrogen peroxide to the hydroxyl radical (OH.), and is a prominent mechanism leading to the formation of reactive carbonyls (Amici, Levine et al. 1989; Goldstein, Meyerstein et al. 1993). Depending on the location of the metal-ion catalyzing the Fenton reaction, the resulting

Table 1. Summary of endogenously formed reactive carbonyls

Mechanism	Reactive Carbonyl Products	Adduct Structure	Targeted Residues
Metal-catalyzed Oxidation (MCO)	Glutamic semialdehyde	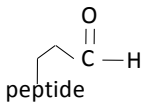	Arg, Pro, Thr
Metal-catalyzed Oxidation (MCO)	Aminoadipic semialdehyde	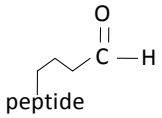	Lys
Lipid-peroxidation	HNE, ONE, Acrolein	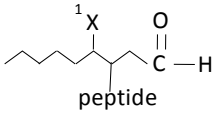	Cys, His, Lys
Lipid-peroxidation	A2/J2-ISPs	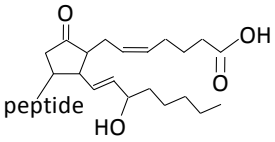	Cys
Protein glycation	Glyoxal (G), Methylglyoxal (MG), 3-deoxyglucosone (3-DG)	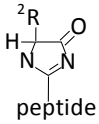	Arg

[1] X = -OH (HNE: 4-hydroxynonenal), =O (ONE: 4-oxo-nonenal)

[2] R = H (G); CH_3 (MG); or H_2C-$(CHOH)_2$-CH_2OH (3-DG)

reactive $OH^{\cdot}$ molecule will either directly carbonylate proteins, or generate reactive carbonyl intermediates capable of modifying proteins downstream (Amici, Levine et al. 1989). Generation of Fenton $OH^{\cdot}$ radicals by protein-bound metals results in the direct carbonylation of proteins, and is known as metal catalyzed oxidation (MCO) (Amici, Levine et al. 1989; Stadtman and Berlett 1991; Stadtman and Oliver 1991). In this reaction, electron donors such as NAD(P)H and ascorbate react with Fe^{3+} or Cu^{2+} to produce H_2O_2. The reduced metal ions (Fe^{2+} or Cu^{+}) that are also generated bind metal-binding sites on proteins where they subsequently participate in a one electron reduction of H_2O_2 to produce the $OH^{\cdot}$ radical. The free-radical electron from the $OH^{\cdot}$ radical is transferred to the sidechains of metal-bound residues and subsequently quenched by a dehydration event. Finally, release of the ion-metal by the addition of water triggers the chemical reconfiguration of the sidechain, leaving an aldehyde moiety in place of the original functional group. Thus, it follows that proteins interacting with metal cofactors, and more specifically, amino acid residues located within metal-coordination sites are prime candidates for modification. Indeed, this reaction is moderately selective, as characterization of MCO carbonyl adducts has been limited to lysine, arginine, proline, and to a lesser extent threonine residues (Stadtman and Oliver 1991) . The primary protein conjugates produced in these reactions are glutamic and aminoadipic semialdehydes, which have been shown to exist at detectable levels in biological samples (Requena, Chao et al. 2001). Infact, it was estimated in this same study that MCO-

derived protein carbonylation accounted for upwards of 60 percent of the endogenous protein carbonylation detected in rat liver extracts.

Lipid peroxidation

Alternatively, Fenton $OH^{\cdot}$ radicals generated within or proximal to lipid membranes readily oxidize free and membrane-bound omega-6 polyunsaturated fatty acids (PUFAs), producing a variety of reactive lipid carbonyl intermediates that readily form protein adducts (Figure 1B)(Esterbauer, Schaur et al. 1991; Refsgaard, Tsai et al. 2000; Requena, Chao et al. 2001; Sayre, Lin et al. 2006). Known as lipid peroxidation, this reaction is initiated by the free radical attack on the conjugated double bonds within PUFAs by $OH^{\cdot}$.

The resulting lipid radicals undergo free-radical rearrangement and formation of lipid hydroperoxides, which are further processed to produce stable bifunctional α,β-unsaturated lipid carbonyls (Schneider, Tallman et al. 2001; Schneider, Porter et al. 2008). The stable and hydrophobic nature of these molecules enables their diffusion throughout the cell, where they function as "second messengers" of $O_2^{\cdot-}$ insult by effecting oxidative damage to cellular compartments distal to the initial site of ROS production. Specifically, these bifunctional lipid carbonyls possess an electrophilic carbon atom within their double bond, which is readily attacked by the sidechains of nulceophilic residues (i.e. Cysteine, Histidine, and Lysine) to form stable Michael addition adducts. (Esterbauer, Schaur et al. 1991). The high susceptibility of proteins to carbonylation by lipid peroxidation products compared to metal catalyzed oxidation was recently demonstrated in an elegant study that placed the two mechanisms in direct

competition with each other, suggesting lipid carbonyls are of greater biological significance (Yuan, Zhu et al. 2007).

Cyclopentanone-isoprostanes (IsoPs), specifically the A2 and J2 diastereomers, are a relatively new found class of lipid carbonyls and represent the most abundant and best characterized endogenous bifunctional α,β-unsaturated ketones (Chen, Morrow et al. 1999; Chen, Zackert et al. 1999; Milne, Musiek et al. 2005). The A2/J2-IsoPs are lipid peroxidation products of arachadonic acid derived via the IsoP free-radical degradation pathway (Milne, Musiek et al. 2005). Specifically, O_2 is incorporated into radicalized arachadonic acid at the site of hydrogen abstraction, and the resulting peroxyl radical rearranges to form endocyclized intermediates. The addition of a second O_2 molecule quenches the radical forming a bicycloendoperoxide which is further processed by a series of reduction steps to produce the A2/J2-IsoPs, among others. As diastereomers, the resulting A2 and J2-IsoPs are only distinguishable by the location of the ketone and unsaturated carbon atoms within the cyclopentenone ring. Their abundance *in vivo* has been quantified in untreated rat livers (5ng/g liver) and is magnified dramatically following oxidative insult by CCl4 treatment (Chen, Morrow et al. 1999; Chen, Zackert et al. 1999). The cyclopentanone-isoprostane isomer 15-A2t-IsoP is particularly abundant and is known to form endogenous Michael-addition adducts with sulfur atoms from both small molecule nucleophiles (i.e. glutathione) and cysteine residues within proteins (Chen, Morrow et al. 1999; Chen, Zackert et al. 1999; Hubatsch, Mannervik et al. 2002; Levonen, Landar et al. 2004). The potential of this molecule to regulate protein

function through conjugate formation is best exemplified in a recent study suggesting that 15-A2t-IsoP modification of the redox sensitive protein Keap1triggers its dissociation from the Nrf2 transcription factor, enabling Nrf2 translocation to the nucleus where it drives expression of various antioxidant genes (Levonen, Landar et al. 2004).

Lipid peroxidation of ω-6 PUFAs (i.e arachadonic and linoleic acid) has also been shown to generate a variety of bifunctional α,β-unsaturated lipid aldehydes in the form of alkenals (Esterbauer, Schaur et al. 1991). The most reactive of these, including 4-hdroxynonenal (HNE), 4-oxo-nonenal (ONE), and acrolein contain substituted electron withdrawing groups proximal to the unsaturated double bond, which effectively increase the partial positive charge and electrophilic strength of the reactive carbon atom (Esterbauer, Schaur et al. 1991). 4-hydroxynonenal has been especially recognized for its cytotoxic and mutagenic potency, and significant effort has been spent on elucidating the mechanisms leading to its formation *in vivo* (Noordermeer, Feussner et al. 2000; Lee, Oe et al. 2001; Schneider, Tallman et al. 2001; Liu, Raina et al. 2003; Schneider, Porter et al. 2004; Zhang, Sun et al. 2006; Gu, Zhang et al. 2007; Schneider, Porter et al. 2008). It appears from the work of Schneider and colleagues that the lipid peroxidation pathway leading to HNE formation progresses similarly to the IsoP pathway up to the formation of the first lipid hydroperoxide intermediate (Schneider, Tallman et al. 2001). At this point, a second molecule of O_2 is added to the non-cyclized lipid radical, generating a dihydroperoxide intermediate which is subsequently cleaved via Hock rearrangement to produce 4-hydroperoxy-nonenal (4-HPNE). Reduction of the hydroperoxide group

completes the mechanism, yielding HNE as the end product. Numerous examples demonstrating loss-of-function phenotypes for proteins conjugated by HNE and other α,β-unsaturated lipid aldehydes illustrate the biological significance of these relatively abundant carbonyl adducts, and will be discussed in subsequent sections .

Protein glycation

Reactive carbonyls are also generated in the absence of free radical attack as seen during metabolism of non-enzymatically glycated proteins, which affects an estimated 0.1-0.2% of cellular and extracellular lysine residues (Monnier 1990; Thornalley 1999; Thornalley, Battah et al. 2003; Zhang, Ames et al. 2009). In this reaction, the Schiff-base adduct formed between the exposed aldehyde of a reducing sugar and the side-chain amine from lysine is rearranged to form a more stable ketoamine compound, known as an Amadori product . Subsequent oxidative decomposition of the Amadori product via retroaldolization yields small dicarbonyl compounds, including glyoxal (G), methylgloxal (MG), and 3-deoxyglucosone (3-DG), that readily form Schiff-base adducts on arginine residues (Rabbani and Thornalley 2008). With one carbonyl remaining unquenched, these protein carbonyls are susceptible to forming higher ordered cross-linked compounds known as advanced glycation end products (AGEs). The deleterious functional consequences associated with adduction of dicarbonyl intermediates, has been demonstrated for human serum albumin (HSA) where formation of a MG adduct on Arg410 in the drug-binding site II inhibited the HSA's esterase activity (Ahmed, Dobler et al. 2005).

Clearly, reactive carbonyl biology is complex. The variety of endogenous sources, mechanisms of formation, and chemically distinct structures involved in protein carbonylation is unique among posttranslational modifications (see table 1 for summary). Indeed, discerning this information for even a single carbonylated protein remains a formidable task in the field.

Prevention and metabolism of protein carbonyls

Under physiological conditions reactive oxygen species (ROS) are maintained at low levels by a complex antioxidant defense system (Lin and Beal 2006; Ellis 2007). Composed of small molecule scavengers and dedicated enzymes, this system works passively and actively to prevent the formation and to quench the reactivity of ROS at every stage in their biogenesis. During heightened oxidative stress many of these antioxidant molecules exhibit reduced function, possibly due to their putative modification by reactive carbonyls (Figure 1B & 1C) (Del Corso, Dal Monte et al. 1998; Park, Koh et al. 2003; Honzatko, Brichac et al. 2005; Doorn, Hurley et al. 2006; Fang and Holmgren 2006; Roede, Carbone et al. 2008; Reed, Pierce et al. 2009). Although it may not be the initial cause of declining anti-oxidant capacity, protein carbonylation likely contributes to its progression. In this section I'll touch on the various anti-oxidants involved in the prevention and metabolism of ROS, noting those whose activity is affected following protein carbonylation.

The initiating phase of ROS formation involves the generation of superoxide radicals ($O_2^{\cdot-}$), which are themselves classified as ROS. A variety of small molecule scavengers are known to quench $O_2^{\cdot-}$ radicals, with the greatest attention given to Vitamin C (ascorbic acid) and Vitamin E (i.e. α-tocopherol). Vitamin C is a hydrophilic molecule that reduces $O_2^{\cdot-}$ in non-membranous environments to H_2O. As such, Vitamin C is most likely the primary scavenger of $O_2^{\cdot-}$ radicals, which are also hydrophilic due to their ionic nature. In contrast, Vitamin E, specifically α-tocopherol, is hydrophobic and responsible for quenching free-radicals in lipid bilayers (Ham and Liebler 1995). Interestingly, Vitamin C has been shown in vitro to increase ROS levels by reducing transition metals and stimulating Fenton reactions.

Superoxide Dismutases (SODs) are a family of three enzymes responsible for converting superoxide radicals to hydrogen peroxide (McCord and Fridovich 1988; Zelko, Mariani et al. 2002). SOD1 uses copper and zinc cofactors to reduce $O_2^{\cdot-}$ in the cytoplasm (Tainer, Getzoff et al. 1983; Reed, Pierce et al. 2009). SOD2 requires manganese cofactors to quench mitochondrial $O_2^{\cdot-}$ and has been found to be carbonylated in early Alzheimer's disease brain. The very existence of a SOD enzyme specifit to the mitochondria further supports the idea that this organelle is the major endogenous source of $O_2^{\cdot-}$. The third enzyme in the family, SOD3, also uses copper and zinc cofactors and is exclusively responsible for reducing extracellular $O_2^{\cdot-}$. The distribution of SODs throughout the cell, including the extracellular matrix, stresses the importance $O_2^{\cdot-}$

metabolism, even though the resulting ROS metabolite H_2O_2 appears to be more detrimental to cells.

Given the propensity of H_2O_2 to fuel Fenton reactions and generate the highly reactive hydroxyl radical ($OH^{\cdot}$), it's not surprising that mammalian cells have evolved multiple enzymes dedicated to H_2O_2 metabolism (Nohl H 1980). Many of the enzymes involved with the metabolism of H_20_2 contain active-site cysteine (Cys) or selenocysteine (Sec) residues, indicating that they may be candidates for inactivation by reactive carbonyls. Interestingly, the few studies addressing this possibility indicate that the susceptibility of these H_2O_2 metabolizing proteins does not necessarily result in their inactivation, and where it does, the active site Cys and Sec residues are not targets of carbonylation. Modification of Peroxiredoxin 6 (Prx-6) by 4-hydroxynonenal in the livers of ethanol fed rats provides an example of the former situation, as adduct formation of various non-active site residues did not change the enzymes activity (Roede, Carbone et al. 2008). Conversely, Glutathione peroxidase (GPx) inactivated by exposure to varying concentrations of methylgloxal (MG) contained MG adducts only on Arg184 and Arg185 in the enzymes glutathione binding domain (Park, Koh et al. 2003). Still, the possibility that other H_2O_2 metabolizing enzymes may be inactivated by reactive carbonyl adduction to active-site Cys and Sec residues cannot be discarded. In fact, the inhibition of Thioredoxin (Trx) and Thioredoxin Reductase (TrxR) following adduction of HNE to the active site residues Cys32/Cys35 and Cys496/Sec497, respectively, supports the

likelihood that some H_2O_2 metabolizing proteins are regulated in a similar manner (Fang and Holmgren 2006).

Many of the enzymes responsible for detoxifying H_2O_2 and maintaining redox balance in mitochondria are dependent on the availability of reduced glutathione (GSH), which is primarily generated by NADPH-dependent mechanisms (Lin and Beal 2006). Nicotinamide adenine dinucleotide phosphate (NADP)-isocitrate dehydrogenase (IDH), the major supplier of mitochondrial NADPH, is carbonylated in aged-rat skeletal muscle and in the heart of spontaneously hypertensive rats (Benderdour, Charron et al. 2003; Feng, Xie et al. 2008). The latter study further demonstrated that HNE-modification of IDH, following treatment of isolated heart mitochondria with a moderate amount of HNE (20uM), promoted its impaired activity. Thus, carbonylation of IDH *in vivo* likely slows the production of NADPH, which directly impairs the maintenance of the NADPH-dependent thioredoxin system, and reduces turnover of GSSG to GSH. As a result, the mitochondrial antioxidant capacity is compromised, rendering the organelle more susceptible to oxidative stress.

Reactive carbonyls, capable of transmitting oxidative damage to compartments distal to the original site of insult, are themselves detoxified by a number of enzymes, several of which are sensitive to adduct formation by their own reactive carbonyl ligands. Aldehyde dehydrogenase (ALDH) prevents reactive aldehyde mediated cross-linking by oxidizing aldehydes to carboxylic acids (Canuto, Ferro et al. 1994; Honzatko, Brichac et

al. 2005; Poli, Schaur et al. 2008). The mitochondrial isoform (ALDH2) forms 4-oxo-nonenal (ONE) adducts at the active site cysteine (cys-302) upon ONE treatment, resulting in abrogated activity (Doorn, Hurley et al. 2006). Conversely, aldose reductase (ALR) prevents cross-linking by reducing aldehydes to alcohols (Poli, Schaur et al. 2008). Inhibition of ALR2 activity following HNE treatment has been demonstrated and is thought, based on indirect evidence, to involve adduct formation at the active site cysteine (cys-298)((Del Corso, Dal Monte et al. 1998)). An alternative mechanism for detoxifying reactive carbonyls is provided by Glutathione-transferases (GSTs), which catalyze the adduction of glutathione to electrophilic carbons on α,β-unsaturated lipid carbonyls, and thus prevent Michael-addition adduct formation. Excessive HNE-modification of GSTs has been observed in Alzheimer's disease brain, which, according to functional assays conducted by Mitchell and colleagues, likely contributes to its declining activity (Mitchell, Morin et al. 1995; Sultana and Butterfield 2004). It would be interesting to find out if the GSTA4 isoform specifically is affected by HNE-conjugation, as it is the primary GST involved in quenching HNE and other lipid carbonyls (Bruns, Hubatsch et al. 1999; Engle, Singh et al. 2004).

Proteasomal degradation of carbonylated proteins prevents their accumulation within cells, and is thus an essential mechanism of detoxification (Breusing and Grune 2008). The 20S free proteasome is primarily responsible for this task, and degrades carbonylated proteins in an ubiquitin- and ATP-independent manner (Shringarpure, Grune et al. 2003). It has been proposed that the 20S proteasome recognizes exposed hydrophobic surfaces

on carbonylated proteins resulting from carbonyl-induced conformational changes (Breusing and Grune 2008). While enhanced during mild oxidative stress, proteasomal activity is decreased in aged tissues where oxidative stress is elevated, such as Alzheimer's brain (Keller, Hanni et al. 2000; Bulteau, Szweda et al. 2002). Two models have emerged that may explain this observation. First, recent studies indicate that various subunits within the 20S proteasome complex form debilitating HNE-adducts when exposed to slightly elevated levels of HNE (Ferrington and Kapphahn 2004; Farout, Mary et al. 2006). That the proteasomal catalytic subunits (β1, β2 and β4) are themselves spared from modification suggests that HNE induces conformational changes in neighboring subunits which allosterically affect proteasomal activity. The second model postulates that protein aggregates formed through intermolecular oxidative protein crosslinks inhibit proteasomal activity by clogging both the 20S and the 26S proteasome complexes. A number of well controlled experiments using HNE-crosslinked proteins, and the observation that lipofuscin induces inhibition of proteasomal activity in aging fibroblasts, provide the supporting this model (Friguet and Szweda 1997; Shringarpure, Grune et al. 2000; Sitte, Huber et al. 2000). In either case, inhibition of proteasomal activity by reactive carbonyls produces a positive feedback loop, whereby accumulation of dysfunctional proteins leads to greater production of reactive carbonyls, and thus to more proteasomal inhibition and even more damaged proteins.

Mitochondrial targets of protein carbonylation

Mitochondria are the greatest endogenous source of ROS and are thus considered most susceptible to oxidative damage. Mitochondrial dysfunction, as characterized by decreased ATP production, increased generation of ROS, decreased antioxidant capacity, increased lipid peroxidation, and increased protein carbonylation, correlates well with aging and several age-related diseases (Lin and Beal 2006; Trifunovic and Larsson 2008). An attractive hypothesis for explaining mitochondrial dysfunction postulates that oxidation of mitochondrial proteins contributes to their functional decline, and exacerbates the generation of additional ROS and additional oxidative damage to the organelle (Harman 1972). Indeed, endogenously carbonylated mitochondrial proteins have been reported following experimentally induced traumatic brain injury (Opii, Nukala et al. 2007), throughout the progression of Alzheimer's disease (Reed, Pierce et al. 2009) (Reed, Perluigi et al. 2008), and in various tissues of aged rats, including brain (Prokai, Yan et al. 2007), heart (Yarian, Rebrin et al. 2005), (Choksi, Boylston et al. 2004), kidney (Choksi, Nuss et al. 2007), and skeletal muscle (Meany, Xie et al. 2007; Choksi, Nuss et al. 2008; Feng, Xie et al. 2008). In many cases, carbonylation of the identified proteins correlates with decreased protein, and protein complex activity. The mitochondrial proteins affected by protein carbonylation are involved in multiple tasks, and their impairment likely contributes to increased oxidative stress.

Electron Transport Chain

The impact of protein carbonylation on various complexes within the mitochondrial respiratory chain has been most acutely illustrated in a pair of studies by Choksi and

colleagues, whereby the functional consequences of endogenous protein carbonylation on mitochondrial respiration was investigated in aging rat kidney and skeletal muscle (Choksi, Nuss et al. 2007; Choksi, Nuss et al. 2008). In each tissue, protein carbonylation of individual subunits correlated with age-associated declines in the activity of their respective complex. In many cases, the protein adducts were further defined as HNE and MDA adducts. That the carbonylation of several protein subunits was consistent between samples supports the idea that carbonylation is a selective rather than a global event. Interestingly, while all five electron transport complexes exhibited declining activity as a function of age in skeletal muscle, all but complex III was affected in kidney, despite the fact that in kidney, the same complex III protein subunit was carbonylated (Figure 1A). These tissue specific effects may be explained by the adduction of different lipid carbonyls in the two tissues, with complex III in kidney modified by MDA, and in skeletal muscle by HNE. In addition, carbonylation may occur at different amino acids within the complex III subunits which could elicit different structural and functional affects. To resolve this quandary, advanced technologies capable of localizing the site of carbonylation to specific residues are needed.

Citric Acid Cycle

Several enzymes of the citric acid cycle are also known to be functionally impaired by protein carbonylation under varying conditions (Figure 1D). Pyruvate dehydrogenase converts pyruvate and coenzyme-A (CoA) to acetyl-CoA, and is detrimentally carbonylated (HNE) following experimental traumatic brain injury in rats (Opii, Nukala

et al. 2007). Carbonylated (MDA) aconitase has been identified in numerous studies, and correlates with its reduced ability to convert cis-aconitate to D-isocitrate in aged cardiac and malarial infected livers from mouse (Yarian, Rebrin et al. 2005; Dey, Guha et al. 2009). α-ketoglutarate dehydrogenase (KGDH) is functionally impaired in reperfused rat heart (Lucas and Szweda 1999). This phenotype was recapitulated by treating healthy rat heart mitochondria with low micomolar levels of HNE, and correlated with increased HNE-modification of KGDH's ligand, lipoic acid (Humphries and Szweda 1998). Interestingly, Morneau and colleagues subsequently contested these claims reporting that endogenous HNE-modification of KGDH's ligand binding subunit in aged heart mitochondria was not accompanied with decreased function (Moreau, Heath et al. 2003). The discrepancy may result from different degrees of modification incurred by reperfusion versus aging. In any case, functional decline of the citric acid cycle enzymes cited likely reduces the supply of NADH in the mitochondrial matrix, slowing ATP production as a result. Given that decreased NADH/NAD+ ratios correspond with less production of superoxide by the ETC, carbonylation of these enzymes appears to act as a negative feedback signal preventing increased generation of ROS.

Carbonylation of mitochondrial proteins clearly impacts many of the major biochemical processes that occur in mitochondria (Figure 1A,C,D). By impairing various ETC complexes and decreasing the supply of reducing equivalents in the mitochondrial matrix, reactive carbonyls likely stimulate increased ROS production, promote decreased antioxidant capacity, and thus intensify oxidative stress. Several more mitochondrial

proteins involved in various other processes (i.e. fatty acid oxidation) show age related increases in carbonylation, the result of which is sure to be the focus of future experiments (Feng, Xie et al. 2008). In addition, the carbonylation of numerous extramitochondrial proteins has also been reported, with several involved in glycolysis, protein maintenance, and translation. In all, protein carbonylation is an *in vivo* modification that often compromises protein function and contributes to oxidative stress associated with aging and related diseases.

Identifying carbonylated proteins by mass spectrometry

Mass spectrometry (MS) has been the primary analytical tool used to characterize carbonylated proteins since the emergence of two technological advancements in the late 1980's that enabled the ionization of large non-volatile biomolecules, such as proteins. Earning their inventors the Nobel Prize, matrix-assisted laser desorption ionization (MALDI) and electrospray ionization (ESI) are considered soft ionization techniques, as they deliver unfragmented, charged biomolecules to mass spectrometers, thus ensuring the measurement of consistent and predictable masses for each analyte (Tanaka 1982; Karas and Hillenkamp 1988; Fenn, Mann et al. 1989). The rapid rise of MALDI and ESI, coupled with advances in MS instrumentation and automation, has provided a platform for the high throughput analysis of carbonylated proteomes.

Equally important to the ascension of MS as a workhorse in oxidative proteomics was the sequencing of whole genomes in the 1990's, which provided the necessary information

for building proteomic databases of every organism sequenced. With databases containing theoretical proteomes available, it became possible to use MS not only as a means for studying known quantities, i.e. model proteins, but also as a tool for identifying unknowns within interesting biological samples. Considering that a single sample can generate tens of thousands of MS data files each needing to be measured against a database, the development of automated database search engines provided a crucial step forward in establishing MS as a mainstream analytical tool for analyzing carbonylated proteins.

As with other post-translational modified proteins, carbonylated proteins represent a small fraction of the total protein content in endogenous systems, and thus require enrichment prior to their analysis by MS. As a result, a number of enrichment methods targeting carbonylated proteins en masse or proteins modified by a specific carbonyl (i.e HNE) have been described, and their incorporation into large-scale MS-based proteomic experiments has enabled the full complement of carbonylated proteins associated with ageing and various disease states to be characterized (Reed, Perluigi et al. 2008; Sorolla, Reverter-Branchat et al. 2008; Reed, Pierce et al. 2009). In this section I will touch on several examples in the literature demonstrating the power of carbonyl targeted MS-based proteomics to identify, quantify, and ultimately localize the exact site of carbonylaton within protein targets. (See Appendix 1 for a more in-depth discussion of mass spectrometry.)

Mass spectrometry and two-dimesional gel electrophoresis

Historically, 2-dimensional gel electrophoresis (2-DE) has been the primary platform for resolving and visualizing carbonylated proteins in complex mixtures, upstream of their analysis by mass spectrometry (Klose 1975). In this approach, carbonylated proteins separated first by mass and then by isoelectric point, are detected via immunostaining and selected for identification by MS. Depending on the goals of the experiment, immunodetection may involve use of antibodies against a specific carbonyl group (i.e anti-HNE antibodies) so as to target a select group of carbonylated proteins. Alternatively, and often in parallel, carbonylated proteins may be first derivatized with the carbonyl-reactive reagent dinitrophenylhydrazine (DNPH), then separated by 2-DE, and ultimately detected by an anti-DNP antibody. The mechanism by which DNPH labels carbonylated proteins is well known, and involves the formation of acid labile Schiff-base bonds with aldehydes and ketones, which can be further stabilized upon reduction using the weak reductant sodium cyanoborohydride ($NaBH_3CN$) (Figure 2C). This DNPH-based method for detecting total protein carbonyls in gel-separated samples is commonly used and often referred to as Oxyblot^{TM} (Figure 2A). While necessary for tracking carbonylated proteins, the described immuno and chemical labeling reagents complicate protein identification by MS. As such, the 2-DE approach is usually conducted by running two gels in parallel, one probed with antibody to track the migration of carbonylated proteins, and the other stained for total protein. In this way, spots on the stained gel that correspond with carbonylated proteins can be extracted, subjected to in-gel proteolytic cleavage, and the resulting peptides analyzed by mass spectrometry.

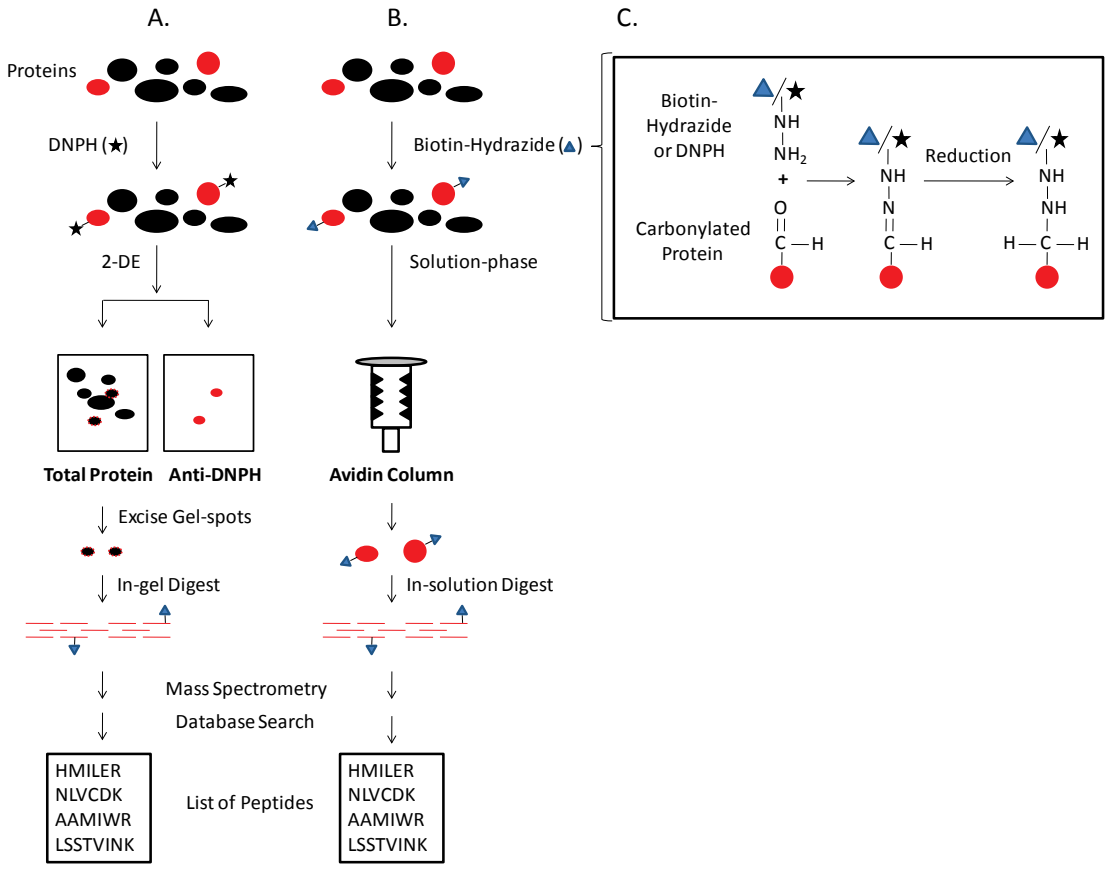

Figure 2. Gel-based Oxyblot™ detection, and solution-phase enrichment of carbonylated proteins for analysis by mass spectrometry. **A**. Complex protein mixtures treated with dinitrophenylhydrazine (DNPH) are divided-in-two, subjected in parallel to two-dimensional gel electrophoresis (2-DE), and either stained for total protein, or probed with anti-DNPH antibodies. Gel-spots on the total protein stained gel that migrate identically to spots appearing in the immunostained gel are excised and processed for analysis by mass spectrometry. Red circles, carbonylated proteins; Black circles, non-carbonylated proteins. **B**. Carbonylated proteins in complex mixtures are covalently labeled with biotin-hydrazide via Schiff-base bond formation, enriched by avidin-affinity column chromatography, digested in-solution, and the resulting peptides analyzed by mass spectrometry. **C**. Generic reaction mechanism for conjugation of DNPH and biotin-hydrazide to carbonylated proteins.

The utility of 2-DE for guiding the targeted identification of carbonylated proteins by mass spectrometry has been consistently demonstrated across various studies. For example, the 2-DE approach enabled the identification of specific 20S proteasomal subunits in purified heart and liver proteasomes that form HNE-adducts *in vivo* and in response to HNE treatment (Ferrington and Kapphahn 2004; Farout, Mary et al. 2006). That HNE-modification preceded loss in proteasomal function, impairing chymotrypsin-like activity specifically, suggests an inhibitory mechanism whereby elevated levels of HNE during conditions of oxidative stress leads to increased modification of specific subunits and impairment of the 20S proteasome. Similarly, 2-DE coupled with anti-HNE antibodies was also successfully employed to identify 11 serum proteins whose endogenous modification by HNE was increased with age (Kim, Zou et al. 2006). Many of the proteins identified are involved in blood coagulation, lipid transport, and blood pressure regulation, indicating the multitude of pathways likely affected by HNE. To investigate the impact of oxidative stress on degenerating brain, Butterfield and colleagues have used the 2-DE approach to characterize the complement of HNE-modified proteins at different stages in Alzheimer's progression (Reed, Perluigi et al. 2008; Reed, Pierce et al. 2009). Based on the early and consistent HNE-modification of select proteins the authors conclude that protein adducts involving reactive lipid carbonyls, HNE specifically, is an early event in the oxidative degeneration of brain tissue. In addition to the above studies, the combination of 2-DE and anti-HNE immunostaining has also been used to identify endogenously HNE-modified proteins in retinal pigment epithelium extracted directly from human donor eyes, and in cultured

retinal pigment epithelial cells (Kapphahn, Giwa et al. 2006). In a separate 2-DE study, epithelial fatty-acid binding protein (EFABP) from rat and murine retinal cells was also identified as an *in vivo* target of HNE, which curiously appears to increase its affinity for ligand (Bennaars-Eiden, Higgins et al. 2002). In sum, 2-DE combined with carbonyl-specific immunostaining has provided a useful tool for identifying endogenously carbonylated proteins in diverse biological samples.

Total carbonyl staining via the Oxyblot™ approach has also proven useful for identifying oxidatively damaged proteins *in vivo*. The identification of six DNPH-reactive proteins in Alzheimer's disease (AD) motivated Butterfield and colleagues to conduct a more precise characterization of the carbonyl adducts formed throughout the progression of AD, as described above (Castegna, Aksenov et al. 2002; Castegna, Aksenov et al. 2002). Increased levels of DNPH-derivatized proteins has also been identified in Huntington disease (HD) brain, further implicating oxidative carbonylation as an important event in neurodegeneration (Sorolla, Reverter-Branchat et al. 2008). Importantly, Oxyblot™ and other hydrazide-based approaches indiscriminately label all reactive carbonyls and are thus insufficient for determining the mechanism by which the labeled carbonyl was formed (i.e lipid peroxidation, direct addition by metal-catalyzed oxidation (MCO), protein glyoxidation).

Mass spectrometry and solution-phase (Gel-free) proteomics

Although 2-DE remains a standard tool for proteomic research, it is clear that this strategy has significant analytical limitations in addressing the many challenges presented by the system-wide analysis of complex protein mixtures. These limitations include (i) limits in sample capacity and detection sensitivity, which constrain 2-DE to identifying relatively abundant proteins, especially apparent when analyzing un-fractionated protein mixtures from whole-cell lysates (Gygi, Corthals et al. 2000); (ii) the separation of insoluble membrane spanning proteins remains a challenge, despite incremental advances in operating conditions making 2-DE more amenable to this class of proteins (Gorg, Weiss et al. 2004); (iii) co-migration of different proteins, and differentially modified proteins migrating to multiple locations on the gel, complicating the quantitative analysis of visualized spots (Gygi, Corthals et al. 2000); and (iv) the labor intensive nature of the method, relying on the sequential identification of protein spots, with limited amenability to automation, thus limiting its throughput. This fact has motivated the development of alternative MS-based strategies to effectively expand the "toolbox" of methodologies available to biological researchers studying protein carbonylation at the proteomic level.

One approach that has gained traction in recent years is solution-phase redox proteomics (Figure 2B). In this approach, carbonylated proteins labeled with biotin-hydrazide are enriched by avidin affinity column chromatography, digested by proteases in-solution, and the resulting peptides analyzed by automated microcapillary reverse-phase liquid chromatography tandem mass spectrometry (μLC-MS/MS). Originally described by Soreghan and colleagues as a tool for identifying carbonylation of low abundant signaling

proteins in tissue homogenates from aged rat brain, the value of the solution-phase approach for characterizing protein targets of carbonylation in various other complex biological mixtures has since been demonstrated(Soreghan, Yang et al. 2003). In a follow-up study, the same group used this approach to describe the carbonylation of the Golgi-resident enzyme glucuronlytransferase protein (GlcAT-P) following β-amyloid induced oxidative stress in cultured primary cortical mouse neurons (Thomas, Soreghan et al. 2005). The associated decline in expression of Human Natural Killer (HNK-1), a neural-specific carbohydrate epitope implicated in regulating inter-neural synaptic transmission, was observed in both β-amyloid treated neurons and in brains of Alzheimer's Disease (AD) mouse models, and lead the authors to postulate that carbonylation of GlcAT-P inhibits its biosynthesis of HNK-1, contributing to the impaired synaptic transmission and increased memory loss observed in AD. To explore the possible connection between protein carbonylation and obesity-associated diabetes, a similar solution-phase redox proteomic approach was used to characterize the carbonyl proteome of adipose tissue from obese insulin-resistant C57BL/6J (MCP 6, 624-637). Of the proteins identified, adipocyte fatty acid binding protein (AFABP), a protein involved in regulating insulin-sensitivity, provided the most intrigue as its carbonylation was associated with declined function.

Several modifications/additions to the basic solution-phase redox proteomic approach described above have been successfully implemented. By differentially labeling controls and samples with amine reactive stable isotope tags (iTRAQ), Meany et al. were able to

conclusively identify and discard from their dataset background proteins non-specifically bound to the avidin resin by virtue of their unchanging abundance levels (Ross, Huang et al. 2004; Meany, Xie et al. 2007). To improve the coverage of carbonylated proteins identified using the solution-phase approach, Mirzaei and colleagues incorporated C8 reverse-phase column chromatography to further fractionate the avidin-enriched biotin-hydrazide labeled proteins from healthy rat plasma prior to their digestion and analysis by mass spectrometry (Mirzaei, Baena et al. 2008). Finally, Feng et al. combined solution-phase redox proteomics with multiplexed stable isotope labeling of peptides to quantitate age-associated abundance changes of carbonylated proteins in rat skeletal muscle (Feng, Xie et al. 2008). An in-depth discussion of the use of stable isotope labels (i.e iTRAQ and ^{18}O) for conducting such comparative proteomic analysis is provided in Appendix I.

Localizing sites of carbonylation by mass spectrometry

Although the gel-based and solution-phase methods described above offer valuable insights pertaining to protein carbonylation in complex biological mixtures, the depth of information provided is very limited. Relying on no-biotin hydrazide control samples run in parallel to distinguish between carbonylated and non-carbonylated proteins, these approaches only reveal the putative protein targets of carbonylation, as the specific amino acid residues carrying the carbonyl are seldomly discovered. Thus, important information concerning the biochemical nature of the modifying carbonyl (i.e. HNE, Acrolein, ONE) is also lost. Although challenging, unveiling these details is crucial for expanding our knowledge of the oxidative mechanisms leading to protein carbonylation

in various disease contexts, and will lay the groundwork for future studies aimed at defining the biochemical consequences associated with site-specific *in vivo* carbonylation of proteins.

To address this need, a number of techniques designed to enhance the detection of carbonylated peptides via mass spectrometry have recently been described (table 2). One approach seeks to improve detection by selectively enhancing the ionization of carbonylated peptides. For example, using dinitrophenylhydrazine (DNPH) as the reactive matrix for MALDI mass spectrometry analysis has been shown to preferentially amplify the signal and thus fragmentation of carbonylated peptides (Fenaille, Tabet et al. 2004). Alternatively, derivatization of aldehyde-modified peptides with 4-(2-(trimethylammonio)ethoxy)benzenaminium halide (4-APC) increases their charge state, and has been shown to improve their detection by electrospray mass spectrometry (Eggink M, Wijtmans M, et al. Anal Chem 2009).

Another approach involves the selective enrichment of carbonylated peptides prior to analysis by mass spectrometery, which serves to minimize suppression of their signal by the more abundant non-modified peptides present in complex mixtures. Immunosorbent materials designed to bind HNE and DNPH modified peptides have been used to enrich carbonylated peptides from proteins treated with HNE and other lipid carbonyls (Fenaille, Tabet et al. 2002; Codreanu, Zhang et al. 2009). In fact, 18 sites of HNE-modification were mapped on proteins isolated from RKO cells treated with 100uM HNE (Codreanu,

Table 2. Summary of chemical reagents used for improving detection of carbonylated peptides by mass spectrometry

Reagent Name	Chemical Structure	Reactivity	Function	Relative Quantitation	Reference
[1]HICAT	See below	Carbonyls	Peptide enrichment	Yes	Han et al. 2007
[2]ARP	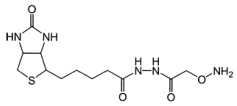	Carbonyls	Peptide enrichment	No	Chavez et al. 2006
HNE-antibody column		HNE	Peptide enrichment	No	Codreanu et al. 2009
Girard P Reagent (GRP)	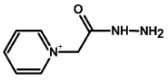	Carbonyls	Signal enhancement	Yes	Mirzaei & Regnier 2006 A, 2006 B
[3]4-APC	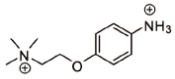	Aldehydes	Signal enhancement	No	Eggink et al. 2009
[4]DNPH	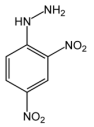	Carbonyls	Signal enhancement	No	Fenaille et al. 2004
HICAT structure	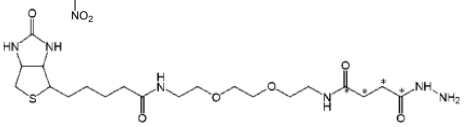				

[1]HICAT = Hydrazide-functionalized isotope-coded affinity tag
[2]ARP = Aldehyde reactive probe
[3]4-APC = 4-(2-(trimethylammonio) ethoxy) benzenaminium halide
[4]DNPH = Dinitrophenylhydrazine

Zhang et al. 2009). Alternatively, avidin affinity capture of biotinylated peptide carbonyls has also aided the identification of several sites of carbonylation in modified proteins. In a pair of studies, Maier's group employed two chemically distinct carbonyl reactive probes (ARP and HICAT) to isolate *in vivo* carbonylated peptides from ADP/ATP translocase 1 and the long-chain-specific acyl-CoA dehydrogenase protein extracted from rat cardiac muscle mitochondria (Chavez, Wu et al. 2006; Han, Stevens et al. 2007). In addition, the HICAT reagent was among the first attempts at profiling quantitative changes to carbonylated peptides between samples. In a third approach, carbonylated peptides are derivatized with Girard P reagent, which introduces an additional positive charge into the peptides, enabling their selective enrichment via cation exchange chromatography, and enhancing their detection by MALDI mass spectrometry (Mirzaei and Regnier 2006). While this approach was initially used to convincingly identify seven sites of MCO carbonylation artificially introduced into transferrin, its subsequent application to protein lysates from untreated *S. cerevisiae* inexplicably mapped sites of carbonylation to tryptically cleaved amino acids, raising skepticism about the utility of Girard P reagent (GPR) for complex mixture analysis. Even so, Mirzai and Regnier further demonstrated the use of isotope coded GPR for tracking quantitative changes to carbonylated peptides.

Although providing important steps forward, these approaches have largely been limited in their ability to map sites of protein carbonylation in complex biological mixtures. One potential explanation is that biotin-conjugated and other bulky reagents readily dissociate

into smaller ions during MS/MS fragmentation, which often dominate the resulting MS/MS spectrum and preclude confident identification of the modified peptides. In addition, the peptide enrichment strategies so far reported rely on two different chemical interactions: labeling of the peptide with a carbonyl-reactive tag, and subsequent affinity-capture of the labeled peptides. As such, the inefficiencies of each reaction are compounded, which likely results in decreased sampling of carbonylated peptides. Finally, identification of carbonylated peptides by mass spectrometry relies completely on confident database matches, as a lack of carbonyl-specific diagnostic ions are available to validate both the very presence and site of carbonylation on any given peptide. As a result, many lower confident true matches to carbonylated peptides are often ignored so as preserve high data quality, while false positive matches receiving high marks are blindly accepted as real. Clearly there is a need for new technologies that address these current limitations and move the field of redox proteomics closer to the end goal of systematically mapping sites of *in vivo* carbonylation.

Thesis objectives and brief outline of thesis

My thesis project seeks to address some of the aforementioned limitations in redox proteomics, and is defined by the following aims:

1) Design a label-free methodology for systematically enriching carbonylated peptides in complex mixtures so as to improve their detection and identification by mass spectrometry

2) Develop a methodology for improving the spectral visualization of carbonylated peptides analyzed by mass spectrometry.

Aim 1 will be addressed in chapter 2 where the solid-phase hydrazide reagent (SPH) is introduced and demonstrated on a cell lysate exogenously treated with HNE. Aim will be presented in chapter 3 with a discussion and demonstration of the utility of partial ^{18}O-labeling for both tracking carbonylated peptides detected by mass spectrometry, and assessing the accuracy and coverage of carbonylated peptides matched by database searching. In chapter 4, I will touch on three preliminary experiments that extend from my thesis aims and guide my future directions. Finally, I will close with some concluding remarks concerning the state of the field and the direction it may be headed.

Chapter 2

Proteomic Mapping of 4-Hydroxynonenal Protein Modification Sites by Solid-Phase Hydrazide Chemistry and Mass Spectrometry

This chapter is reprinted from Analytical Chemistry, vol. 79, Mikel R. Roe, Hongwei Xie, Sricharan Bandhakavi, and Timothy J. Griffin, **Proteomic Mapping of 4-Hydroxynonenal Protein Modification Sites by Solid-Phase Hydrazide Chemistry and Mass Spectrometry**, 3747-3756,

Summary

The modification of proteins by the cytotoxic, reactive aldehyde 4-hydroxynonenal (HNE) is known to alter protein function and impair cellular mechanisms. In order to identify susceptible amino acid sites of HNE modification within complex biological mixtures by microcapillary liquid chromatography and linear ion trap tandem mass spectrometry, we have developed a solid-phase capture and release strategy that utilizes reversible hydrazide chemistry to enrich HNE-modified peptides. To maximize the detection of fragment ions diagnostic of HNE modification, both neutral-loss dependent acquisition of MS/MS/MS spectra and the pulsed Q dissociation operation mode were employed. When the solid-phase hydrazide (SPH) enrichment strategy was applied to a yeast lysate treated with HNE, 125 distinct amino acid sites of HNE modification were mapped on 67 different proteins. The endogenous susceptibility of many of these proteins to HNE modification was demonstrated by analyzing HNE treated yeast cell cultures with a complementary biotin hydrazide enrichment strategy. Further analysis revealed that the majority of amino acid sites susceptible to HNE modification were histidine residues, with most of these sites being flanked by basic amino acid residues, and predicted to be solvent exposed. These results demonstrate the effectiveness of this novel strategy as a general platform for proteome-scale identification of amino acid sites susceptible to HNE modification from within complex mixtures.

Introduction

Under oxidative stress an imbalance in prooxidant and antioxidant molecules causes an altered redox potential in the cell, leading to increased levels of reactive oxygen species (ROS). One common consequence of oxidative stress is the ROS-mediated introduction of carbonyl groups into protein amino acid side chains via a number of mechanisms(Sies 1991; Chevion, Berenshtein et al. 2000): Metal catalyzed oxidation directly converts side chains to reactive carbonyls (Requena, Chao et al. 2001); the adduction of lipid derived carbonyls, such as 4-hydroxynonenal (HNE), is also a common mechanism of protein carbonylation, and a frequently used marker of oxidative damage (Sies 1991; Chevion, Berenshtein et al. 2000).

In addition to being recognized as a marker of oxidative stress, HNE has been associated with aging in organisms ranging from from *C. elegans* to humans (Esterbauer, Schaur et al. 1991; Chiarpotto, Biasi et al. 1995; Ayyadevara, Engle et al. 2005; Asselin, Bouchard et al. 2006; Dalle-Donne, Rossi et al. 2006; Gil, Siems et al. 2006). Furthermore, elevated cellular levels of HNE-modified proteins have been implicated in the onset and progression of various diseases including atherosclerosis (Uchida, Itakura et al. 1995; Itakura, Oya-Ito et al. 2000), neurodegenerative diseases (Yoritaka, Hattori et al. 1996; Calingasan, Uchida et al. 1999; Butterfield, Reed et al. 2006) and cancer (Okamoto, Toyokuni et al. 1994). Hence, an improved understanding of the biochemistry that regulates HNE adduct formation could provide new insights into the mechanisms of

oxidative stress-associated changes in cellular function and the pathologies of a plethora of diseases.

HNE is known to diffuse throughout the cell away from its origin within cell membranes to covalently modify proteins and alter their function (Benedetti, Comporti et al. 1980; Uchida, Shiraishi et al. 1999; Uchida 2003). Biochemical analysis of the mechanisms governing the formation of HNE protein adducts indicates that the side chains of the nucleophilic residues cysteine, histidine, and lysine form Michael-addition adducts with HNE at carbon position three (Esterbauer, Schaur et al. 1991; Uchida and Stadtman 1992). Importantly, previous work using carbonyl-reactive probes has shown that the reactivity of the free aldehyde on bound HNE molecules is not quenched by intramolecular cyclization events which are heavily favored by oxo-cyclo equilibrium (Esterbauer, Schaur et al. 1991; Uchida and Stadtman 1992; Uchida and Stadtman 1993; Nadkarni and Sayre 1995).

While a number of general strategies have been described for identifying proteins susceptible to carbonyl modification (Soreghan, Yang et al. 2003; Mirzaei and Regnier 2005; Mirzaei and Regnier 2006), the strategies described for mapping sites of HNE modification on proteins within complex mixtures are limited. Identifying amino acid sites of modification is critical to understanding potential functional effects of these modifications on specific proteins and pathways, as well as elucidating potential conserved amino acid sequences and/or structural motifs susceptible to these modifications. The challenge of mapping HNE modification sites within complex

mixtures is defined by the dynamic range of the sample and the substoichiometric nature of the modification. The difficulty of this task is greatly magnified in bottom-up proteomic approaches where samples are made significantly more complex by digesting proteins into multiple peptides. As a result, the vast majority of investigations seeking to identify sites of HNE modification have been conducted on single, purified proteins (Bennaars-Eiden, Higgins et al. 2002; Louie, Kapphahn et al. 2002; Ishii, Tatsuda et al. 2003; Carbone, Doorn et al. 2004; Drake, Petroze et al. 2004; Isom, Barnes et al. 2004; Aldini, Dalle-Donne et al. 2005; Carbone, Doorn et al. 2005; Carbone, Doorn et al. 2005; Ozeki, Miyagawa-Hayashino et al. 2005; Fang and Holmgren 2006; Temple, Yen et al. 2006). In one such study, Bolgar and Gaskell used apomyoglobin as a model protein to demonstrate the potential utility of various instrumental methods, such as precursor-ion and neutral-loss scanning, to facilitate the detection HNE-modified peptides by mass spectrometry (Bolgar 1996). Although yet to be shown, these methods are likely applicable for the detection of HNE-modified peptides within complex mixtures.

To overcome the challenges of mapping sites of HNE modification within complex mixtures, a limited number of strategies for isolating and identifying modified peptides have been developed. These include a method that incorporates the carbonyl derivatizing agent 2,4-dinitrophenylhydrazine (DNPH) into the MALDI matrix for identifying gel separated HNE modified proteins (Fenaille, Tabet et al. 2004), and the use of immobilized anti-HNE and anti-DNPH antibodies (Fenaille, Tabet et al. 2002) for the enrichment of HNE modified peptides. Notably, these strategies have yet to demonstrate utility in the analysis of complex mixtures on a proteome-scale.

Here we describe a label-free strategy based on the development of a solid-phase hydrazide (SPH) reagent for the enrichment of aldehyde-containing HNE-modified peptides from within complex mixtures. HNE-modified peptides are captured on hydrazide coated glass beads via the formation of a covalent but reversible hydrazone bond enabling their specific enrichment and release under acidic conditions. By combining this front-end enrichment strategy with neutral-loss dependent acquisition of MS/MS/MS (MS^3) spectra and pulsed-Q-dissociation (PQD) operation on a linear ion trap mass spectrometer, a comprehensive catalogue of amino acid sites susceptible to HNE modification in treated yeast protein mixtures was obtained. These results demonstrate the utility of this novel SPH-based strategy for the general, proteomic characterization of HNE-modified peptides from within complex mixtures, providing new and useful information on proteins susceptible to this important class of post-translational modification.

Materials and Methods

Construction of the Solid-phase Hydrazide (SPH) Reagent

One-hundred milligrams of aminopropyl glass beads (Sigma), having an average pore size of 170 Å, were prewashed with anhydrous dimethylformamide (DMF) in a 2 milliliter disposable fritted spin column (BioRad). The amine groups were derivatized with carboxylic groups by incubating the beads for 90 minutes in a mixture of succinic anhydride (541 mM) and diisopropylethlamine (2.5%) dissolved in DMF. After washing with 3 column volumes of DMF, the beads were primed for the attachment of FMOC-

carbazate (Sigma) by incubating them for 30 minutes in a solution of DMF containing 1-hydroxybenzotriazole (140 mM) and N,N'-diisopropylcarbodiimide (2%). To this mixture, FMOC-carbazate (200 mM) dissolved in DMF was added and the beads allowed to incubate for an additional 90 minutes. After a second wash step with DMF to remove unreacted FMOC-carbazate, bound FMOC groups were removed by incubating the beads in a DMF solution containing 20% piperidine for 30 minutes in the dark. The molar capacity of the resulting hydrazide bound glass beads was estimated by measuring the amount of FMOC in the flow through fraction as determined by the change in absorbance at 290 nm relative to a piperidine/DMF blank. The beads were further washed with two column volumes of methanol, dried via vacuum centrifugation, and stored at -20°C. All incubations were conducted at room temperature.

Preparation of HNE-Modified peptide and protein standard samples.

To test the reactivity of the SPH reagent towards peptides modified at histidine, lysine, and cysteine residues three standard peptides, anaphylatoxin, substance-P fragment 1-7, and urinary trypsin inhibitor (SigmaAldrich), were independently reacted with 5 mM HNE (Cayman Chemical) in 50 mM Tris pH 8.3 for 4 hours at 37ºC. The resulting HNE-modified peptide stocks were then passed through a strong-cation-exchange cartridge (Applied Biosystems) to remove free HNE. The eluates, containing the HNE-modified standard peptides, were lyophilized via vacuum centrifugation, resuspended with 0.1% trifluoroacetic acid and then desalted by SepPak reverse phase solid phase extraction

(Waters). The resulting eluates were again lyophilized via vacuum centrifugation, resuspended with 0.1% acetic acid and stored at -20ºC.

To generate a mixture of modified and unmodified peptides of minimal complexity, 10 nmol of horse myoglobin (Sigma) was first incubated with 2 mM HNE for 2 hours at 37°C in 50 mM potassium phosphate pH 7.4. The remaining free HNE was removed by applying the sample to a 5000 MW cutoff centrifugal spin column (Millipore). The retained protein was then digested with trypsin overnight (1:50 Trypsin to protein) in 50 mM Tris buffer pH 8.3. The resulting peptides were then acidified with 0.1% TFA and desalted using a Sep-Pak reverse phase cartridge. The eluate was subsequently lyophilized via vacuum centrifugation and then resuspended with 0.1% TFA. 100 pmol of these HNE-modified myoglobin peptides was then combined with 100 pmol of unmodified tryptic peptides from a standard 10 protein mixture composed of commercially available proteins (Sigma). To this mixture, 50 pmol of HNE-modified anaphylatoxin peptide was added as a positive control.

Preparation of HNE-Modified Protein Samples from Yeast Whole Cell Extracts

To generate HNE-modified proteins from yeast lysates, unsynchronized cultures of *S. cerevisiae* (BJ5465) were grown at 30°C to an OD600 of 0.5 and then lysed with glass beads in the presence of a cocktail of protease inhibitors (Roche). The proteins were isolated by mild centrifugation, quantified via the BCA assay (Pierce), and then treated with HNE. Briefly, 1 mg of protein, dissolved in 50 mM potassium phosphate (pH 7.4), was reacted with 250 μm HNE for two hours at 37°C. The remaining free HNE was

removed using 4 ml centrifugal ultrafiltration columns (Amicon 5000 MW cutoff, Millipore). The resulting proteins were digested with trypsin (1:100 enzyme to substrate) at 37°C for 16 hours in the following digestion buffer: 100 mM ammonium bicarbonate (pH 8.0), 10% acetonitrile, and 5 mM of the reducing agent Tris(2-Carboxyethyl)-phosphine hydrochloride (TCEP). The resulting tryptic peptides were acidified, desalted using a Sep-Pak reverse phase solid-phase extraction cartridge (Waters), and finally lyophilized via vacuum centrifugation.

To generate HNE-modified proteins within growing yeast cultures, a slight modification to the above protocol was made. After achieving an OD600 of 0.5, experimental and control cultures were incubated for an additional 2-hours in the presence of 250 μm HNE (dissolved in ethanol) or an equal volume of ethanol alone, respectively. Subsequent preparation of the proteins was conducted as described above.

Enrichment of HNE-Modified Peptides using the SPH Reagent

In all enrichment experiments, the SPH reagent (3 mg) was added to peptides dissolved in 100 μl of reaction buffer (0.2% acetic acid, 10% acetonitrile pH 3.6) and the resulting mixture shaken (Eppendorf Thermomixer R) at 25°C and 1200 rpm. The HNE-modified standard peptides were mixed with the unmodified fibrino peptide in a molar ratio of 1:1:10:100 fibrino:anaphylatoxin:substance-P fragment 1-7:urinary trypsin inhibitor and then incubated with the SPH reagent for two hours. This molar ratio was chosen to produce similar MALDI peak intensities from the four peptides so as to better follow

their capture and release from the SPH reagent. To analyze a minimally complex mixture, 200 picomoles of tryptic peptides from a 10 protein mix, containing peptides from HNE-modified myoglobin, were reacted with the SPH reagent for 4-hours. Fifty picomoles of the HNE-modified anaphylatoxin peptide was spiked into this sample as a positive control.

To analyze yeast samples, 1-2 mg of tryptic peptides were reacted with the SPH reagent overnight. Following all incubations, the SPH reagent was pelleted to the bottom of the 1.5 ml eppendorf tube, and the supernatant (i.e. the flow through fraction) was extracted and saved for MS/MS analysis. The pellet was subsequently washed four times each with 400 µl of reaction buffer followed by, 1 M NaCl, distilled water, 80% acetonitrile, and a second round of distilled water. All washes were conducted by mild vortexing (20 seconds) and bench-top microcentrifugation (13,000 rpm) in succession. To release the hydrazide-bound peptides, 200 µl of 10% formic acid was added to the washed SPH pellet and the mixture was incubated for 30 minutes at 60°C. The supernatant containing the released peptides was collected and the SPH pellet was washed one time with an additional 200 µl of 10% formic acid. The wash supernatant was added to the released peptides and the combined solution was lyophilized.

Enrichment of HNE-Modified Proteins by Biotin-Hydrazide

Proteins (2.5 mg) extracted from cultures of *S. cerevisiae* incubated with 250 uM HNE as described above were suspended in an aqueous buffer containing 100 mM sodium acetate

and 150 mM sodium chloride, pH 5.5. Biotin-hydrazide, dissolved in dimethylsulfoxide, was added to a final concentration of 5 mM and the resulting mixture was shaken (700 rpm) for 2-hours at room temperature. The hydrazone bonds formed between protein carbonyls and the biotin-hydrazide reagent were then reduced by incubating with sodium cyanoborohydride (15 mM) on ice for 40 minutes. Unreacted biotin-hydrazide was subsequently removed by dialyzing the samples in 1x PBS at 4°C. Affinity purification of the biotinylated proteins was achieved by using a monomeric avidin column. The columns were washed using 12 mL PBS buffer followed by 12 mL of 50 mM HEPES buffer to get rid of excess salt and 12 mL of 2mM D-biotin in 50 mM HEPES buffer to elute the biotinylated proteins. Trypsin (20 μg) and 5 mM TCEP-HCl was added to the eluate to digest the proteins overnight at 37°C. After tryptic digestion, the excess D-biotin was removed using mixed mode cation exchange (MCX, Waters Corp.) cartridges. Before applying the digested peptides to the MCX cartridge, the pH of the peptide solution was adjusted to 3 or less with formic acid and the cartridge was equilibrated with 2 mL of 1:1 mixture of methanol and water using a large pipette bulb to apply positive pressure. Acidified peptide samples were loaded on the cartridge 3 mL at a time and the flow rate across the cartridge was about 1 drop per second. After loading, the cartridge was washed with 3 mL of 0.1% formic acid, followed by 2 mL of methanol to remove hydrophobic contaminants. To elute the bound peptides, 1ml of freshly prepared elution buffer containing 150 μL of ammonium hydroxide and 850 μL of methanol was used. The eluted peptides were dried by vacuum centrifugation.

MALDI-TOF MS

Prior to analysis by mass spectrometry, standard HNE-modified peptide samples were desalted with Millipore's reverse-phase micro C18 ZipTips per manufacturer's instruction, and then mixed with α-cyano-4-hydroxycinnamic acid matrix. Full scan mass spectra were collected using a Qstar XL quadrapole-TOF mass spectrometer with MALDI ion source (Applied Biosystems Inc., Foster City, CA) in positive ion detection mode, and averaging together 30 spectra. The TOF region acceleration voltage was 4 kV, and the injection pulse repetition rate was 6.0 kHz. A 337 nm nitrogen laser was used to generate laser pulses at a repetition rate of 10 Hz having a laser energy of ~14uJ.

LC-MS/MS

All microcapillary liquid chromatography (μLC) separations were done on an automated Paradigm MS4 system (Michrom Bioresources, Inc., Auburn, CA). Samples were automatically loaded across a Paradigm Platinum Peptide Nanotrap (Michrom) pre-column (0.15 x 50 mm, 400 μL volume) for sample concentrating and de-salting, at a flow rate of 50 μL/min in HPLC buffer A (5% acetonitrile, 0.1% formic acid, aqueous). The inline analytical capillary column (75 um x 12 cm) was home-packed using C18 resin (5um, 200Å Magic C18AG, Michrom BioResource, Auburn, CA) and Picofrit capillary tubing with an integrated 15 μm ESI tip (New Objective, Cambridge, MA). Peptides were eluted using a linear gradient of 10-35% buffer B (80% acetonitrile, 0.1% formic acid, aqueous) over 60 minutes, followed by isocratic elution at 80% buffer B for 5 min with a flow rate of 0.25 μL/min across the column. Peptides were analyzed by

MS/MS using a Finnigan linear ion trap mass spectrometer system (LTQ, Thermo Electron Corporation, San Jose, CA). The electrospray voltage was set to 2.0 kV. A collision energy of 30% was determined to be optimal for generating quality MS/MS fragmentation patterns by collision-induced-dissociation. For pulsed-Q-dissociation, an optimized collision energy of 42% was used. Peptides generated by the biotin-hydrazide experiment were exclusively fragmented using standard CID operating mode using the defined instrumental parameters.

Sequence Database Searching and Data Analysis

All generated MS/MS and MS^3 spectra were searched against a concatenated *Saccharomyces cerevisiae* database, containing both the forward and reverse sequences of all yeast open reading frames, using the SEQUEST algorithm (Eng 1994). The differential search parameters were specified for detecting both the oxidation of methionine (+16) and the addition of HNE (+156) to cysteine, histidine and lysine residues. The precursor mass tolerance was set at 2.0, and no enzyme was specified, thereby enabling the filtering of peptide matches for those containing tryptic cleavage sites. Peptides were assigned probability scores (P score) by Peptide Prophet (Keller, Nesvizhskii et al. 2002) and the data organized using the tool Interact. An initial false positive rate of less than 1% was determined for all HNE-modified peptides with scores of 0.87 or higher (Peng, Elias et al. 2003). Given that all the false positive hits at this threshold derived from peptides modified by HNE at cysteine and/or lysine residues, a separate analysis was conducted on histidine modifications alone. A probability score of

0.4 or greater was found to provide a false positive rate of less than 1% for all histidine modified peptides. This value was thus used as the threshold for accepting histidine modifications without further validation. Manual confirmation of all histidine modified peptides with scores below this threshold adhered to the following criteria: 1) 80% of the major spectral peaks were accounted for by expected b and y-ions; and 2) at least one of the diagnostic ions of HNE-peptide fragmentation, as described in the Results section was present. In addition, all peptides modified at cysteine and/or lysine residues, independent of probability scores, were manually inspected and verified using the same criteria as stated above.

Results

HNE-modified peptide enrichment strategy

To address the current lack of proven strategies capable of enriching HNE-modified peptides from complex mixtures, we designed a solid-phase approach that utilizes hydrazide chemistry to covalently and reversibly isolate HNE-modified peptides via Schiff-base (i.e. hydrazone bond) formation with the reactive aldehyde residue (Figure 1). Capture of HNE-modified peptides was conducted under mildly acidic conditions (pH 3.6) to capitalize on the reactivity of hydrazide with aldehydes at this pH, while limiting the reactivity of other nucleophiles (e.g. primary amines) (Nguyen and Huc 2003; Lees, Sen et al. 2006), and also to maximize the formation of hydrazone bonds relative to their hydrolysis (Bunyapaiboonsri, Ramstrom et al. 2001). To limit the occurrence of non-specifically bound peptides in the final peptide analysis, the reacted beads were washed

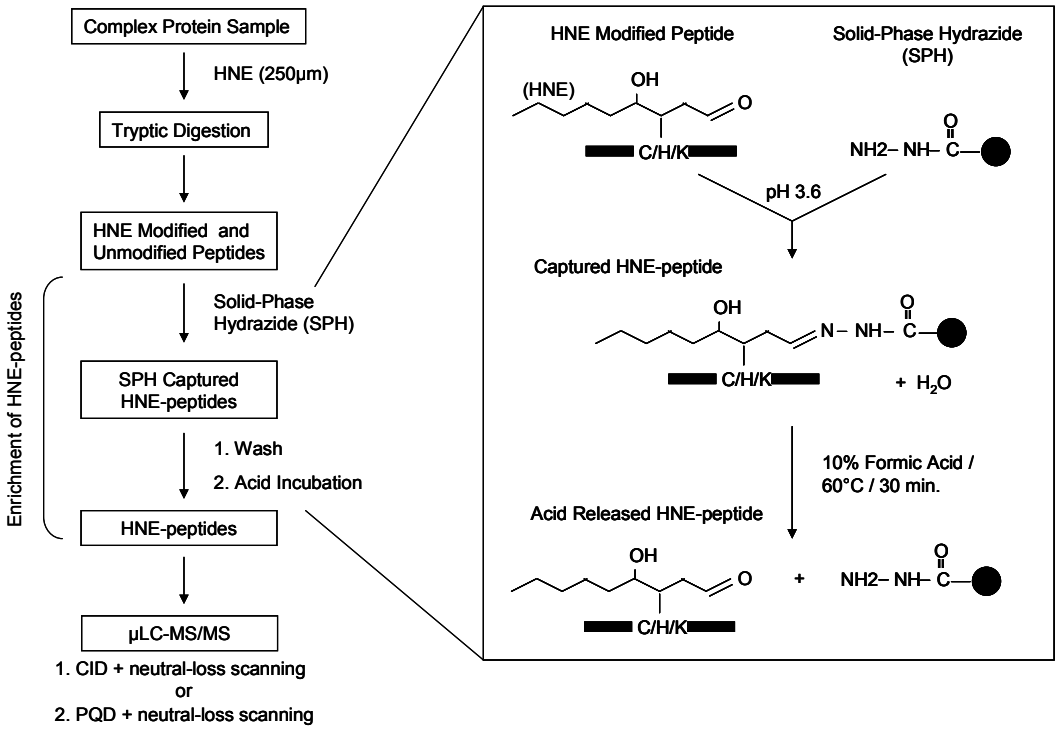

Figure 1. Scheme for solid-phase hydrazide (SPH) enrichment and analysis of HNE-modified peptides within complex mixtures. The details of the enrichment and instrumental analysis strategies are described in the text.

thoroughly with reaction buffer, high salt, and organic solvents in succession. Importantly, these wash steps were conducted under mild pH conditions where the hydrazone formed between the SPH and HNE-modified peptide remains stable (Nguyen and Huc 2003; Levrand, Ruff et al. 2006). The bound peptides were finally released by heating the beads in strong acid (10% formic acid) (Chelius and Shaler 2003). Under these hydrolyzing conditions the hydrazone bonds are reversed, and the released HNE-modified peptides are readily analyzed by mass spectrometry. (Chelius and Shaler 2003; Nguyen and Huc 2003; Skene and Lehn 2004). Importantly, the controlled-pore glass beads used as a solid support in the synthesis of the SPH reagent are compatible with the conditions used for eluting the peptides, unlike other supports such as agarose gel based beads, which may breakdown and introduce contaminants under such conditions.

Optimization of the SPH strategy using HNE-modified peptide and protein standards

In initial experiments, three standard peptides, HNE-modified *in vitro* at histidine, lysine, and cysteine residues respectively, were combined with an unmodified, negative control peptide. The resulting mixture was then used to optimize reaction conditions and to demonstrate the ability of the SPH reagent to effectively capture and release HNE-modified peptides (Figure2). As shown in Figure 2a, all three modified peptides (labeled 1-3 for His, Lys and Cys modified peptides, respectively) and the unmodified peptide were present in solution prior to adding the solid-phase hydrazide reagent. However, after reacting with the SPH reagent for two hours, only the unmodified peptide remained in solution (Figure 2b), indicating that the three HNE-modified peptides were bound to the reagent. The reappearance of peaks 1, 2 and 3 at equal relative intensities after the

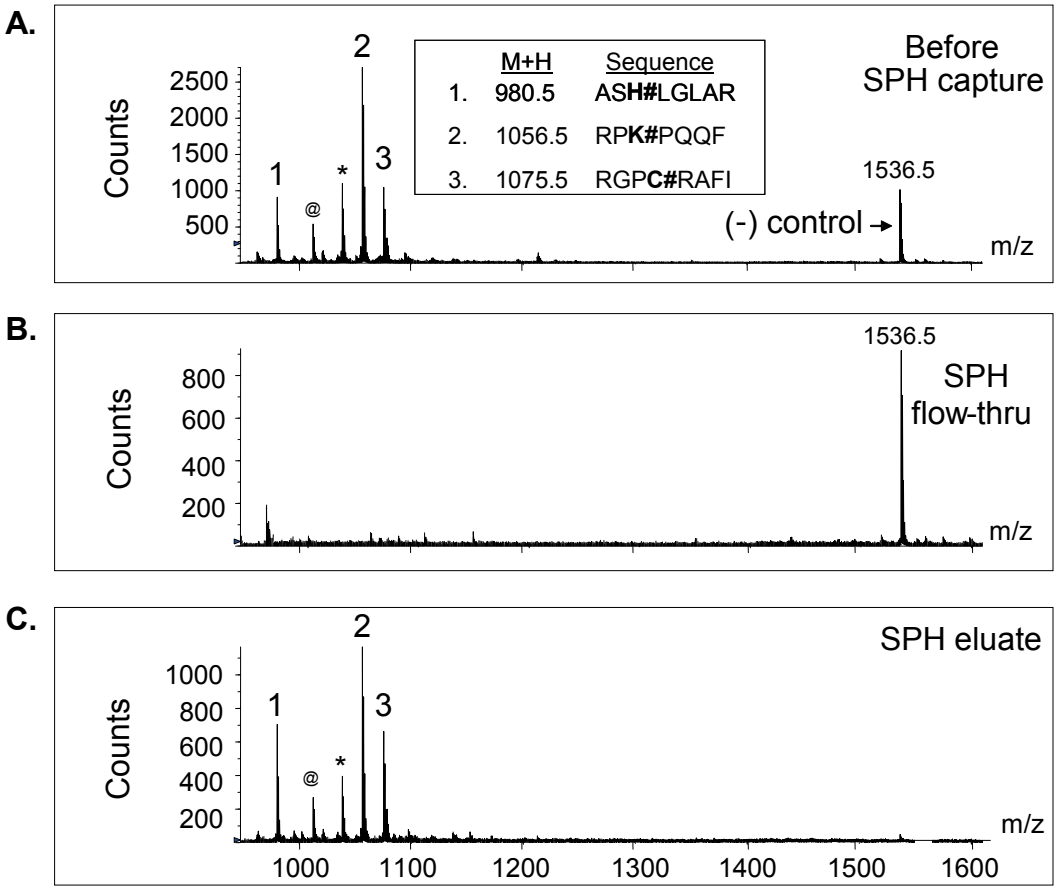

Figure 2. MALDI-TOF MS spectrum showing the efficient capture and release of HNE-modified standard peptides from the SPH reagent. (a) Three standard peptides modified by HNE (#) at histidine (1), lysine (2), and cysteine (3) residues were combined with an unmodified, negative control peptide (at m/z 1536.5) prior to reaction with the SPH reagent. * and @ designate loss of water and an unknown in-source fragmentation product consistently detected (loss of 44 Da) using both MS and MS/MS from the lysine modified peptide. (b) After reacting for two-hours, only the unmodified, negative control peptide remains in the supernatant, defined as the Flow-through fraction. (c) The reappearance of the HNE-modified standard peptides (labeled 1-3) in the Eluate fraction, after acid release from the SPH reagent.

SPH reagent is heated in acid demonstrates that each class of HNE-modified peptide (His, Lys, Cys) is effectively released from the solid structure without further chemical modification (Figure 2c). Importantly, the unmodified peptide was virtually absent in the eluate fraction as it was removed in the washing stage prior to acid treatment. Taken together this data indicates that the SPH reagent specifically captures and releases HNE-modified peptides. In these optimization experiments, percent recoveries of approximately 80% were consistently attained as determined by comparing the ratio of mass spectrometric signal intensities between HNE-modified anaphylatoxin and an externally added peptide observed in the Before enrichment and Eluate fractions (data not shown). Additionally, in experiments measuring recovery from the SPH reagent, starting peptide amounts of less than 1 picomole were routinely enriched and reliably detected (data not shown).

Enrichment of HNE-modified peptides within a 10 protein mix

To demonstrate the utility of the SPH reagent for enriching HNE-modified peptides from within a mixture of limited complexity, a tryptic digest containing equimolar amounts of *in vitro* HNE-modified myoglobin and 10 other unmodified standard proteins was utilized. As expected, signal suppression of the HNE-modified peptides analyzed in the presence of a large background of non-modified peptides greatly limited their detection by mass spectrometry (Figure 3A). Here, however, two HNE-modified peptides from myoglobin were observed just above the noise (peaks labeled 1 and 2 in Figure 3A). After using the SPH reagent to enrich for HNE-modified peptides out of the digest, the same two modified peptides from myoglobin were again observed, this time with much

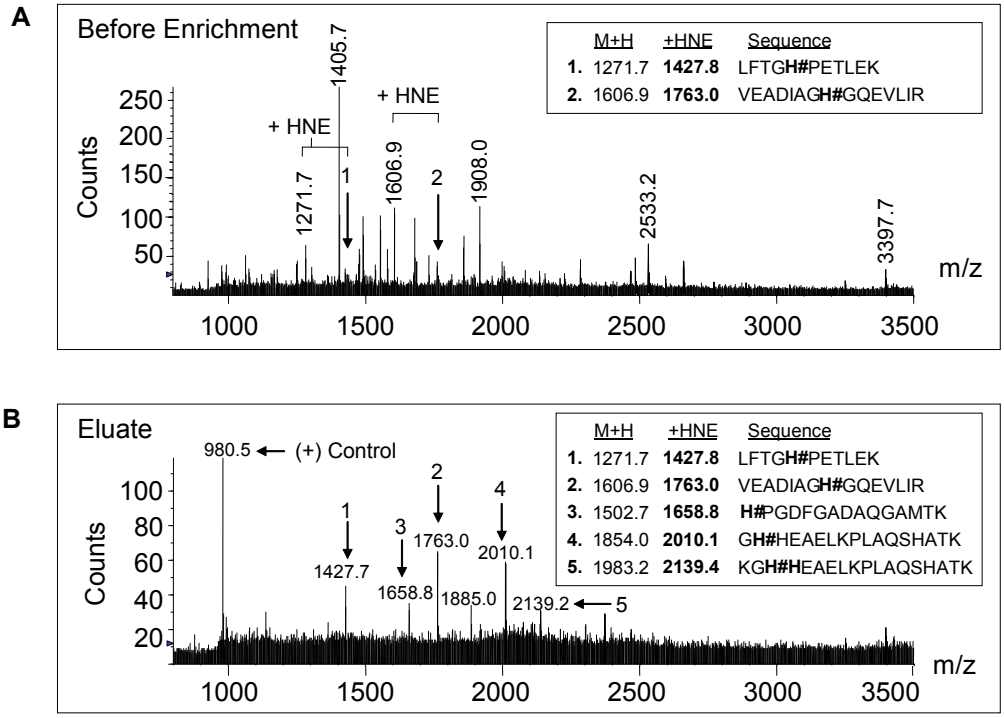

Figure 3. SPH enrichment of HNE-modified peptides within a mixture of limited complexity. (a) MALDI-TOF MS spectrum of a minimally complex tryptic digest, containing ten unmodified proteins and HNE-modified myoglobin, prior to addition of the SPH reagent. Numbers 1 and 2 designate HNE-modified peptides from myoglobin. (b) MALDI-TOF MS spectrum of SPH enriched fraction from a 10 protein digest. Numbers 1-5 designate five distinct HNE-modified peptides from myoglobin, with their sequences indicated in the inset table. Histidines marked with a # sign are HNE-modified.

improved signal-to-noise ratios (Figure 3B). In addition, three new HNE-modified myoglobin peptides, previously masked by the background of unmodified peptides, were enriched and detected. The m/z values for all five modified myoglobin peptides detected are consistent with values previously reported for this protein, and correspond to histidine modified tryptic peptides (Alderton, Faustman et al. 2003) (See inset of Figures 3A and 3B). Importantly, these modified myoglobin peptide sequences at the m/z values indicated in Figure 3B were also confirmed by MS/MS analysis on the hybrid MALDI instrument (data not shown). This data indicates that the hydrazide beads are capable of enriching HNE-modified peptides from within a mixture of non-modified peptides.

SPH enrichment of HNE-treated yeast lysates

With this proof-of-principle data in hand, we next sought to determine the effectiveness of the SPH reagent to enrich HNE-modified peptides mixtures with increased complexity. For these experiments we chose to incubate proteins isolated from total yeast lysates with excess HNE (250 μM) in a PBS buffer and under native conditions. After incubation and removal of excess HNE, the proteins were digested with trypsin, and the peptides reacted with the SPH reagent. The enriched eluate was analyzed by μLC-ESI-MS/MS on a linear two dimensional ion trap.

Figure 4 is a representative MS/MS spectrum from an HNE-modified peptide that was matched with high confidence using the Sequest search algorithm (Peptide Prophet assigned P score of 0.98). Within this MS/MS spectrum, characteristic peaks derived from CID of HNE-modified peptides are labeled. The neutral-loss of HNE from the

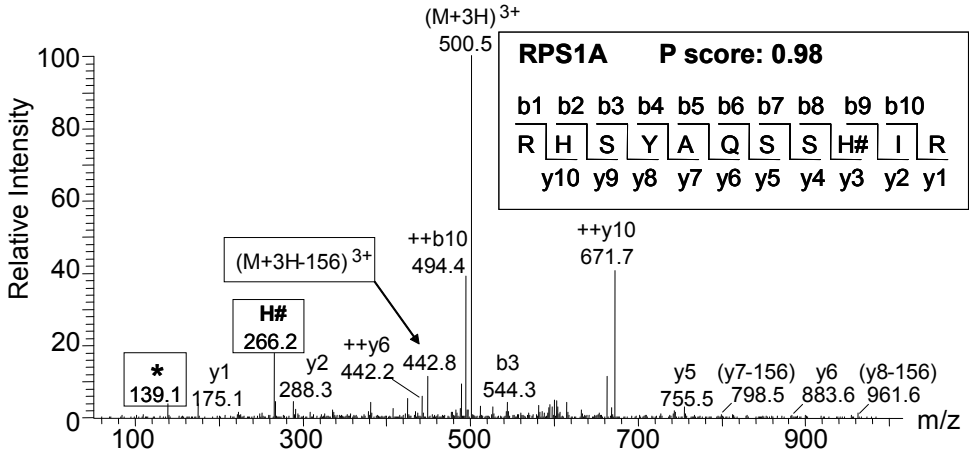

Figure 4. Example MS/MS spectrum of HNE-modified peptides generated by PQD operating mode. The peak at 448 m/z, corresponds to the neutral- loss of HNE (-52m/z) from the triply charged precursor ion. The released, HNE moiety dehydration fragment ion at 139m/z, is denoted with a (*), and the HNE-modified histidine immonium ion peak at 266 m/z is denoted as (H#).

triply-charged peptide, in this spectrum at 448.4 m/z, is a common and prominent peak within the spectrum of HNE-modified peptides analyzed by electrospray ionization (Bolgar 1996; Carbone, Doorn et al. 2004; Aldini, Dalle-Donne et al. 2005; Carbone, Doorn et al. 2005). The released HNE-derived moiety often fragments further via a dehydration event to form the observed ion at 139.1 m/z. While both of these fragmentation patterns are characteristic of HNE-modified peptides, independent of the site of modification, the ion at 266.2 m/z represents the immonium ion of histidine modified with one molecule of HNE and is consistently present in the MS/MS spectrum of peptides HNE-modified at histidine residues (Bolgar 1996; Isom, Barnes et al. 2004).

Characteristic fragment ions observed in the MS/MS spectrum of HNE-modified peptides can be both a limitation and benefit to the characterization of these peptides. For example, while prominent neutral-loss may preclude reliable fragmentation on the peptide backbone, and thus limit reliable identification of the peptide sequence, the characteristic neutral-loss peak is diagnostic of HNE-modified peptides and therefore provides a means to confirm and validate the identification of putatively modified peptides (Bolgar 1996). Thus, we sought to capitalize on this beneficial aspect of the observed diagnostic fragments by implementing instrumental strategies on the LTQ linear ion trap accounting for these fragments.

Given the success of neutral-loss dependent data acquisition methods for detecting covalent peptide modifications, such as phosphorylation (Beausoleil, Jedrychowski et al. 2004), a similar approach was used here to identify sites of HNE modification.

Specifically, when a fragment peak with an m/z value corresponding to the neutral-loss of HNE from the precursor ion was among the ten most intense peaks in a given MS/MS spectrum, it was selected for an additional round of fragmentation. The resulting MS^3 spectrum, which lacks the various fragmentation peaks ascribed to HNE modification, leads to a cleaner fragmentation pattern of the peptide and thus a better peptide match by the database search algorithm. Thus, MS^3 spectra served two purposes: first, they enabled the identification of modified peptides when MS/MS spectra proved insufficient, and second, they provided further supporting data to confirm the identification of modified peptides determined from reliable MS/MS spectra.

While the majority of meaningful MS^3 generated from this approach confirmed highly confident identifications derived from MS/MS spectrum, there were several instances where the MS^3 spectrum was either the primary source for identifying HNE-modified peptides, or provided the necessary information required to validate the identification of a low scoring HNE-modified peptide identified by MS/MS. An example of the latter is depicted in Figure 5 where the MS/MS spectrum is matched with very low confidence to a peptide from the heat-shock 70 protein (SSA1) that is modified at a cysteine residue. When the prominent neutral-loss fragment in the MS/MS spectrum was selected for an additional round of CID, it produced a MS^3 spectrum wherein all the resulting peaks could be accounted for by the series of b and y ions expected for the unmodified version of the SSA1 peptide. Manual inspection of the MS/MS spectrum further confirmed the identification and modification of the SSA1 peptide.

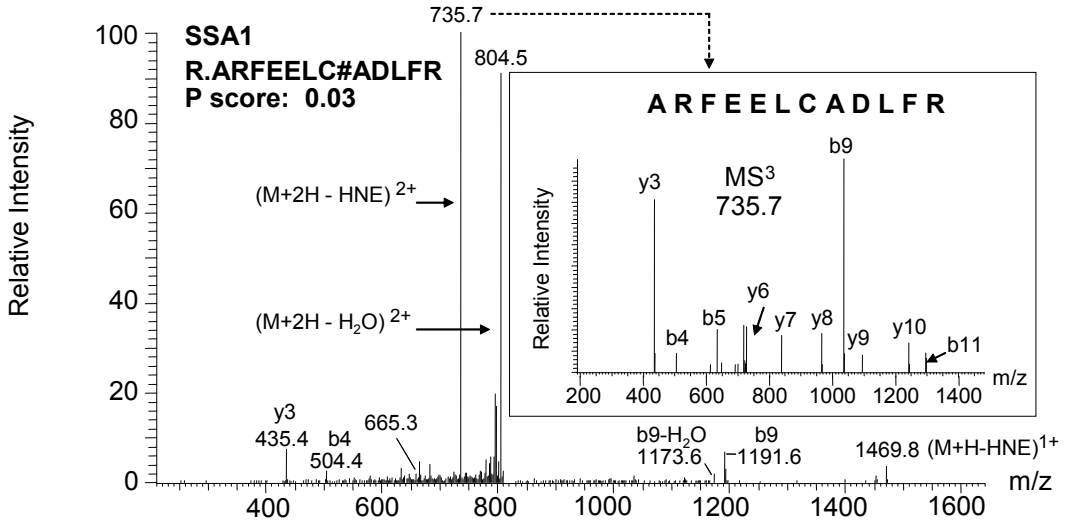

Figure 5. Utility of neutral-loss dependent MS^3 spectra for confirming low confidence HNE-modified peptide matches. The dominance of the neutral loss peak (735.6m/z) in this spectrum effectively suppresses the series of b and y ions produced by the doubly charged precursor ion (814.m/z), and results in a low P score assignment to the peptide match. The HNE-modified peptide sequence match was confirmed after manual validation of the MS^3 spectrum generated from the neutral loss ion.

Other than the neutral loss ion, the other diagnostic fragment ions common to HNE peptides are at low m/z values (139 and 266 m/z). Traditionally, ion trap instruments operating in standard CID mode have been limited in their detection of low mass fragments in MS/MS experiments. However, a new improvement called pulsed Q dissociation (PQD) has overcome this limitation, providing the ability to detect low mass ions from collisionally activated peptide fragmentation in all MS/MS acquired (Schwartz, Syka et al. 2005). Thus we sought to use this new PQD operation mode in order to maximize the detection and utility of these diagnostic fragment ions in the identification of enriched HNE-modified peptides. The ability to monitor the low mass range of every PQD generated MS/MS spectrum significantly increased the coverage of both diagnostic fragment ions. With this improved detection of the 139 and 266 m/z ions, added confidence was provided in the identification of HNE-modified peptides that derived from MS/MS spectra having assigned probability scores both well above (e.g. Figure 4) and well below (e.g. Figure 6) the 1% false positive threshold. The latter example demonstrates the utility of the diagnostic ions for identifying HNE-modified peptides that would usually be considered invalid based on their low probability scores (i.e. false negatives). In fact, the presence of the 266 m/z ion alone in several MS/MS spectra guided the manual validation of 18 peptides modified at histidine residues with assigned probability scores below the threshold for providing a 1% false positive rate. These peptides, which would not have otherwise been considered correct, demonstrate the utility of the diagnostic ions and the PQD operation mode for enabling the identification of more modified peptides with increased confidence.

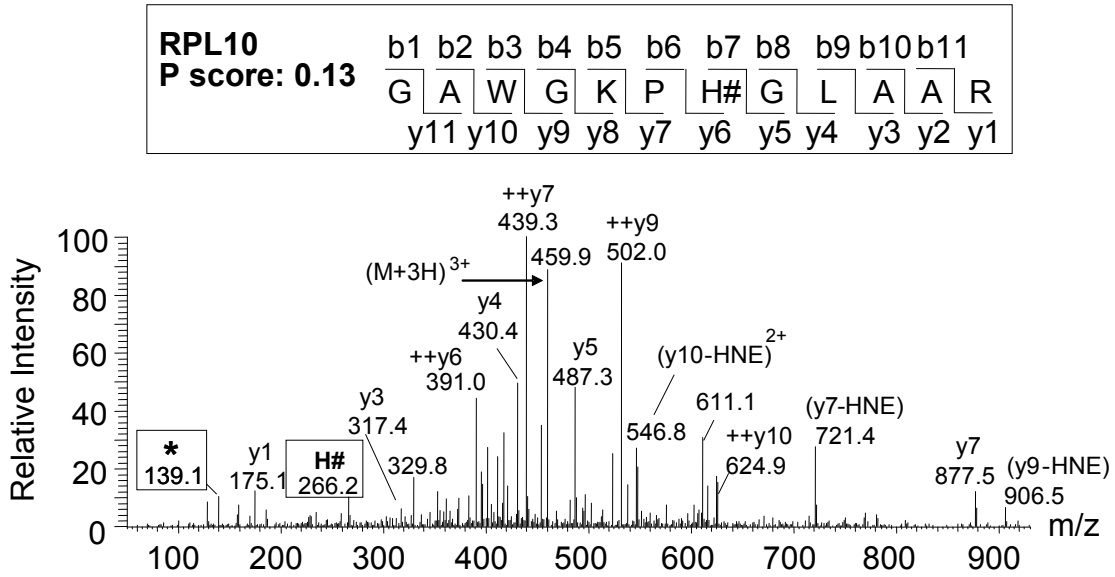

Figure 6. PQD MS/MS spectrum of a HNE-modified histidine peptide with a low P score assignment. The presence of the 139 and 266 m/z diagnostic fragment ions in the spectrum, generated by PQD operating mode, helped confirm its identity and the HNE modification of the peptide, despite its low P score assignment.

Further adding to the dataset of HNE-modified peptides, many additional MS/MS spectra incorrectly matched to unmodified peptides were identified based on the presence of the 266 m/z fragment ion within the spectrum. Most common were peptides mistakenly identified by Sequest as containing an amino-terminal arginine (R) miscleavage, which results in the same mass shift (+156 Da) produced by the addition of HNE to reactive amino acids. As a result, the precursor masses of these peptide sequences are indistinguishable using a linear ion trap. However, in the case of histidine containing peptides, careful examination of the peptide fragmentation pattern of these MS/MS spectra (Figure 7), together with the presence of the 266 m/z diagnostic fragment ion, provided the necessary evidence for identifying novel HNE-modified peptides. Clearly, the reliable identification of histidine adducts via the 266 m/z fragment ion both increases the confidence of, and significantly adds to, the peptide matches within the dataset. In all, the CID and PQD methods described above were used in parallel to provide a comprehensive analysis of multiple replicates of SPH reagent enriched HNE-modified peptides derived from *in-vitro* treatments of yeast lysates. From these experiments, 125 sites of HNE modification spanning 67 different proteins were characterized (Supplemental Table 1). The vast majority of the HNE-modified peptides identified were supported either by the presence of diagnostic fragment ions (139 and/or 266 m/z) or by MS^3 spectrum that resulted from the neutral-loss of HNE. Furthermore, all MS/MS spectra were searched against a chimeric database containing both a forward and reverse sequence database, facilitating the estimation of false positive rates for sequence matches (Peng, Elias et al. 2003). Therefore, all HNE-modified peptides shown in the

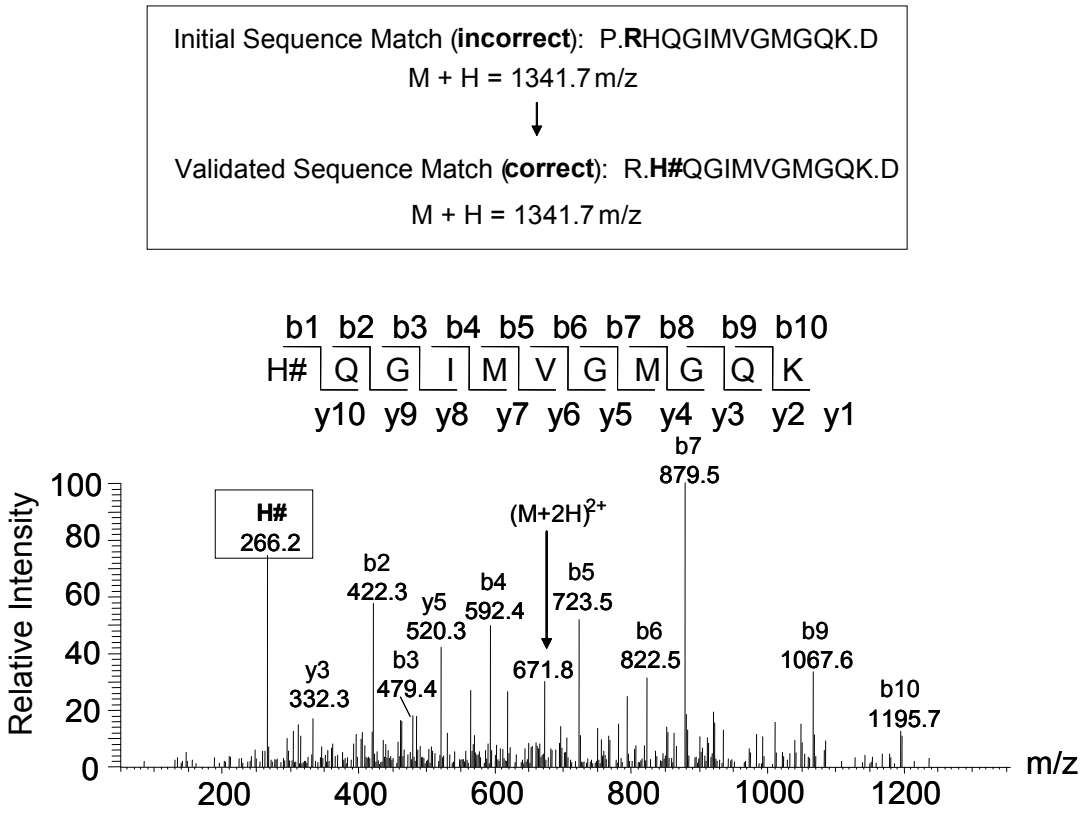

Figure 7. MS/MS spectrum of an incorrectly assigned, miscleaved N-terminal arginine peptide. MS/MS initially matched incorrectly to a miscleaved N-terminal arginine peptide. The prominence of the 266 m/z fragment ion corresponding to the HNE-modified histidine immonium ion helped to confirm the correct match to a HNE-modified histidine containing peptide. The MS/MS spectrum for the HNE-modified peptide match is shown.

Supplementary Table were assigned a Probability score above a threshold which provided for an estimated false-positive rate below 1% (see Experimental Methods for details). Some peptide matches are also included which were assigned Probability scores below the 1% false positive rate threshold; each of these matches was manually validated, using either the indicated HNE diagnostic fragments and/or MS^3 spectrum to aid in the validation process.

SPH enrichment of yeast cultures treated with HNE

While characterizing HNE-modified peptides within yeast lysates treated *ex vivo* with HNE demonstrates the utility of the SPH reagent for mixture analysis, the actual data collected provides limited information on protein susceptibility *in vivo*. Thus, to identify sites of HNE-modification in a system that better resembles endogenous conditions, the SPH enrichment strategy was applied to yeast whole cell extracts isolated from cell cultures that were treated with 250 μm HNE for 2 hours. These treatment conditions followed those described by others in previous fundamental studies on cellular response to HNE using budding yeast as a model organism (Wonisch, Hayn et al. 1997; Wonisch, Kohlwein et al. 1998). While treatment with HNE significantly slowed cell growth compared to control cultures, indicating a profound effect on the cellular machinery, only two HNE-modified peptides, from two separate proteins, were identified with confidence from these experiments (Supplemental Table 1). In successive experiments, we were unable to expand on this dataset, indicating a potential limitation in the sensitivity of the SPH method. Thus, a complementary method for identifying endogenously HNE modified proteins was pursued, as described below.

Complementary use of the SPH reagent and biotin hydrazide-based enrichment of HNE-modified proteins

Given the challenge presented in the detection of HNE-modified peptides derived from HNE treated cell cultures, we pursued a complementary and established biotin-hydrazide labeling strategy for enriching HNE-modified proteins via affinity chromatography (Soreghan, Yang et al. 2003; Yoo and Regnier 2004) in order to characterize these proteins. These studies were conducted with the hypothesis that the biotin hydrazide strategy might provide a complementary catalogue of endogenously HNE-modified proteins from yeast, at least some of which would be in common with proteins identified using the SPH method to identify modification sites from *in vitro* treated proteins as described above. As a negative control, a non-HNE treated yeast lysate was also labeled with the biotin hydrazide reagent and processed similarly to the HNE-modified sample, in order to identify background proteins binding to the avidin column, or proteins containing carbonyl modifications other than HNE. Proteins identified exclusively in the HNE-labeled sample with Peptide Prophet probability scores of 0.9 or above were deemed to be HNE-modified proteins.

As shown in Table 1, 15 proteins identified using the biotin hydrazide strategy also were proteins from which HNE-modified peptides were identified using the SPH strategy on *in vitro* treated yeast lysates. Analysis of the peptides from these proteins indicates that HNE adduct formation at all three of the known amino acid targets (Cys, His, Lys) was

Table I. HNE-modified yeast proteins common to both the biotin-hydrazide analysis of HNE-treated yeast cultures and the SPH reagent enrichment of modified peptides from HNE-treated yeast lysates.

[1] A probability score (P score) for each peptide match was determined by Peptide Prophet (Keller, Nesvizhskii et al. 2002).

[2]NA (not applicable) indicates that the ion was outside the mass range of the standard CID generated spectrum.

# Denotes cysteine (C), histidine (H), or lysine (K) residue modified by HNE.

* Peptides identified by Sequest from MS^3 spectrum.

† Peptides originally identified by Sequest as unmodified peptides containing amino-terminal arginine miscleavage, which, following manual validation, were determined to be HNE-modified based on the presence of 139m/z and 266m/z diagnostic markers. The (#) indicates the HNE-modified amino acid in each sequence as determined from the MS/MS spectrum.

◊ Peptide derived from HNE treated yeast cultures, rather than HNE treated yeast lysates (see text for details).

Gene Name	Protein Name	Modified Peptide(s)	Probability Score [1] (P score)	139m/z Peak? [2]	266m/z Peak? [2]	Neutral Loss? [2]
Protein Folding						
SSA1	Stress-Seventy subfamily A	R.ARFEELC#ADLFR.S	0.03	NA		√
SSB1	Stress-Seventy subfamily B	K.STSGNTH#LGGQDFDTNLLEH#FK.A	0.54	NA	√	√
		K.STSGNTH#LGGQDFDTNLLEHFK.A *	1.00	NA	√	-
		K.STSGNTHLGGQDFDTNLLEH#FK.A	0.60	NA	√	√
Nutrient Metabolism						
CDC19	Pyruvate kinase	K.YRPNC#PIILVTR.C ◊	0.94	√		√
		R.FSH(#)LYR.G †	0.28	√	√	
		R.FSH#LYR.G	0.12	√	√	√
		R.FSHLYR.G *	0.99			-
		R.MNFSH(#)GSYEYHK.S †	0.94	√	√	√
		R.MNFSH#GSYEY.H	0.24	NA	√	
PGK1	3-phosphoglycerate kinase	R.H(#)ELSSLADVYINDAFGTAH#R.A †	0.69	NA	√	√
		L.SSLADVYINDAFGTAH#R.A	0.99	NA	√	
		R.AH(#)SSMVGFDLPQR.A †	0.91		√	
		K.YVLEH#H(#)PR.Y *	0.97			-
		K.YVLEH(#)HPR.Y *	0.96	√	√	-
		Y.VLEH#H(#)PR.Y *	0.25			-
ENO1	Enolase I	K.NVPLYK#HLADLSK.S	0.42		√	
		K.NVPLYKH#L.A	0.73		√	
		R.IGSEVYH#NLK.S	0.41	NA	√	NA
		R.IGSEVYHNLK.S *	0.79			-
		R.SGETEDTFIADLVVGLRTGQIK#TGA.P	0.99	NA	NA	
FBA1	Fructose 1,6-bisphosphate aldolase	F.H#GGSGSTVQEFH#TGIDNGVVK.V	1.00	NA	√	√
		F.H#GGSGSTVQEFHTGIDNGVVK.V *	1.00	NA	√	-
		F.HGGSGSTVQEFH#TGIDNGVVK.V	1.00	NA	√	√
		K.ALH#PISPNF.S	0.82	NA	√	NA
		K.GAIAAAH#YIR.S	0.88	NA	√	√
		K.GAIAAAHYIR.S *	0.94	NA		-
		K.GISNEGQNASIKGAIAAAH#YIR.S	0.78	√	√	
		K.TGVIVGEDVH#NLFTYAK.E	1.00	√	√	
		L.RPEILAEH#QK.Y	0.94	√	√	√
		L.YAGDIALRPEILAEH#QK.Y	0.43	NA	√	√
Protein Synthesis						
RPS1A	Ribosomal Protein of the Small subunit	D.IFPLQNIH#VR.K	0.12	NA		NA
		F.H#GMDFTTDKLR.S	0.50	NA	√	NA
		K.DIFPLQNIH#VR.K	0.97	NA	√	√
		K.DIFPLQNIHVR.K *	0.63	NA		-
		K.FDVGALMALH#GEGSGEEK.G	1.00	NA	NA	NA
		K.RHSYAQSSH#IR.A	1.00	NA	√	NA
		R.H(#)SYAQSSH#IR.A †	0.99	√	√	√
		R.HSYAQSSH#IR.A	0.96	√	√	
RPS12	Ribosomal Protein of the Small subunit	R.TALVH#DGLAR.G	0.99	NA	√	√
RPL3	Ribosomal Protein of the Large subunit	K.GH#GFEGVTH#R.W	1.00	√	√	
		K.GH#GFEGVTHR.W *	0.91	√		-
		K.GHGFEGVTH(#)R.W *	0.34			-
		K.H#AFMGTLK.K	0.95	NA	√	
		R.H#GHLGFLPR.K †	1.00	√	√	
		R.HGHLGFLPR.K *	0.58			-
RPL4A	Ribosomal Protein of the Large subunit	K.VGYTLPSH#IISTSDVTR.I	1.00		√	√
RPL17B	Ribosomal Protein of the Large subunit	K.LYVSH#IQVNQAPK.Q	1.00		√	
		K.YLDQVLDHQR.A *	0.19			-
TEF2	Translational elongation factor EF-1 alpha	K.SH#INVVVIGHVDSGK.S	0.91	√	√	√
		K.SHINVVVIGH#VDSGK.S	0.46	NA	√	√
		K.STTTGH#LIY.K	0.44	NA	√	NA
		K.SVEMH#HEQLEQGVPGDNVGFNVK.N	0.85	√	√	
		V.VVIGH#VDSGK.S	0.92	NA	√	√
KAP123	Karyopherin beta	K.H#WNAIDESTR.A	0.70	NA	√	NA
Other						
PMA1	Plasma membrane H+-ATPase	E.NADGFAEVFPQH#K.Y	0.12	NA	√	NA
		K.TVEEDH#PIPEDVH#ENYENK.V	0.69	NA		NA
		K.VLEFH#PFDPVSK.K	0.50	NA	√	NA
ALD6	Cytosolic aldehyde dehydrogenase	A.HLVFDDANIKK.T *	0.95			-

detected, with modification of histidine residues predominating. These results suggest that the large-scale *in vitro* analysis of detected, with modification of histidine residues predominating. These results suggest that the large-scale *in vitro* analysis of HNE-modified complex mixtures by the SPH reagent may provide important information regarding the sites of modification within endogenous targets of HNE modification. Clearly, these findings demonstrate the utility of using the SPH and biotin hydrazide strategies in a complementary manner.

Discussion

Detecting and characterizing peptides carrying post-translational modifications from within complex mixtures often requires the implementation of front-end enrichment strategies (Roe and Griffin 2006). Here we describe a novel solid-phase approach based on hydrazide chemistry for the enrichment of peptides modified by the lipid peroxidation product HNE. Characterization of modified peptides was further improved by implementing advanced instrumental methodologies on the back-end that maximize the utilization of diagnostic MS/MS fragment ions of HNE-modified peptides. When applied to yeast cell lysates treated with excess levels of HNE, this overall strategy enabled the mapping of 125 sites of modification from 67different proteins. Manual inspection of the data, guided by the generation of MS^3 spectra and the presence of the diagnostic fragment ions of HNE-modified peptides (139 m/z and 266 m/z), led to the validation of many modified peptides matching with low probability scores, and to the identification of false negative sequence matches and incorrectly matched sequences (i.e. N-terminal arginine miscleavages). Forty-three of these sites were mapped to peptides derived from proteins

which were also enriched and identified via biotin hydrazide labeling and avidin chromatographic selection of yeast cell cultures treated with HNE. This suggests that the SPH strategy for enriching HNE-modified peptides can be used complementary to protein enrichment strategies for generating data on susceptible sites of HNE modification with potential endogenous relevance.

The SPH approach is one of the first described capable of enriching and identifying HNE-modified peptides from within complex mixtures on a proteome-wide scale, and has several advantages as an analytical strategy. These include: 1) Direct capture, release and restoration of aldehyde groups on modified peptides. As such, this approach does not add extra molecular tags to the aldehyde group (e.g. biotin and carbon linkers (Mirzaei and Regnier 2005; Lee, Young et al. 2006; Mirzaei and Regnier 2006)), which may complicate the MS/MS fragmentation and interpretation of results; 2) The ability to scale up the enrichment step for the analysis of milligram amounts of starting protein, enabling the enrichment and detection of lower abundance HNE-modified peptides. This is in contrast to gel based strategies which are limited in amounts of starting material (Conrad, Choi et al. 2001; Fenaille, Tabet et al. 2004); 3) Facile and cost-effective synthesis of the SPH reagent using a controlled pore glass support, which is compatible with washing and elution conditions using organic solvents and extremes of pH and heat.

In terms of limitations, the handling steps (e.g. tryptic digestion and peptide purification) involved in processing the HNE-modified proteins prior to their reaction with the SPH

beads increases the potential for highly reactive aldehyde to cross react with nucleophilic groups (e.g. primary amines) on other peptides. Such cross reactions would effectively block these modified peptides from enrichment and limit the ability to detect many modified peptides. This may have contributed to our inability to reliably identify larger numbers of modified peptides from the HNE treated cell cultures. As such, others have suggested (Mirzaei and Regnier 2005) that the most effective approach to enriching carbonyl modified proteins is to introduce hydrazide labeling reagents early on in the processing steps, in order to react with these groups on the intact proteins, prior to tryptic digestion. Although this is a reasonable precaution to consider, our studies with HNE-modified peptides indicate that this cross-reactivity is fairly limited. In control studies incubating the HNE-modified anaphylatoxin standard peptide with reactive amine compounds at neutral and basic pH, little or no reactivity was observed (data not shown). This may be because of the propensity of HNE to form a hemiacetal at these pH values, effectively minimizing the reactivity of the aldehyde group. Furthermore, other than the tryptic digestion step, all handling steps as well as the incubation with the SPH reagent were performed at acidic pH levels (< 4), which not only favors the reaction of aldehydes with hydrazide groups, but should also minimize the reactivity of primary amines found in other proteins or peptides.

To our knowledge, our use of the SPH enrichment strategy, together with the instrumental methods described above, has provided one of the most comprehensive catalogues of susceptible sites of HNE modification from a complex protein mixture to

date. This proteomic-scale dataset provides important new insights into protein susceptibility to modification by HNE. For example, a strong preference for the formation of histidine versus cysteine HNE adducts is observed. Although incongruent with the order of reactivity reported for these residues by Esterbauer and colleagues (Esterbauer, Schaur et al. 1991), this tendency toward histidine adduct formation reinforces previous observations made wherein histidine residues out competed intramolecular (Fenaille, Parisod et al. 2005) and intermolecular cysteines (Orioli, Aldini et al. 2005) for reaction with HNE. Results from initial optimization experiments indicated that hydrazide is equally reactive to HNE adducts on histidine and cysteine, and that these adducts are both equally stable to acid elution from the SPH beads, precluding these as reasons for our preferred detection of histidine peptides. While the above observation may be explained simply by the higher frequency of histidine amino acids across the proteome compared to cysteine, further investigation is required to define why histidines are preferentially detected as sites of HNE modification.

The acquisition of a large dataset of HNE modification sites enables a variety of follow-up analyses on protein susceptibility to this modification, including the discovery of potentially conserved sequence motifs susceptible to HNE adduct formation. In order to investigate this possibility, we used the publicly available TEIRESIAS Pattern Discovery Tool (Rigoutsos and Floratos 1998) and compared our set of identified histidine modified peptide sequences (total of 121) to a control set of peptide sequences. These control sequences were histidine containing tryptic peptides (also 121 different sequences in

total) identified in a separate MS/MS analysis of a non-HNE modified yeast lysate. Based on this pattern analysis, we found the HNE-modified sequences in the dataset showed a 1.5 fold increase in the number of basic residues (K, R) positioned within 4 residues of modified histidine, compared to the control dataset. The local chemistry imparted by basic residues on neighboring histidines would likely involve the removal of the immidazole hydrogen, effectively lowering the pKa of the histidine residue and increasing its nucleophilic attraction to HNE. This may also partly explain the prominence of highly basic ribosomal proteins identified in our study as being susceptible to histidine modification by HNE. Consistent with the notion that these charged residues typically localize to solvent exposed surfaces within protein structures, greater than 85% of the modified sites mapped in the yeast lysate dataset are solvent exposed, with an average accessible surface area (ASA) of 45 $Å^2$, as predicted by the NETASA algorithm (Ahmad and Gromiha 2002). This observation is in keeping with the described tendency of HNE to modify solvent exposed residues in studies conducted on single proteins (Alderton, Faustman et al. 2003; Ishii, Tatsuda et al. 2003; Isom, Barnes et al. 2004). Although a relatively simple analysis of this data is presented here, these results do demonstrate the utility of the large-scale data obtained using the SPH reagent in identifying potential conserved amino acid sequences and protein structural features with propensity to HNE modification, leading to the possibility of predicting protein susceptibility to these modifications.

To conclude, we have developed a strategy that takes a significant step towards the goal of proteome-wide analysis of amino acid sites susceptible to HNE modification by combining a novel chemical enrichment strategy with instrumental methods tailored to characterizing HNE-modified peptides. The SPH strategy can be used in parallel with complementary enrichment strategies capable of isolating HNE-modified proteins, such as biotin-hydrazide labeling and avidin enrichment, to identify susceptible endogenous targets of HNE modification. Finally, the general hydrazide chemistry central to the SPH enrichment strategy suggests that it should be applicable to other commonly known carbonyl modifications to proteins, such as those resulting from metal catalyzed oxidation of amino acid side chains (Mirzaei and Regnier 2005; Mirzaei and Regnier 2006).

Chapter 3

Targeted ^{18}O-labeling of HNE-modified peptides for improved detection by mass spectrometry

The data in this chapter has been submitted the Journal of The American Society for Mass Spectrometry for publication.

Summary

Protein carbonylation refers to the covalent modification of proteins with reactive aldehyde- or ketone-containing molecules, and is a classic marker of oxidative stress correlating well with aging and age-associated diseases, presumably due to its deleterious effect on protein function. Current practice for mass spectrometry-based proteomic identification of protein amino acid sites susceptible to carbonylation combines the following steps: proteolytic digestion, enrichment of modified peptides, generation of high quality peptide fragmentation data by tandem mass spectrometry (MS2), and sequence identification via sequence database searching. Despite incremental improvements in this general practice, reliable proteomic identification of carbonylated peptides remains a challenge in need of new, enabling tools. To this end, we developed a method which complements the current practice, capable of detecting carbonylated peptides via mass spectrometry without reliance on confident matching of modified peptide fragmentation spectra to a sequence database. The basis of our method is the partial incorporation of ^{18}O into reactive carbonyls to produce an observable mass defect, resulting in a unique isotope signature specific to modified peptides, observed both in MS and MS2 spectra. Our method is composed of carefully optimized measures integral to its success, designed to eliminate protease-catalyzed incorporation of ^{18}O into the carboxy-termini of peptides, and stabilize the incorporated ^{18}O molecule, which not only preserves the ratio of ^{16}O:^{18}O in carbonylated peptides, but also ensures compatibility with online liquid chromatography electrospray mass spectrometry analysis. We

demonstrate the value of ^{18}O isotope signatures detected in both MS and MS2 spectra for confirming the presence and the amino acid position of 4-hydroxynonenal (HNE) modifications in HNE-treated myoglobin, and in enriched HNE-modified peptides from a HNE-treated rat skeletal muscle homogenate. In addition to confirming correct database sequence matches, our results further demonstrate the utility of the ^{18}O-labeling method for identifying carbonylated peptides missed by the database search, information that ultimately provides a novel means for evaluating the efficiency by which HNE-modified peptides are identified via MS2 and sequence database searching. Also, to automatically detect spectra produced by ^{18}O-labeled, carbonylated peptides, we developed novel software that uses stringent mass accuracy and relative isotopologue abundance criteria to interrogate raw mzXML-formatted mass chromatogram data for candidate ^{18}O-labeled, carbonylated peptides. In sum, our method and software provide valuable new tools for investigators endeavoring to study protein carbonylation from complex biological mixtures via mass spectrometry-based proteomics.

Introduction

The post-translational introduction of reactive ketone and aldehyde moieties into proteins, known as protein carbonylation, is a classic marker of oxidative stress that correlates well with both the aging process itself as well as various age-associated diseases, ranging from Alzheimer's and Parkinson's disease to amyotrophic lateral sclerosis and diabetes (Dalle-Donne, Giustarini et al. 2003). While a definitive role in disease etiology has yet to be established, the deleterious effect carbonylation has on protein function provides a putative biochemical mechanism through which this irreversible modification may contribute towards the initiation and propagation of disease (Grimsrud, Xie et al. 2008). In order to further characterize the basic biology of protein carbonylation and thus better define its potential pathologic role, the specific proteins and amino acids carbonylated throughout disease progression need to be identified (Grimsrud, Xie et al. 2008).

Characterizing protein carbonylation on a proteome-wide scale is a core objective in the emerging field of redox proteomics, which seeks to characterize proteins susceptible to oxidative or nitrosative modifications (Dalle-Donne, Scaloni et al. 2005). Tandem mass spectrometry (MS2)-based proteomics enables both the identification of carbonylated proteins and the localization of the corresponding carbonyl to a specific residue, thus providing a powerful tool in redox proteomics. However, such studies for protein carbonylation are not routine, as several challenges complicate the process. One challenge is due to the complexity of carbonyl modifications, which involves a number of

mechanisms generating various chemically unique reactive carbonyls of differing masses that target several amino acids. For example, carbonyls may be directly introduced into the sidechains of Lys, Arg, Pro, and Thr via metal catalyzed oxidation, and into the sidechain of Glu and the N-termini of peptides via α-amidation of the protein backbone (Berlett and Stadtman 1997; Requena, Chao et al. 2001).

By comparison, reactive carbonyls generated as secondary products of protein glycation and ROS mediated lipid peroxidation, the most common of these being 4-hydorxynonenal (HNE), target the sidechains of Lys and Arg, and Cys, His, Lys, and Arg, respectively (Monnier 1990; Sies 1991; Chevion, Berenshtein et al. 2000). Importantly, most of these reactive carbonyl moieties (in the form of aldehydes or to a lesser extent ketones) retain their reactivity following conjugation, independent of the mechanism by which they were introduced, save those adducts formed by Schiff-base reactions with Lys.

Another challenge lies in the relatively low abundance of carbonylated proteins within complex biological mixtures. To address this challenge, front-end enrichment methods that target this substochiometric protein population have been developed. The primary strategy used for capturing carbonylated proteins relies on covalent chemistry-based enrichment methods exploiting the reactivity of hydrazides with reactive carbonyls, enabling the global analysis of carbonylated proteomes (Grimsrud, Xie et al. 2008).

One common approach is to enrich carbonylated proteins labeled with reagents such as biotin-hydrazide, or variations there-of, via avidin-affinity chromatography prior to their identification by mass spectrometry. This approach has proven useful for characterizing the carbonyl proteomes of various mammalian-derived protein lysates generated from plasma (Mirzaei, Baena et al. 2008), tissue homogenates (Soreghan, Yang et al. 2003; Mirzaei and Regnier 2005; Grimsrud, Picklo et al. 2007), mitochondrial extracts (Meany, Xie et al. 2007), and tissue-derived cell lines (Thomas, Soreghan et al. 2005; Codreanu, Zhang et al. 2009). An important caveat regarding the biotin-hydrazide approach is that carbonylation of the proteins identified is inferred based on their enrichment by avidin alone, as the specific carbonylated residue is very rarely determined due to signal suppression from the remaining non-carbonylated peptides in the sample. Also, biotin-hydrazide itself readily fragments into a number of abundant ions which can also preclude identification of biotin-hydrazide labeled peptides (Yi, Li et al. 2005).

Efforts to unequivocally identify sites of carbonylation to specific residues have thus relied on methods for enriching carbonylated peptides, followed by MS2 analysis and matching to peptide sequences via automated sequence database searching. One promising approach, involving the avidin-affinity enrichment of biotinylated peptides rather than labeled proteins, has been used to successfully localize sites of carbonylation within both simple and complex protein mixtures (Chavez, Wu et al. 2006; Han, Stevens et al. 2007) . However, biotin labels are known to hamper sequence identification by

complicating MS2 fragmentation patterns and by increasing peptide hydrophobicity (Yi, Li et al. 2005).

As an alternative to label-based approaches, we developed a solid-phase hydrazide (SPH) reagent that directly and reversibly captures carbonylated peptides via formation of Schiff-base bonds (Roe, Xie et al. 2007), and demonstrated its utility on a complex mixture of HNE-modified proteins. Importantly, captured peptides are reversed-off the reagent by hydrolyzing the Schiff-base, and are thus restored to their native forms as the carbonyl is replenished. While this label-free method produced MS2 spectra free of fragment ions derived from a biotinylating reagent which may confound identifications, we observed that many spectra, for unknown reasons, still did not confidently match to HNE-modified peptide sequences. Based on these observations, new methods to assist in the detection and identification of modified peptides are needed.

Here we have sought to develop a method by which enriched, carbonylated peptides could be unambiguously detected by mass spectrometry, without a dependence on successfully matching their MS2 spectra to sequences via database searching. Such a method would have potential value in: confirming carbonylated peptides that are matched via database searching; differentiating enriched, carbonylated peptides from non-carbonylated background peptides, which could then be targeted for MS2 analysis; and evaluating the efficiency by which these peptides are identified by MS2. Taking advantage of the non-enzymatic solvent-exchangeable properties of reactive carbonyl

oxygen molecules, our method is based on the partial incorporation of ^{18}O into carbonylated peptides so as to introduce a mass defect that results in a unique isotope signature readily detected in their MS and/or MS2 spectra. Using both HNE-modified myoglobin as a standard, and a HNE-modified complex protein mixture derived from rat skeletal muscle, we have developed an optimized protocol for the specific and stable incorporation of ^{18}O into reactive carbonyls that complements label-free enrichment methods and improves the detection of carbonylated peptides. Our results demonstrate the value of this method for confirming putatively HNE-modified peptide sequences identified from MS2 spectra, decreasing false negative identifications of such sequences, and providing a novel means to assess the efficiency of the identification of these peptides via MS2 and sequence database searching. As such, our method provides a valuable new tool for investigators endeavoring to study protein carbonylation via mass spectrometry-based proteomics.

Materials and Methods

Preparation of ^{18}O-labeled HNE-Modified Myoglobin Digest

Five-hundred micrograms of myoglobin from horse heart (Sigma) was treated with 2mM 4-hydroxynonenal (HNE, Cayman Chemical) for two-hours at 37°C in 100mM sodium phosphate, pH 7.2. The modified sample was filter centrifuged using an Amicon Ultra spin column with a 10kD cutoff (Millipore) to remove excess HNE, and the resulting retentate was reconstituted in 100mM sodium phosphate, pH 7.2. After measuring the protein concentration by the BCA assay (Pierce), the entire HNE-modified myoglobin

sample was trypsinized overnight (1:50 protease-to-substrate) and subsequently stored at -20□C for future experiments.

^{18}O-labeling of HNE-peptides

The following protocol for labeling HNE-modified peptides with ^{18}O was applied to a 2ug aliquot from the HNE-modified myoglobin digest and to the enriched peptide fraction from the HNE-modified rat skeletal muscle tissue lysate. Lyophilized samples were reconstituted in 100ul of ^{18}O-labeling buffer (70% v/v of 97% $H_2{}^{18}O$ (Sigma), 100mM sodium phosphate, pH 7.2) and then incubated at room temperature for 2 hours. Next, a small volume of concentrated sodium hydroxide was added to adjust the sample pH to about 8, followed by the addition of alkaline sodium borohydride to a final concentration of 10mM. After incubating at room temperature for an additional hour, the samples were desalted by C18 Ziptips and the resulting eluates vacuum centrifuged to dryness. To back-exchange any ^{18}O molecules incorporated into peptide carboxylates during labeling, each sample was reconstituted in 100ul $H_2{}^{16}O$ supplemented with 1ug Trypsin, incubated at room temperature for 24 hours, vacuum centrifuged to dryness, and stored at -20□C.

Comparing Methods for Eliminating the Oxygen-exchange Activity of Trypsin

One-hundred micrograms of the HNE-modified myoglobin digest was spiked with 2 additional micrograms of trypsin and divided into 20ug aliquots, with each subjected to a different method for depleting the oxygen-exchange activity of trypsin. One 20ug aliquot was diluted to 1mL with water and filter centrifuged using an Amicon Ultra filtered spin column (10 kD cutoff) per manufacturer's specifications. Following a single pass

through the spin column, the peptides in the flow-through fraction were vacuum centrifuged to dryness and ^{18}O-labeled according to the protocol described above. A second aliquot was vacuum centrifuged to dryness and subsequently reconstituted in alkaline ^{18}O-labeling buffer (supplemented with 100mM sodium hydroxide, pH >12). The sample was then reduced and processed for analysis according to the ^{18}O-labeling protocol described above. A third aliquot was boiled for 15 minutes prior to labeling with ^{18}O so as to denature the trypsin and thus inactivate its activity. Seventy microliters of $H_2{}^{18}O$ and 10ul 1M sodium phosphate, pH 7.2, was then directly added to the boiled sample so as to establish ^{18}O-labeling conditions consistent with those used for the other methods. Again, the sample was reduced and analyzed according to the ^{18}O-labeling protocol described above. Still a fourth aliquot was ^{18}O-labeled according to the protocol described above without concern for ^{18}O incorporation into the c-terminus of peptides by trypsin-catalyzed oxygen exchange. The reduced, ^{18}O-labeled sample was then desalted by C18 Ziptip and the eluate vacuum centrifuged to dryness. The dried sample was subsequently reconstituted with 100ul of 100% $H_2{}^{16}O$ supplemented with 2ug trypsin, incubated overnight at room temperature, and vacuum centrifuged to dryness. All ^{18}O-labeled peptides from each aliquot were were analyzed according to the MALDI-TOF protocol described herein.

Preparation of HNE-treated Lysate from Rat Skeletal Muscle Tissue

Skeletal muscle tissue containing both type I (slow-twitch) and type II (fast-twitch) muscle fibers was isolated from the hind limb muscles of young adult Fisher 344 rats (12 months old). One-and-half grams of muscle tissue was then minced with scissors and

washed thrice with ice-cold 1X PBS (Sigma) by pelleting the tissue each time at 200g. The final tissue pellet was reconstituted in Tissue Lysis Buffer (1:10 w/v, 150mM sodium chloride, 50mM Tris-HCl pH 7.4, 1mM ethylenediaminetetraacetic acid, 1% Triton X-100, 1% deoxycholic acid, 0.1% sodiumdodecylsulfate, and 1X Protease Inhibitor cocktail (Roche)) and vortexed vigorously for 20 seconds. Next, the tissue was homogenized using a PowerGen tissue homogenizer on the lowest setting with two 20 second mixes. The cellular debris was then pelleted by centrifuging the sample at 700g for 10 minutes at 4°C. The supernatant was carefully removed and the proteins extracted by methanol-chloroform precipitation as previously described (Meany, Xie et al. 2007). The resulting delipidated protein pellet was reconstituted in 100mM sodium phosphate, pH 7.2, containing 0.1% SDS and quantified by the BCA assay. HNE-modified proteins were then generated by incubating 3mg of the tissue lysate with 250uM HNE for two hours at 37°C. Excess HNE was subsequently removed by filter centrifugation using an Amicon Ultra spin column (10kD cutoff) per manufacturer's instruction. The retentate was diluted to 2mL with trypsin friendly buffer (100mM sodium phosphate pH 7.2, 5 mM TCEP, 10% acetonitrile) and then digested overnight following the addition of 60ug of trypsin.

Enrichment of HNE-modified peptides from HNE-treated Rat Skeletal Muscle Tissue Lysate

Carbonylated peptides within the HNE-treated tissue lysate digest were enriched using UltraLink Hydrazide Gel (Pierce), a commercially available solid-phase hydrazide reagent that is traditionally used for building antibody affinity columns. Briefly, 500 ul

of Hydrazide Gel slurry was washed with water in a 1.5ml eppendorf tube by vortexing vigorously. The resin was then pelleted by bench-top microcentrifugation, resuspended with 500ul of the sample digest buffer (100mM sodium phosphate, pH 7.2), combined with the sample digest, and mixed overnight on an Eppendorf Thermomixer R tube shaker (1200RPM, 25°C). After spinning down the resin, the non-bound peptides in the supernatant were removed and saved for future analysis. The remaining resin pellet was washed four times each with 1mL of 1% SDS, 1M NaCl, 80% acetonitrile, and distilled water by vigorous vortexing (20 s) and benchtop microcentrifugation in succession. To release the hydrazide-bound peptides 1mL of 1% acetic acid was added to the washed resin and the mixture was incubated for two hours on an Eppendorf Thermomixer R tube shaker (1200RPM, 25°C). Importantly, 1% acetic acid proved optimal for releasing UltraLink Hydrazide bound peptides while minimizing the resin-derived contaminates generated by stronger acidic conditions. After spinning down the resin the enriched peptides present in the supernatant were collected and the resin was washed one time with and additional 300ul of distilled water. The wash supernatant was added to the released peptides and the combined solution was vacuum centrifuged to dryness.

MALDI-TOF MS/MS

The lyophilized ^{18}O-labeled HNE-treated myoglobin digests were reconstituted with 1.5ul of MALDI sample buffer (80% Acetonitrile, 0.1% Trifluoroaceticacid), mixed with α-cyano-4-hydroxycinnamic acid matrix, and spotted on a MALDI plate. Both full-scan and MS/MS spectra were collected in the positive ion detection mode on a Qstar XL quadrapole-TOF mass spectrometer fitted with a MALDI ion source (Applied Biosystems

Inc., Foster City, CA). Spectra were generated using the instrument parameters previously described (Roe, Xie et al. 2007).

LC-MS/MS

Enriched peptides from the HNE-treated rat skeletal muscle tissue lysate were reconstituted in 5ul of sample buffer (2% ACN, 0.1% formic acid, aqueous) and fractionated by microcapillary liquid chromatography (μLC) using Ekisigent's nanoLC - 1D plus HPLC. Specifically, peptides were fractionated by reverse-phase using an in-line analytical capillary column (100um x 13cm) packed in-house with Magic C18 resin (5um, 200 Å Magic C18AG, Michrom BioResource, Auburn CA). A linear gradient of 2-40% buffer B (80% ACN, 0.1% formic acid, aqueous) at a flow rate of 250nL/min. over 60 minutes was used to elute peptides directly into a Finnigan linear ion trap mass spectrometer equipped with an orbital trap mass analyzer (LTQ-orbitrap, Thermo Electron Corp., San Jose, CA.). A top-5 data-dependent method incorporating a 30 second dynamic exclusion window was used to continuously select the top five most abundant precursor-ions in the orbitrap (AGC target; 1 x 10^6 ions, resolution; 60,000, maximum ion accumulation time; 500ms, minimum threshold intensity; 1000) for MS/MS fragmentation in the linear ion trap (AGC target; 1 x 10^4, maximum ion accumulation time; 100ms, normalized collision energy; 35, precursor isolation width; 2m/z, microscan per spectrum; 1). Ions carrying either singly or unassigned charges were excluded from MS/MS fragmentation.

Database Searching and Data Analysis

All MS2 data files extracted from the RAW file for the HNE-modified rat skeletal muscle sample were searched using the Sequest algorithm (Version 27, Revision 12) against a concatenated *R. norvegicus* database (Refseq), containing a composite 77763 protein sequences. A number of variable modifications were specified in the search parameters including the oxidation of methionine (+15.994915), the addition of ^{18}O-labeled and reduced HNE (+160.134924) to cysteine, histidine, and lysine residues, and the incorporation of one ^{18}O molecule into the peptide c-terminus (+2.004244). Mass tolerances of 0.8 amu and 1.0 amu were used for the precursor and fragment ions, respectively, and a partially tryptic constraint was applied. A statistical measure of confidence was assigned for all prospective database matches via the Peptide Prophet scoring algorithm, and the resulting data was evaluated and organized using Scaffold (version 2_02_03, Proteome Software, Portland, Oregon, USA). To obtain a high confidence dataset, an 8ppm mass accuracy constraint was applied to the subset of spectra matching to carbonylated peptides, which resulted in zero hits to the reverse database. This dataset was subsequently used to compare against the number of spectra containing ^{18}O isotope signatures as detected by our software.

To systematically identify candidate ^{18}O fragment patterns, a Python (2.5.2 version) program was written and run against the collected data files. The program, findIsoptopePatterns.py, takes as input an mzXML file and outputs a tab delimited file listing candidate MS and MSMS scans. First, the program identifies MS scans that have produced one or more MSMS scans. Then, for each precursor value in the MS scan, the program looks for an mz value that is a fixed AMU difference below the precursor's mz.

In addition, the program checks that the intensity value is a fixed percentage of the precursor's intensity. Second, the program examines the MSMS peak list identifying ^{18}O 4-tuples. Peaks in the 4-tuple must be separated by a set AMU distance. This distance, and tolerance, can be set as a program parameter. The intensities for each of the 4-tuple peaks is normalized to the third peak's intensity value. To be considered a legitimate candidate pattern, the first peak's intensity must be within a minimum and maximum percentage of the third peak. These threshold values are modifiable parameters. The program counts and reports the number of candidate fragment patterns for each MSMS scan as well as the MS pattern discovered in the first step.

Results

Targeted ^{18}O-labeling of protein carbonyls

Our method is based on the partial incorporation of ^{18}O into the oxygen of reactive carbonyls via non-enzymatic oxygen-exchange (Figure 1A). A mass defect specific to carbonylated peptides is introduced by incubating peptide mixtures in a neutral buffer containing 70% $H_2{}^{18}O$, resulting in a 2:1 ^{18}O:^{16}O ratio within the reactive carbonyl. Importantly, this ratio is preserved by subsequently reducing the carbonylated peptides with 10mM sodium borohydride. Once reduced the carbonylated peptides are amenable for additional LC-based fractionations without concern of further back-exchange with aqueous solvents, a limitation of past attempts to use ^{18}O-labeling of carbonylated peptides (Sun and Anderson 2005).

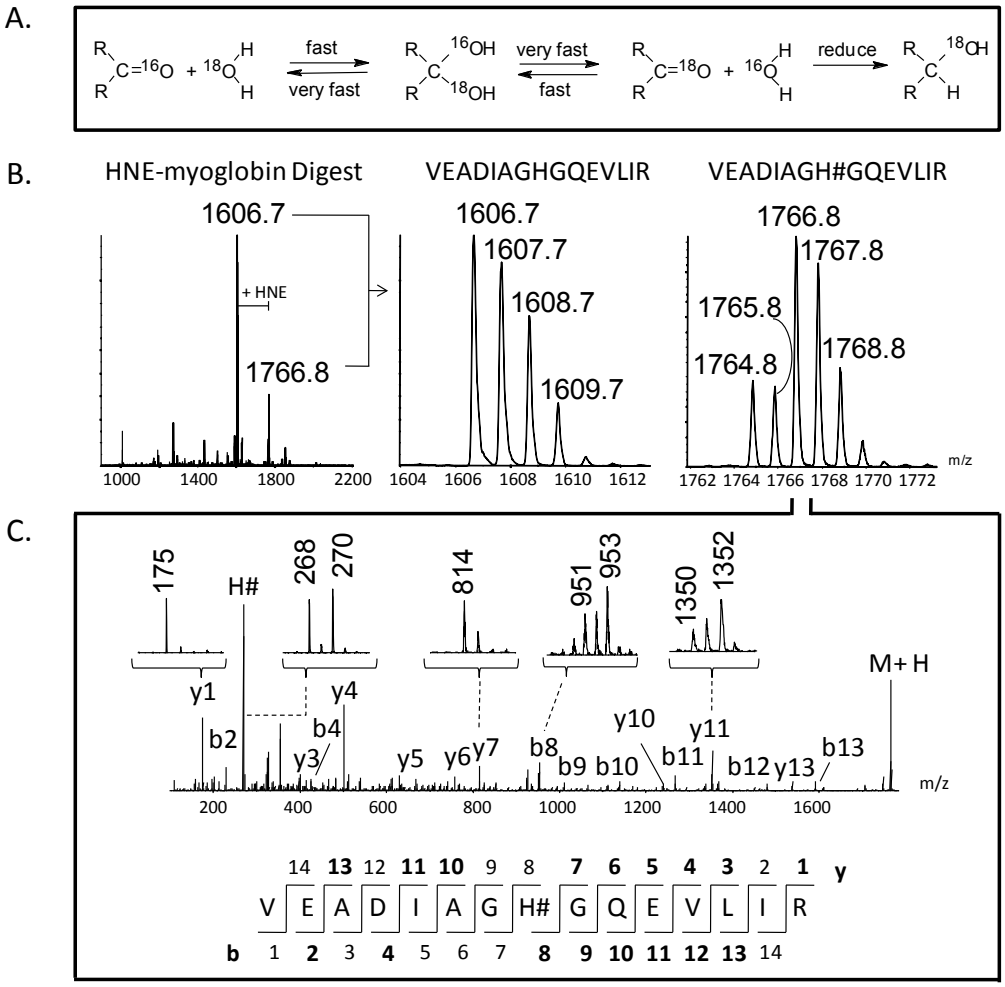

Figure 1. Targeted labeling of carbonylated peptides by non-enzymatic, stable incorporation of ^{18}O. (A) Reaction mechanism for the non-enzymatic incorporation of ^{18}O into carbonyl oxygens. Water supplemented with ^{18}O reacts with carbonyls to form an intermediate diol which undergoes condensation. The resulting ^{18}O-labeled carbonyl is reduced to trap the ^{18}O in an alcohol moiety. (B) MS spectrum of HNE-modified myoglobin digest labeled with 70% ^{18}O, focusing on the isotope envelopes from the non-modified and HNE-modified (#) versions of a single peptide. (C) MS2 spectrum of ^{18}O-labeled (70%) HNE-modified peptide (1766.8m/z), focusing on the isotope envelopes of select fragment ions that demonstrate the utility of 70% ^{18}O-labeling for tracking the HNE-modification. All b and y fragment ions observed are shown in bold in the peptide map below the spectrum. H# designates the HNE-modified immonium ion of histidine.

To demonstrate the effectiveness of our ^{18}O-labeling procedure, a digest of HNE-modified myoglobin was incubated in 70% $H_2{}^{18}O$ for 2 hours followed by reduction in 10mM sodium borohydride for an additional hour. The resulting MS spectrum for the entire digest, together with the magnified isotope envelopes for the non-modified and HNE-modified forms of the peptide VEADIAGHGQEVLIR are presented in Figure 1B. The specific partial incorporation of ^{18}O into the HNE-modified form of the peptide produced a unique isotope signature, characterized by a +2 amu isotopologue that measured about twice the intensity of the monoisotopic ion, making it readily distinguishable from the non-modified form (Figure 1B). Conveniently, this isotope signature was retained in the MS2 spectrum for fragments that carry the carbonyl modification, and thus provides a tool for validating database search results (Figure 1C). Specifically, both the presence of a carbonyl modification and the exact residue to which the carbonyl is localized can be determined. This concept is demonstrated in the MS2 spectrum generated by the aforementioned HNE-modified peptide where fragments from the non-modified portion of the peptide (e.g. y1 and y7) show normal isotope signatures, while those from HNE-modified fragments (e.g. y11 and the histidine immonium ion) show the distinctive ^{18}O isotope signature (Figure 1C, insets).

Eliminating trypsin-catalyzed ^{18}O exchange

Although the proof-of-principle results in Figure 1 are encouraging, a significant potential problem exists. This problem results from the well-described protease-catalyzed exchange of carboxy oxygens from the c-termini of peptides with those from the solvent(Schnolzer, Jedrzejewski et al. 1996). Although useful for global quantitative

proteomic studies (Yao, Freas et al. 2001; Heller, Mattou et al. 2003), for our purposes the potential partial incorporation of ^{18}O into the carboxy terminus of all peptides would result in all peptides showing a mass defect, and hamper our attempts to limit such defects specifically to peptides carrying reactive carbonyl modifications. To address this issue we compared the efficacy of several measures (Hajkova, Rao et al. 2006; Sevinsky, Brown et al. 2007; Petritis, Qian et al. 2009) to eliminate the oxygen-exchange activity of trypsin within a digest of HNE-modified myoglobin, using ^{18}O incorporation as the readout. More specifically, ^{18}O labeled c-termini were detected by the presence of 1 or more, or 2 or more ^{18}O isotopologues in the MS spectra for the non-modified and HNE-modified peptides, respectively. Figure 2 shows results from these comparisons, focusing on a single myoglobin peptide detected both in its non-modified, and HNE-modified form.

In the absence of any measures to inactivate trypsin, the c-termini of both non-modified and HNE-modified peptides were labeled with multiple ^{18}O molecules such that the isotope signatures remained indistinguishable (Figure 2A). Efforts to physically remove trypsin by ultrafiltration almost completely abolished the incorporation of ^{18}O into peptide c-termini (Figure 2B), and while promising, concerns about the reliability and possible sample loss of ultrafiltration devices have been documented (Sevinsky, Brown et al. 2007; Petritis, Qian et al. 2009). Alternatively, Hajkova and colleagues recently characterized the pH dependency observed for the oxygen-exchange activity of trypsin and found a substantial loss of function at more basic conditions

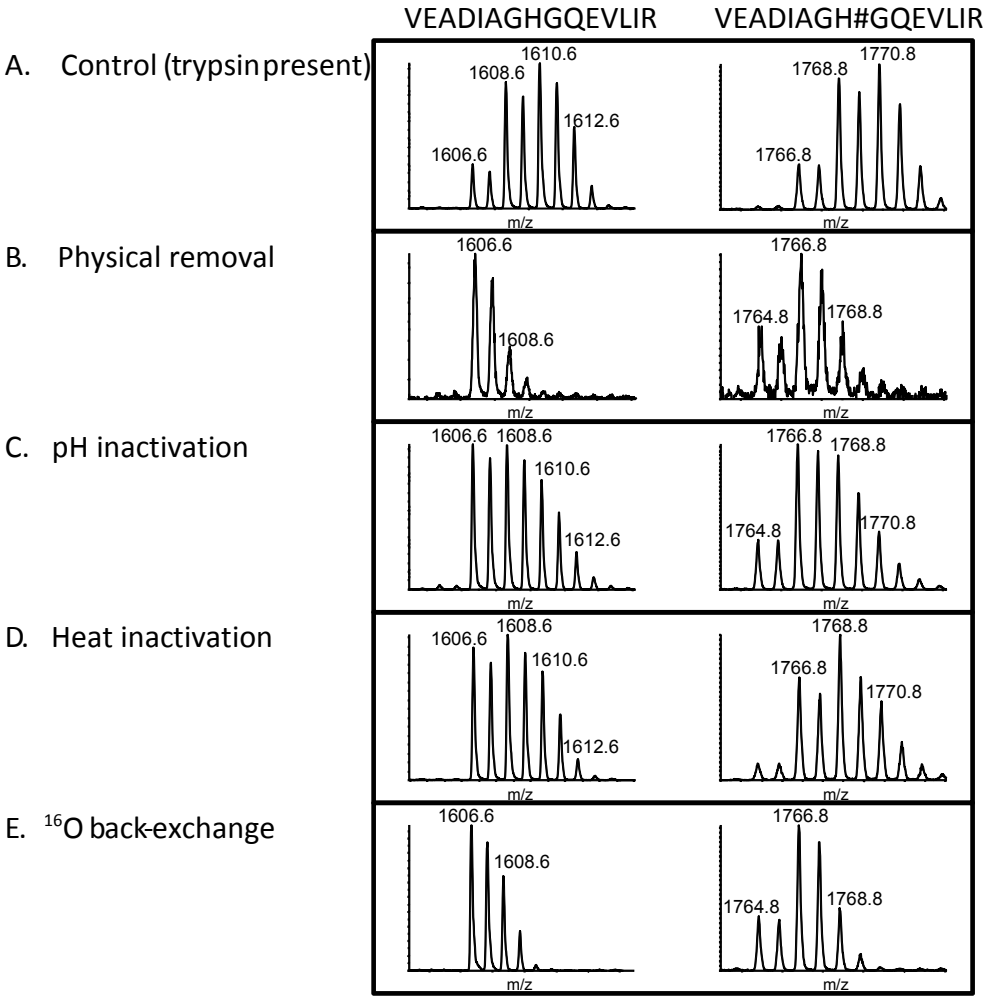

Figure 2. Comparison of methods for eliminating the oxygen-exchange activity of trypsin. A HNE-modified myoglobin digest was incubated with 70% $H_2{}^{18}O$ (aqueous) after exposure to various methods for preventing the trypsin-catalyzed incorporation of ^{18}O into the carboxyl oxygens at the c-terminus of peptides. The isotope envelopes for a single peptide from the digest, in both its non-modified and HNE-modified (#) form as observed in a MALDI-TOF MS spectrum, are presented. (A) The digest was labeled with 70% ^{18}O and reduced without any intervening measures for inactivating trypsin. (B) Trypsin was physically removed by ultrafiltration, and the flowthrough was ^{18}O-labeled (70%) and reduced. (C) The digest was ^{18}O-labeled (70%) and reduced at a pH of 12 so as to inactivate trypsin's oxygen-exchange activity. (D) The digest was boiled for 15 minutes to inactivate trypsin and then labeled with 70% ^{18}O. (E) The digest was labeled with 70% ^{18}O without any intervening measures for inactivating trypsin, vacuum centrifuged to dryness, reconstituted in 100% ^{16}O water supplemented trypsin, and incubated overnight at room temperature.

(Hajkova, Rao et al. 2006). Based on their findings, we attempted to prevent ^{18}O incorporation into the peptide c-termini by shifting the pH of the ^{18}O labeling reaction to 12, which only partially reduced the incorporation of ^{18}O into the c-terminus of peptides (Figure 2C). Another method for inactivating trypsin described by the Smith laboratory involves boiling the samples (Liu, Qian et al. 2004; Qian, Monroe et al. 2005; Petritis, Qian et al. 2009). However, in our hands, boiling th e HNE-Myoglobin digest prior to ^{18}O labeling did not significantly reduce ^{18}O incorporation into the c-terminus of peptides, presumably due to refolding of the enzyme back into its catalytically active state during the subsequent two-hour 18O labeling reaction (Figure 2D).

Given the observed limitations of the measures above, we pursued an alternative approach, exploiting the specificity of trypsin for the c-terminus and its inertness to the reactive carbonyl residue. By further incubating the reduced peptides in 100% ^{16}O water supplemented with tyrpsin (Figure 2E), we hypothesized that the trypsin would completely incorporate ^{16}O back into the c-terminus, while leaving the ^{18}O trapped in the reduced HNE modification unaffected. Indeed, after an overnight incubation virtually all peptides were free of ^{18}O incorporation into their c-terminus, while the signature isotope pattern for HNE-modified peptides was preserved. Given the effectiveness of this simple procedure to remove ^{18}O incorporated into the peptide c-termini of reduced peptides, we decided to incorporate it into our overall method for characterizing carbonylated peptides.

Combining SPH enrichment and ^{18}O-labeling for the analysis of carbonylated peptides from complex mixtures

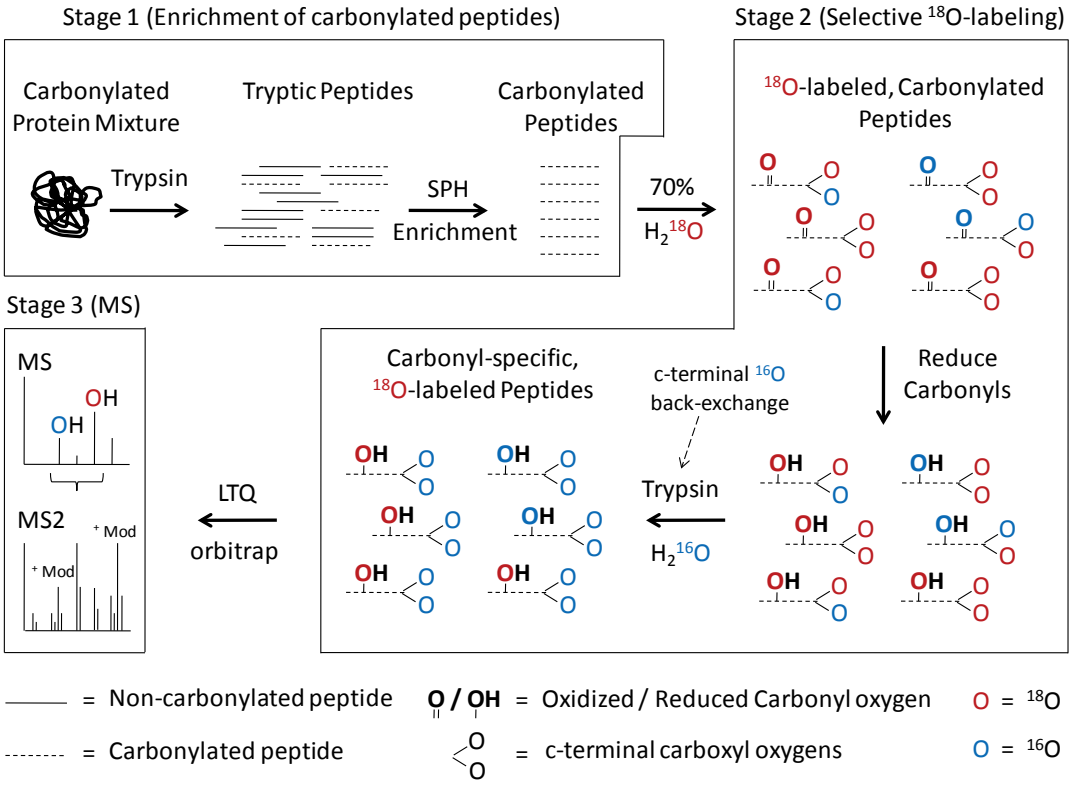

Figure 3. Scheme for the comprehensive analysis of carbonylated peptides by label-free SPH enrichment and targeted ^{18}O-labeling of peptide carbonyls. Details for the enrichment, ^{18}O-labeling, and high resolution mass spectrometry analysis of carbonylated peptides are described in the materials and methods section.

To characterize the carbonyl proteome in complex mixtures we previously described a front-end enrichment method based on the reversible, covalent capture and release of carbonylated peptides to a SPH reagent (Roe, Xie et al. 2007). Here we sought to combine SPH enrichment and ^{18}O labeling to develop an integrated method for enhancing the detection and identification of carbonylated peptides from complex mixtures. This method integrates three stages, 1) enrichment of carbonylated peptides, 2) ^{18}O labeling of enriched peptides, and 3) analysis of labeled peptides by high resolution mass spectrometry (Figure 3). In the first stage, the SPH reagent, described in detail in Materials and Methods, is used to enrich carbonyl modified peptides from a complex mixture, in this case HNE-modified peptides from a rat skeletal muscle lysate. As we have previously described (Roe, Xie et al. 2007), HNE-modified peptides are covalently bound to the resin by formation of acid labile, covalent Schiff-base bonds. As such, both peptide capture and subsequent wash steps were conducted at neutral pH, wherein the Schiff-base bond is stable, while the elution of the bound peptides was performed under acidic conditions. In the second stage the enriched peptides are incubated in 70% $H_2{}^{18}O$ at neutral pH, reduced with sodium borohydride, and subjected to conditions promoting the trypsin-catalyzed removal of any ^{18}O incorporated into the c-terminus of peptides during the labeling reaction. Finally, the ^{18}O-labeled sample is analyzed on an LTQ-Orbitrap mass spectrometer to ensure sufficient resolution of the ^{16}O:^{18}O isotope signature of the carbonylated peptide precursor-ions, and to generate of high quality MS2 using the linear ion trap.

Analysis of HNE-treated tissue lysates from Rat skeletal muscle

To test the value of this integrated method, we applied it to the analysis of a rat skeletal muscle tissue lysate treated with HNE. By comparing database matches from the same SPH enriched sample split into a non-labeled (normal ^{16}O isotope signatures) fraction, and a ^{18}O-labeled fraction, we confirmed that the presence of ^{18}O isotopologues in the MS and MS2 spectra does not alter the ability of sequence database searching to identify these peptides (data not shown). In fact, the ^{18}O-labeled fraction resulted in slightly more confident matches to carbonylated HNE-modified peptides than did the non-labeled one. In total, we identified 60 unique HNE-modified peptides within 8ppm mass accuracy from the ^{18}O-labeled sample.

The MS and MS2 spectra matched to one of the HNE-modified peptides from the ^{18}O labeled sample is shown in Figure 4. The presence of an HNE-modification on the peptide is first supported by the isotope signature of the precursor ion where the monoisotopic and the +2 isotope appear in a 1:2 ^{16}O:^{18}O ratio, specific to HNE-modified peptides (Figure 4A). The preservation of the signature isotope pattern for multiple fragment ions in the MS2 spectrum indicates that both the ^{16}O and ^{18}O precursor-ions entered the collision cell when using a 2.0 amu isolation width, which proved convenient for confirming the accuracy of the peptide sequence match and site of modification (Figure 4B). Importantly, all the fragment ions with the expected ^{18}O isotope signatures were assigned to b-ions carrying the HNE modification, while all the y-ions which lacked the HNE modification were assigned to fragment ions with typical, ^{16}O-only isotope signatures (Figure 4B, insets). The ^{18}O isotope signature was also observed for the HNE-

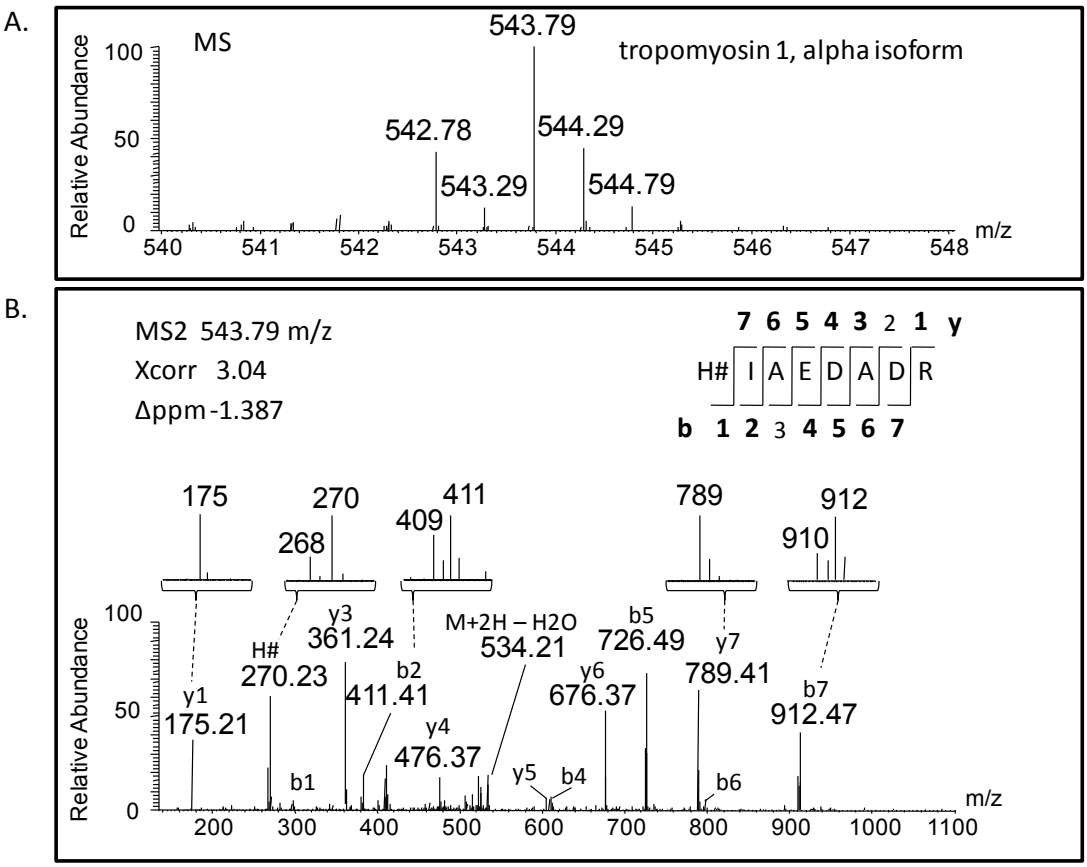

Figure 4. Example MS and MS2 spectra collected on an LTQ-orbitrap that matched confidently to a HNE-modified peptide from a rat muscle protein, tropomyosin 1. (A) MS spectrum showing the signature isotope pattern produced by partial incorporation of ^{18}O into the doubly charged precursor-ion of a carbonylated peptide. The 542.78 and 543.79m/z ions represent the ^{16}O and ^{18}O-labeled versions of the peptide, respectively, which appear in the expected abundance ratio. (B) MS2 spectrum generated by fragmenting the ^{18}O-labeled isotopologue (543.79m/z) in the linear ion trap using an isolation width of 2amu. The observed b and y ions, together with the histidine immonium ion, are labeled in the spectrum andshown in bold in the peptide map. The isotope envelopes for several of the fragement ions have been magnified and are inlayed above the spectrum. As predicted by the sequence, the y-ion series does not contain ^{18}O isotopologues while the series of b-ions, as well as the histidine immonium ion, do.

modified immonium ion of histidine, further validating that the modification was mapped to the correct residue (Figure4B, inset).

As observed with other peptide enrichment methods, it was very difficult to completely remove non-modified peptides that bind the resin non-specifically from the enriched fraction (Ranish, Yi et al. 2003). In this case, such peptides provided a good internal control for evaluating the specificity of the ^{18}O-labeling. One such example was a confidently matched non-HNE-modified peptide from the protein Triosphosphate isomerase. As predicted, neither the MS nor the MS2 spectrum contained isotope signatures reflective of ^{18}O incorporation, indicating the specificity of our method for incorporating ^{18}O within the reactive carbonyl groups.

In addition to the numerous true positive and true negative matches confirmed by ^{18}O labeling, a significant number of false negative matches were also identified by virtue of the absence, or presence, of ^{18}O generated isotope signatures in their MS and MS2 spectra. For example, although the MS and MS2 spectra in Figure 5 clearly contain ^{18}O isotopologues, they were incorrectly matched to a non-modified peptide in the database search. However, further scrutiny of the top ranked peptide sequences as determined by Sequest revealed a candidate HNE-modified peptide from myosin-7 that was the ninth best match. Upon inspection, the expected series of b and y-ions of this sequence matched nicely to the major fragment ions in the spectrum (Figure 5B). In addition, those fragment ions containing ^{18}O isotope signatures matched to b and y ions carrying

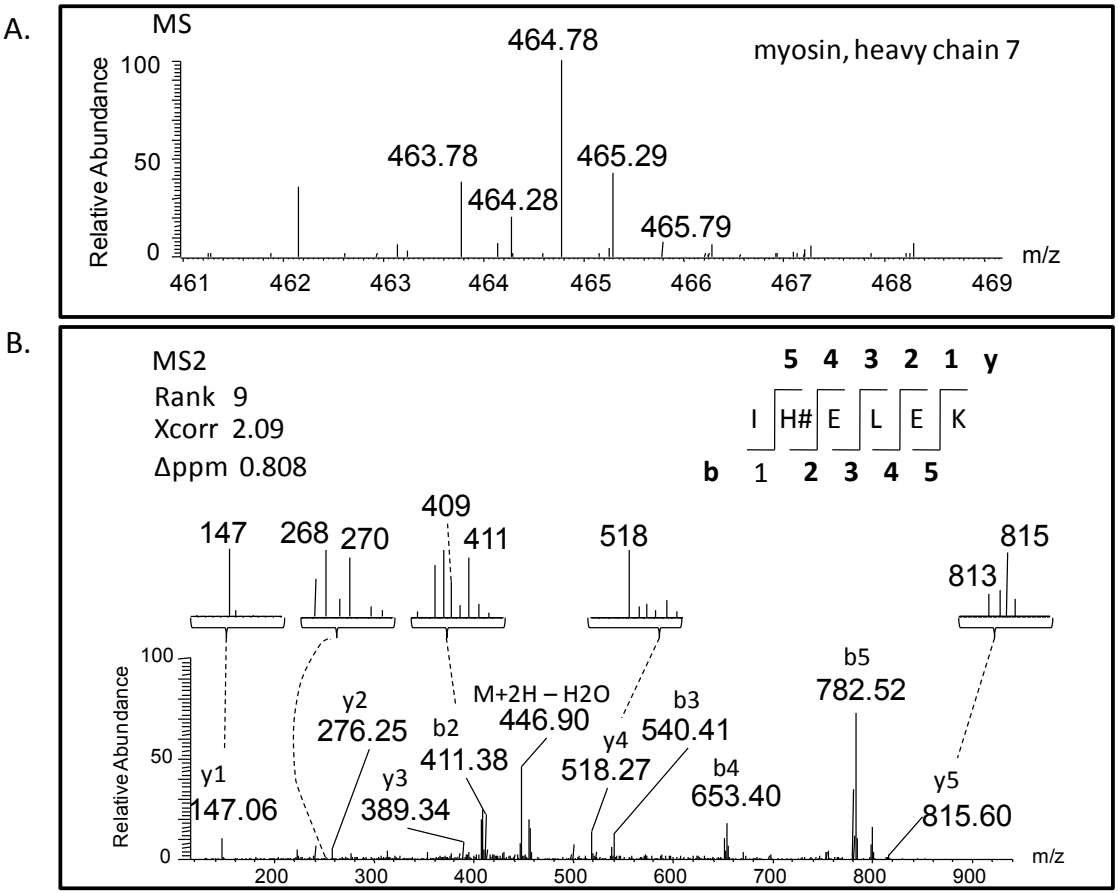

Figure 5. Utility of ^{18}O-labeling for identifying HNE-modified peptides matched with low confidence and ranked low in the Sequest output file. The MS (A) and subsequent MS2 spectrum (B) from a peptide incorrectly matched to a non-modified peptide in the reverse database. The clear presence of ^{18}O isotopologues in both spectra guided further scrutiny of the output file and lead ultimately to the correct identification of the HNE-modified peptide from myosin.

the HNE modification, while b and y ions matching to non-modified fragment ions also lacked the ^{18}O isotope signatures. This is most clearly demonstrated when comparing the non-modified y4 ion, to the HNE-modified y5 ion (Figure 5B, inset).

Given the observed false negative described above, and our past observations revealing many MS2 spectra not successfully matched to HNE-modified peptides, we sought to further investigate the value of ^{18}O incorporation to evaluate the efficiency of MS2 and sequence database searching to identify modified peptides. Upon manual inspection of the LC run for the HNE-labeled rat skeletal muscle sample, it was clear that there were many more ^{18}O isotope signatures for peptide precursors selected for MS2 than were identified by database searching. As an example, a representative MS spectrum is shown in Figure 6. In addition to ions with typical isotope patterns, many more with atypical ^{18}O isotope signatures indicative of HNE-modified peptides were observed, as detailed in this figure. Of the nine such ions pictured, three were not selected for MS2, while only one of the remaining six ions selected for MS2 was correctly matched to an HNE-modified peptide. The presence of an additional isotopologue observed in the envelope for three of the precursor-ions pictured suggests that an additional ^{18}O molecule was incorporated into the peptides (Figure 6, insets). Further scrutiny of the MS2 spectra deriving from these three precursor-ions indicated that while the additional isotopologue may result from incomplete reduction of the carbonyl or the presence of multiple modifications, it is not due to incorporation of ^{18}O into the c-terminus.

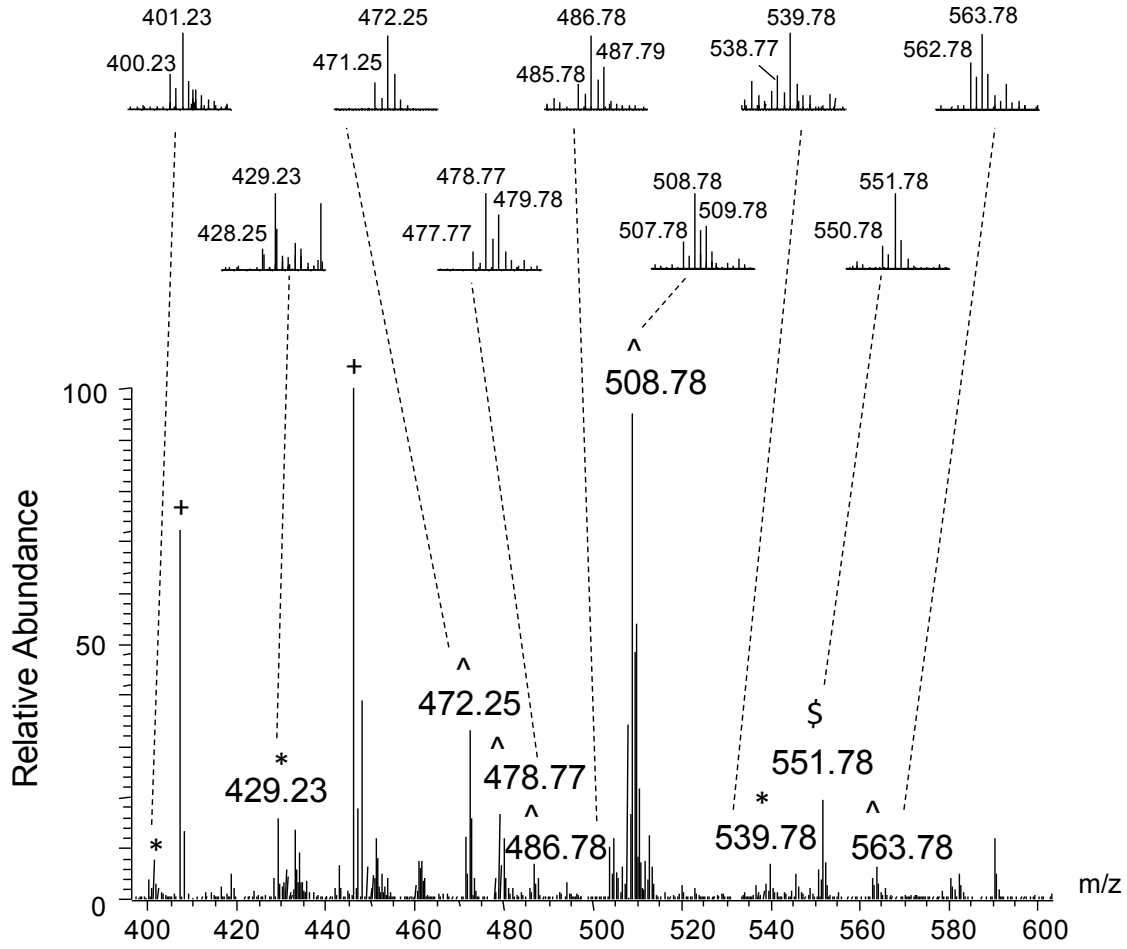

Figure 6. Representative MS spectrum showing inefficiency of the MS2 and database search platform for correctly identifying ^{18}O-labeled peptides. The isotope envelopes for each of the ^{18}O-labeled ions observed over the defined m/z range are inlayed above the spectrum. The MS2 spectrum for peptides that appear to be carrying multiple ^{18}O molecules (478.77, 486.78, and 508.78m/z) are provided in the supplemental data section and indicate the peptides have not been labeled at their c-terminus. *, an MS2 spectrum was not acquired. ^, the MS2 spectrum acquired was not matched to a carbonylated peptide. $, the MS2 spectrum acquired matched to a carbonylated peptide, +, background peptide not labeled with ^{18}O or matched to a carbonylated peptide by the database search.

Given our observation that many peptides showing the ^{18}O isotope signature seemed to be missed when relying on sequence database searching of MS/MS data, we sought to investigate more systematically our ability to identify HNE-modified peptides via μLC-MS/MS and sequence database searching. For this, we generated software that automatically interrogates mzXML files in search of unique isotope signatures attributable to partial ^{18}O incorporation. Specifically, the software was programmed to identify ion clusters in MS and MS2 spectra that adhered to strict m/z spacing and relative abundance constraints for peptide isotopologues (described in detail in Materials and Methods section). The specificity of these criteria to detect ^{18}O isotope signatures was assessed by applying the software to a non-^{18}O labeled negative control sample. This negative control sample was a portion of the same enriched, HNE-modified peptides derived from the rat muscle homogenate used for testing our ^{18}O incorporation method, except the ^{18}O labeling was omitted. In addition, the sample was analyzed using the same μLC-MS/MS method on the LTQ-Orbitrap, with the expectation that the isotope signatures from the detected peptides should show "normal" isotope signatures. Analyzing this negative control sample using our automated software and stringent criteria for the identification of ^{18}O labeled, HNE-modified peptides, we were able to accomplish an estimated false-positive-rate (FPR) of 2%. This FPR estimation was based on the fact that for a comparable number of total MS/MS scans (approximately 5000 MS/MS scans) only seven precursors were identified as carrying the ^{18}O isotope signature in the negative control, versus 336 precursors from the ^{18}O-labeled samples. Therefore,

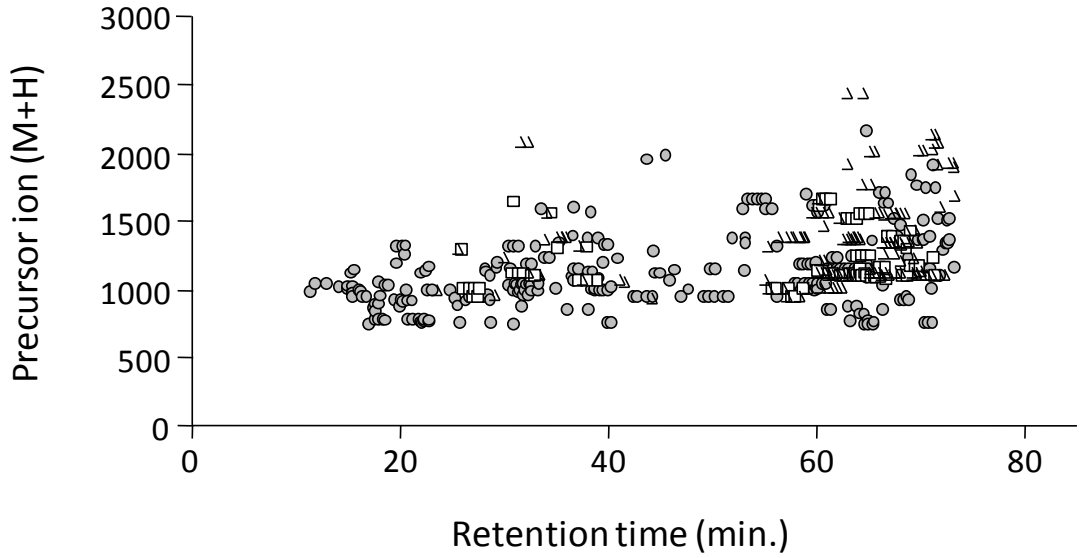

Figure 7. Profile of modified peptides confidently matched via sequence database searching and additional ^{18}O-labeled spectra detected over a representative LC-MS/MS analysis. Shown are individual MS2 spectral scans that were either matched to carbonylated peptides by Sequest (135, open triangles), identified as being ^{18}O-labeled by our software at a false-positive-rate of 2% (261, closed circles), or both (75, open squares). The combined 471 spectral scans provide an estimate of the total number of carbonylated spectra in the sample. Dividing the total number of spectral scans database-matched to carbonylated peptides (210) by the total number of carbonylated scans in the sample (471), indicated Sequest confidently matched carbonylated spectra at a 45% efficiency rate.

we estimated that about 7 of 336 scans in the former sample were false positives, for an estimated false positive rate of about 2%.

By comparison, Sequest confidently matched 210 precursors to HNE-peptides in the rat database. Of these, 75 were also identified by our software (2% FPR) as being ^{18}O-labeled, with an additional 81 adhering to looser criteria at a higher FPR (33%). Specifically, a 2% FPR was achieved by only considering MS2 with 3 or more ^{18}O isotope signatures, while relaxing this constraint to 1 provided a false-positive-rate of 33%. This indicates that the 261 precursors only identified by the software (2% FPR) is a conservative estimate of the carbonylated peptides missed by the database search. By adding these 261 putative false negatives with the 210 precursors confidently matched HNE-modified peptides, a total of 471 precursors comprise our carbonylated dataset (Figure 7). Thus, the rate by which Sequest identified carbonylated precursors in our analysis was estimated at 45% (210 / 471). These results show that a significant number of modified peptides are missed when relying on MS2 and sequence database searching, indicating that our partial ^{18}O-labeling provides a complementary means to detecting carbonylated peptides within a complex mixture.

Discussion

Identifying the full complement of carbonylated peptides from proteins within complex biological mixtures remains a challenging task in the field of redox proteomics. Currently, positive identifications are heavily dependent on the matching of MS2 spectra b- and y-ions to theoretical MS2 spectra in large sequence databases, as a lack of reliable

spectral features unique to carbonylated peptides are available to aid in their identification. Here, we describe a method for detecting carbonylated peptides based on the partial and selective incorporation of ^{18}O into carbonyl oxygens, which is not dependent on matching MS2 via sequence database searching. The resulting ^{18}O isotope signatures produced in the MS and MS2 spectra are diagnostic of carbonylated peptides and provide additional depth of information.

Several novel aspects of our ^{18}O labeling method make it particularly well-tailored for the analysis of carbonylated peptides in complex mixtures. First, the relative amount of ^{18}O (70%) used to label reactive carbonyls ensures that the resulting ^{18}O isotope signature generated is specific to carbonylated peptides, and is thus distinguishable from any other naturally occurring peptide isotope distributions possibly observed within the typical m/z range used for tandem mass spectrometry experiments. Second, we limited the ^{18}O incorporation toreactive carbonyls as the ^{18}O molecules incorporated into peptide c-termini during the labeling reaction were completely back-exchanged into ^{16}O-containing solutionupon addition of trypsin. Third, reduction of reactive carbonyls to alcohol groups following the labeling reaction ensured the preservation of the ^{16}O:^{18}O ratio at the reactive carbonyl not only during the subsequent peptide c-termini back-exchange step, but for all subsequent sample handling processes including LC-based fractionation and analysis by electrospray mass spectrometry. The latter point is especially significant given the infeasibility of conducting LC-MS/MS in $H_2{}^{18}O$-buffer. Finally, our ^{18}O labeling method complements label-free enrichment of carbonylated peptides providing

an in-depth analysis of complex carbonyl proteomes. In addition to these features, we have developed a software program enabling the automated identification of carbonylated peptides by virtue of their ^{18}O isotope signatures from LC-MS and MS2 raw data.

The carbonyl-specific ^{18}O isotope signatures generated by our ^{18}O-labeling method provides added value to redox proteomics studies in a number of ways, as demonstrated here on an HNE-treated complex mixture. For example, the presence of spectral features unique to carbonylated peptides enables independent validation of database search results comfirming the presence and localization of reactive carbonyl medications within the matched peptide (Figure 4). As a result, greater confidence is gained for carbonylated peptides identified by database matching. In addition, the ^{18}O-labeling method also complements the database search results, revealing many additional spectra of modified peptides missed by the search algorithm (Figure 5). Once identified, these so called "false negative" spectra can be selected for manual analysis or possibly de novo sequencing, and may lead to greater understanding about some of the specific spectral features that inhibit the identification of carbonylated peptides by mass spectrometry. Thus, the combination of database searching and ^{18}O-labeling provides a more complete characterization of the carbonylated peptides in a given sample, and informs investigators about the efficiency by which putatively carbonylated peptides are being correctly matched by database search algorithms.

Compared to other diagnostic ions used to screen for carbonylated peptides, ^{18}O isotope signatures enjoy greater applicability and provide more information. Unlike the immonium ion for histidine HNE-adducts (266m/z), or the dehydrated product of HNE (139m/z) oftern observed for all HNE-modified peptides (Bolgar 1996; Roe, Xie et al. 2007), the ^{18}O isotope signatures are not limited to a specific adduct of a given reactive carbonyl, nor even to a single class of reactive carbonyls. They are instead a universal marker of carbonylated peptides, and are thus well suited for improving the detection of peptides modified by the various reactive carbonyls generated *in vivo*.

The software we developed for the systematic identification of ^{18}O-labeled peptides also provides value in a number of ways. It identifies ^{18}O-labeled peptides without dependence on successfully matching MS/MS data to a peptide sequence, thus providing a means for estimating the prominence of reactive carbonyl-modified peptides in a dataset, and assessing the efficiency by which database search algorithms identify carbonylated peptides. Importantly, the software automates detection of ^{18}O isotope signatures, which ensures the consistent application of standardized criteria across the dataset and eliminates the time-consuming process of manual interpretation. Finally, the software was designed to operate on the open-source mzXML file format, and thus should be compatible with all high mass accuracy / high resolution mass spectrometers. Currently, it lacks a user-interface, but both the software and code is available on request.

Applying this software to the analysis of our rat skeletal muscle dataset provided a first-of-its kind, systematic evaluation of the efficiency by which the MS2 and sequence

database search platform identifies HNE-modified peptides. Our results (Figure 7) indicate the database approach provided a limited characterization of the full spectrum of carbonylated peptides, producing an identification efficiency of 45%. This efficiency rate is a conservative estimate for our data collected on a hybrid LTQ-Orbitrap, and likely will vary between experiments conducted on the same and different high mass accuracy instruments (i.e. TOF/TOF, hybrid TOFs). Notably, our ^{18}O-labeling method would enable comparison of the efficiencies for carbonylated peptide identification between these different instrument options.

Given the inefficiency of identifying HNE-modified peptides by MS2 and sequence database searching, two natural questions arise: what limits the identification of these modified peptides, and how can it be improved? One potential limiting factor may be unexpected fragmentation of the HNE group from both precursor and fragment ions, which could complicate analysis. Distinct from neutral-loss, such ill-defined fragmentations are beyond the scope of this study and warrant further investigation. Another possible limiting factor is that the ^{18}O isotope signature observed for some peptides may result from the incorporation of ^{18}O into the c-terminus of peptides, despite our efforts to prevent this. However, we discounted this possibility by including in the database search a differential mass shift on the peptide c-terminus that accounts for ^{18}O incorporation, which showed a negligible number of matches to c-terminal modified peptides. The presence of other modifications on HNE-modified peptides, not accounted for in the sequence database search, may also contribute to the low efficiency of

identifications. In addition to the multitude of biological modifications not included in our search parameters, the potential for unknown chemical modifications introduced by reducing the sample with sodium borohydride may also be of concern. However, proof-of-principle studies on our standard protein indicate that unexpected peaks resulting from additional modifications do not appear following reduction.

Several avenues of study may improve our ability to identify HNE and other carbonyl-modified peptides. Studies directed towards defining unconventional CID fragmentation patterns unique to HNE and other reactive carbonyls as previously mentioned may prove highly valuable. Alternatively, fragmentation of carbonylated peptides by "softer" methods (ETD and ECD) may provide a way to preserve the fragmented peptide in its modified form, thus decreasing the complexity of the spectra and presumably increasing the efficiency by which correct identifications are made. Indeed, a recent study has coupled our SPH enrichment method with ECD analysis, showing the promise of alternative fragmentation methods for analysis of HNE-modified peptides (Rauniyar, Stevens et al. 2009). Our ^{18}O method described here should provide a valuable tool for these future studies seeking to improve the identification of carbonyl-modified peptides using tandem mass spectrometry-based strategies.

In conclusion, we have described a new method for improving the detection and identification of carbonylated peptides which should prove highly valuable for investigators interested in characterizing protein carbonylation via mass spectrometry-

based proteomics. Although demonstrated here on HNE-modified peptides, this method should be amenable to other types of reactive carbonyl modifications. Finally, our initial results also show that our method can be altered to enable complete incorporation of ^{18}O into reactive carbonyls, enabling the measurement of relative abundance levels of modified peptides between different samples, and making it compatible with studies exploring quantitative changes in carbonyl modification state due to age, disease state, or other perturbations.

Chapter 4

Summary and Future Directions

Protein carbonylation is a biologically relevant post-translational modification that correlates with oxidative stress and is implicated in the aging process as well as a variety of age-associated pathologies, including complications from type II diabetes, cancer, and neurodegenerative diseases. Proteomic profiling of carbonylated proteins (redox proteomics) in a number of tissues has produced rather extensive catalogues of proteins that are *in vivo* targets of carbonylation. Many of these proteins are residents of the electron transport chain, the major endogenous source of the superoxide radical, or contribute to the antioxidant defense in the cell. Their carbonylation often results in impaired function, which is believed to further perpetuate the cellular imbalance between ROS and antioxidant defenses, leading to additional oxidative damage.

To better understand the biochemical mechanisms leading to protein carbonylation, novel methods designed to facilitate the identification of both the specific amino acid targets within carbonylated proteins as well as the chemical identity of the modifying reactive carbonyl have been generated. One approach showing value involves mass spectrometric identification of avidin-enriched, biotinylated peptide carbonyls . However, a significant limitation of this approach is that cleavage of the relatively bulky biotin tag during CID produces a number of highly abundant fragment ions that often complicate the MS/MS spectra, suppress the signal of b and y-ions, and thus preclude identification of carbonylated peptides by database searching.

Summary of Chapter 2: Label-free enrichment of carbonylated peptides

As an alternative to this and other label-based enrichment methods, I developed a novel solid-phase hydrazide (SPH) reagent for the label-free enrichment of carbonylated peptides. The SPH reagent works by specifically forming acid-labile Schiff-base covalent bonds with the carbonyl moieties of carbonylated peptides. After washing away all the non-modified peptides, the SPH-bound carbonylated peptides are collected by acid elution and identified by tandem mass spectrometry. When applied to the analysis of yeast lysates treated with the short-chain lipid carbonyl 4-hydroxynonenal (HNE), over a 120 unique sites of modification were confidently identified using a linear ion trap mass spectrometer. Integral to the identification of many of these sites was the novel use of two data acquisition parameters for MS identification of carbonylated peptides, namely PQD and neutral-loss triggered MS/MS/MS (MS^3). While PQD provided the consistent detection of low-mass fragment ions diagnostic of HNE-modified peptides, MS^3 of fragment ions resulting from the neutral-loss of HNE enabled the identification additional peptides whose MS/MS spectrum was not confidently database matched to a HNE-modified peptide.

The label-free enrichment of carbonylated peptides by the SPH reagent is not without limitations. For example, enrichment of peptides rather than proteins requires greater sensitivity as the ratio of non-carbonylated-to-carbonylated analytes is significantly magnified following digestion of complex samples. In addition, by limiting the identification of carbonylated proteins to only those peptides carrying the carbonyl

modification diminishes the confidence with which proteins can be reported as carbonylated. However, if multiple non-carbonylated peptides are also identified from the same protein, the likelihood that the carbonylated peptide is correctly sequenced increases. Similarly, the combination of non-carbonylated and carbonylated peptides for proteins in a dataset enables better relative quantitation of carbonylated proteins than is usually achieved with carbonylated peptides alone. While I attempted to address this issue by complementing peptide enrichment via the SPH reagent with protein enrichment by avidin-affinity capture of biotin-hydrazide conjugated proteins (see Chapter 2), it would be ideal to identify peptides from both the carbonylated and non-carbonylated peptide fractions in a single analysis.

Chapter 2 Future Directions: SPH enrichment of carbonylated proteins for the sequential identification of their non-carbonylated and carbonylated peptides

Using the SPH reagent to enrich carbonylated proteins rather than peptides is an intriguing idea that flows out my published results and may provide a potential solution to the aforementioned limitations. Essential to the success of such an approach would be the use of an SPH reagent containing a larger pore size suitable for capturing proteins. Although marketed as a scaffold for building antibody columns, a hydrazide- conjugated sepharose bead with a 1000Å pore size is commercially available from Pierce. As such, I've generated a working protocol for the enrichment of carbonylated proteins using the Pierce SPH reagent (Ultralink® Hydrazide Gel), and provide a schematic of the workflow in Figure 1. Briefly, carbonylated proteins in complex mixtures are selectively

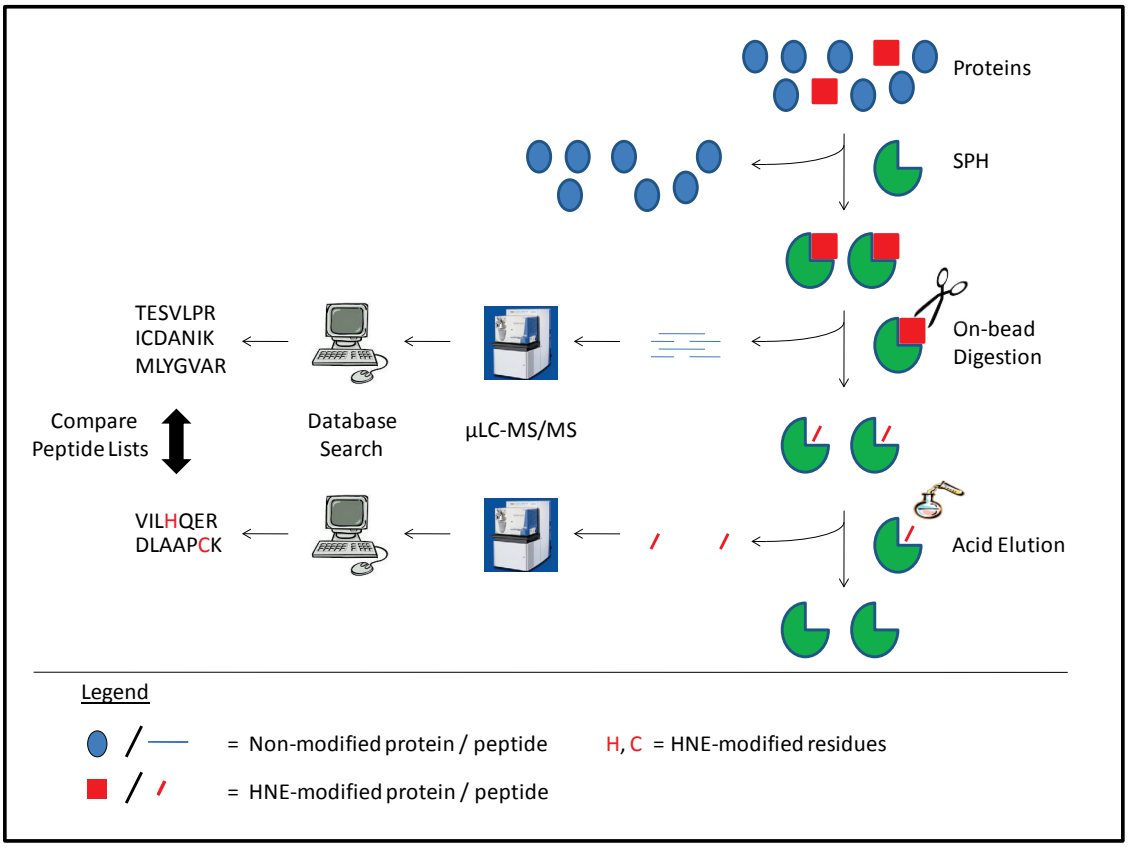

Figure 1. SPH enrichment of carbonylated proteins for the sequential identification of their non-carbonylated and carbonylated peptides

Carbonylated proteins in complex biological mixtures are selectively captured by the SPH reagent (1000Å pore size) and subjected to on-bead digestion with trypsin. In theory, the non-carbonylated peptides should be released from capture while the carbonylated peptides remain bound via Schiff-base interactions. The carbonylated peptides are subsequently released by hydrolyzing the Schiff-base bonds with acid. The two peptide fractions are then separately analyzed by mass spectrometry, and their MS/MS specta screened against a proteomic database to generate lists of identified peptides. Ultimately, the two lists are compared to find peptides, carbonylated and non-carbonylated alike, from the same proteins.

captured by the SPH reagent via formation of acid labile Schiff-base bonds. On-bead digestion of the SPH-bound proteins releases the non-modified peptides, which are collected, while the carbonylated peptides remain bound to the SPH reagent. The carbonylated peptides are then recovered following acid elution and analyzed separately from the non-modified pool of peptides by μLC-MS/MS. Finally, the lists of identified peptides from the two fractions are compared.

To test the utility of this enrichment method, preliminary experiments were conducted to determine first if HNE-proteins are selectively captured by the SPH reagent, and second if the carbonylated peptides are recoverable following on-bead digestion and acid elution. To address the first question, a 1:1 mixture of HNE-modified myoglobin and BSA were reacted overnight with Ultralink Hydrazide Gel using a variety of conditions. A coomassie stain of the before and flow-through fractions reveals that the Pierce SPH reagent selectively captured the HNE-myoglobin, as only the BSA was present in the flow-through fractions (Figure 2A). Similarly, a commassie stain of the before and flow-through fractions from a 1:50 mixture of HNE-myglobin and yeast lysate shows little difference between the two fractions, indicating that the vast majority the proteins were not captured by the SPH reagent (Figure 2B). However, MALDI-TOF analysis of the peptides collected following on-bead digestion (Figure 2C), and after acid-elution (Figure 2D) reveals ions consistent with masses expected for tryptic myoglobin peptides, indicating selective capture of HNE-myoglobin proteins. The complementary nature of the two fractions is demonstrated by the greater abundance of non-modified peptides

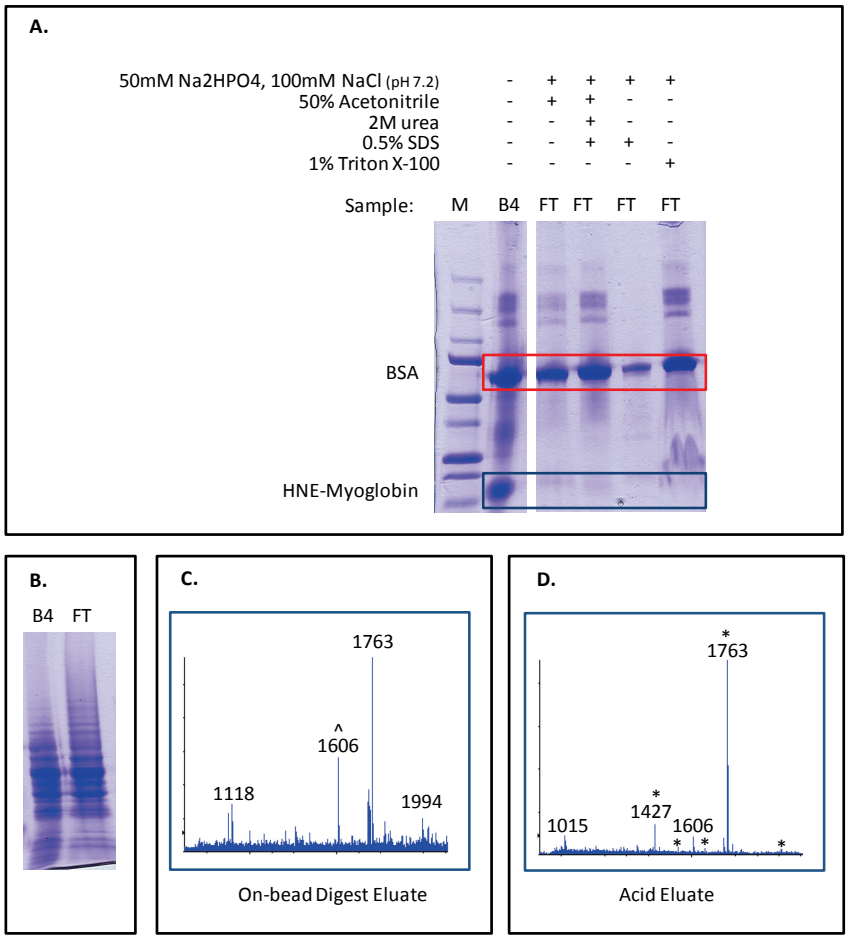

Figure 2. SPH capture and enrichment of HNE-modified myoglobin protein and peptides. A. Coomassie stained gel of the before (B4) and flow-through (FT) fractions from a 1-to-1 mixture of bovine serum albumin (BSA) and HNE-modified myoglobin incubated overnight with a large pore SPH reagent (Ultralink® Hydrazide Gel) in various reaction buffers. Following incubation, only the BSA is observed in the reaction supernatant, indicating the selective capture of HNE-modified myoglobin. **B**. Coomassie stained gel lanes of the before and flow-through fractions from a yeast lysate spiked with HNE-modified myoglobin (1:50) that was incubated overnight with the same SPH reagent. That the two lanes are identical suggests that the vast majority of proteins were not retained by the SPH reagent. **C**. Full-scan MALDI-TOF MS spectrum of the peptides released from the SPH reagent following on-bead digestion. The intense ion at 1606m/z is a prominent non-carbonylated peptide from myoglobin, while the 1763m/z ion is the same peptide modified by HNE. ^, non-modified peptide from myoglobin. **D**. Full-scan MALDI-TOF MS spectrum of the peptides released from the SPH reagent following acid elution. Multiple HNE-modified peptides (*) appear following acid elution that are not present following digestion alone.

following on-bead digestion, while an increased number of HNE-modified myoglobin peptides are detected following acid elution. Whether SPH reagents are sensitive enough to enrich endogenously carbonylated proteins is an important question yet to be addressed. However, preliminary results from a 1:500 mixture of HNE-myglobin and yeast lysate indicated that HNE-myoglobin peptides could be recovered following acid elution, all-be-it with significantly lower intensities. While not necessarily representative of endogenous levels of protein carbonyls, these findings encourage future experiments designed to explore the utility of the SPH protein enrichment approach for analyzing *in vivo* carbonyl proteomes.

Summary of Chapter 3: Targeted ^{18}O-labeling of carbonylated peptides

During the analysis of the SPH-enriched HNE-peptides from yeast lysates it was observed that several MS/MS spectra believed to derive from HNE-peptides were not confidently matched to HNE-peptides in the database. To address this issue, I developed a carbonyl specific ^{18}O-labeling method for improving the detection of carbonylated peptides by mass spectrometry. Based on the non-enzymatic solvent exchangeable properties of the carbonyl oxygen atom, this method involves the exposure of carbonylated peptides to an aqueous solvent containing 70% $H_2{}^{18}O$, so as to generate a carbonyl specific ^{18}O isotope signature by which to distinguish carbonylated peptides from the background. The resulting mass defect is initially observed in the full-scan spectra and subsequently preserved in the MS/MS fragmentation spectra, enabling the facile detection of carbonylated peptides by mass spectrometry. As a visual indicator of

carbonylation, the ^{18}O isotope signatures complement identification of carbonylated peptides by database searching, providing validation of database search results, while also revealing MS/MS spectra from carbonylated peptides either incorrectly matched, or not matched at all by the database search engine.

Several important features to the ^{18}O-labeling method make it particularly well suited for analyzing carbonylated peptides within complex biological mixtures. First, steps are taken to eliminate the potential for trypsin catalyzed incorporatation of ^{18}O into the carboxy-terminus of peptides. Without such action, ^{18}O-labeling of both non-carbonylated and carbonylated peptides renders them virtually indistinguishable and greatly complicates data analysis. Second, incorporation of ^{18}O into peptide carbonyls is stabilized by reducing the carbonyl to an alcohol, which prevents further back-exchange with aqueous solvents, and thus enables downstream analysis by ESI-μLC-MS/MS. Thirdly, the ^{18}O-labeling method is designed to operate in tandem with label-free enrichment of carbonylated peptides by SPH reagents, and is therefore valuable for characterizing the carbonyl proteomes of complex mixtures. Finally, a novel software tool was developed to enable the automatic and high-throughput detection of ^{18}O-labeled MS spectra generated by mass spectrometry analysis.

Chapter 3 Future Direction I: Targeted ^{18}O-labeling for the relative quantitation of carbonylated peptides

Given the well established application of ^{18}O as a stable isotope label for global quantitative proteomic analysis, and the ^{18}O-labeling method described above, the

potential use of ^{18}O-labeling for the specific relative quantitation of carbonylated peptides is an attractive, all-be-it rather obvious idea. To conduct such an experiment, slight modifications to the ^{18}O-labeling protocol described in Chapter 3 are required, which are outlined in Figure 3. In this approach, SPH enriched peptides from two samples are labeled with 100% light (^{16}O) or 97% heavy (^{18}O) oxygen molecules, respectively, reduced with sodium borohydride, and combined prior to analysis by μLC-MS/MS. Importantly, peptides common to both samples co-elute into the mass spectrometer and appear together in the full-scan MS spectra separated by 2 Da. While the preservation of the ^{18}O isotope signature in this experiment is convenient for improving the detection of carbonylated peptides, the overlap of the isotope envelopes for the two peptides complicates analysis of their relative abundance. However, effective isotope deconvolution programs have been described that simplify this process (Johnson and Muddiman 2004).

To examine the feasibility of quantitating carbonylated peptides using the protocol outlined in Figure 3, a proof-of-principle experiment was conducted on an HNE-treated complex protein mixture from rat skeletal muscle. Specifically, one aliquot from the digested sample was labeled with ^{16}O, while a second aliquot containing two-times more peptides was labeled with ^{18}O. The samples were then further processed according the protocol and analyzed on a LIT-Orbitrap mass spectrometer (Thermo's LTQ-Orbitrap). A representative full-scan MS spectrum showing a pair of peptides labeled with ^{16}O and ^{18}O respectively is provided in Figure 4A. The relative peak intensities of the M+H ions

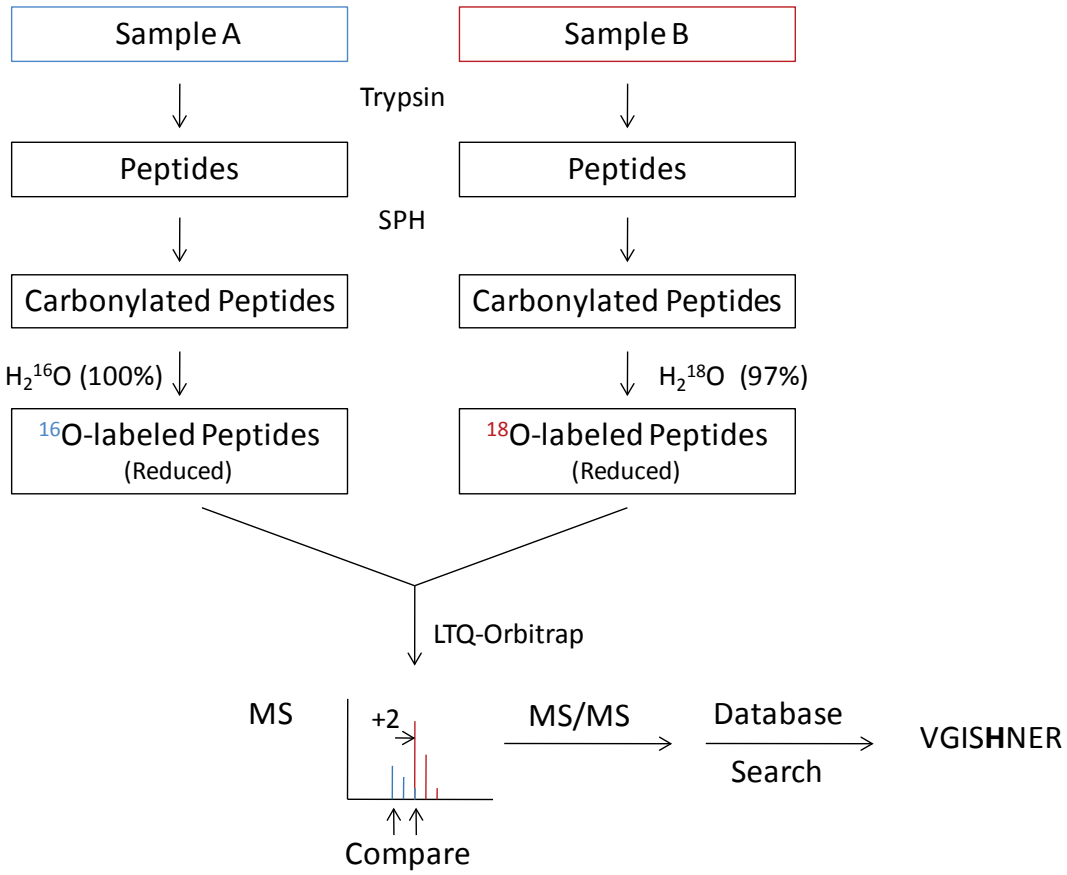

Figure 3. Targeted ^{18}O-labeling for the relative quantitation of carbonylated peptides. SPH enriched carbonylated peptides from two samples are labeled with ^{16}O and ^{18}O respectively, and combined prior to their analysis by µLC-MS/MS on a high resolution mass spectrometer (LTQ-Orbitrap). Peptides common to both samples co-elute into the mass spectrometer and generate an ^{18}O isotope signature in the full-scan MS spectrum. The relative intensity of the ^{16}O and ^{18}O ions in each signature is used to measure the difference in abundance of a given peptide/protein between the two samples. The MS/MS spectrum generated by fragmenting the ions is then submitted to database searching to determine the peptide sequence.

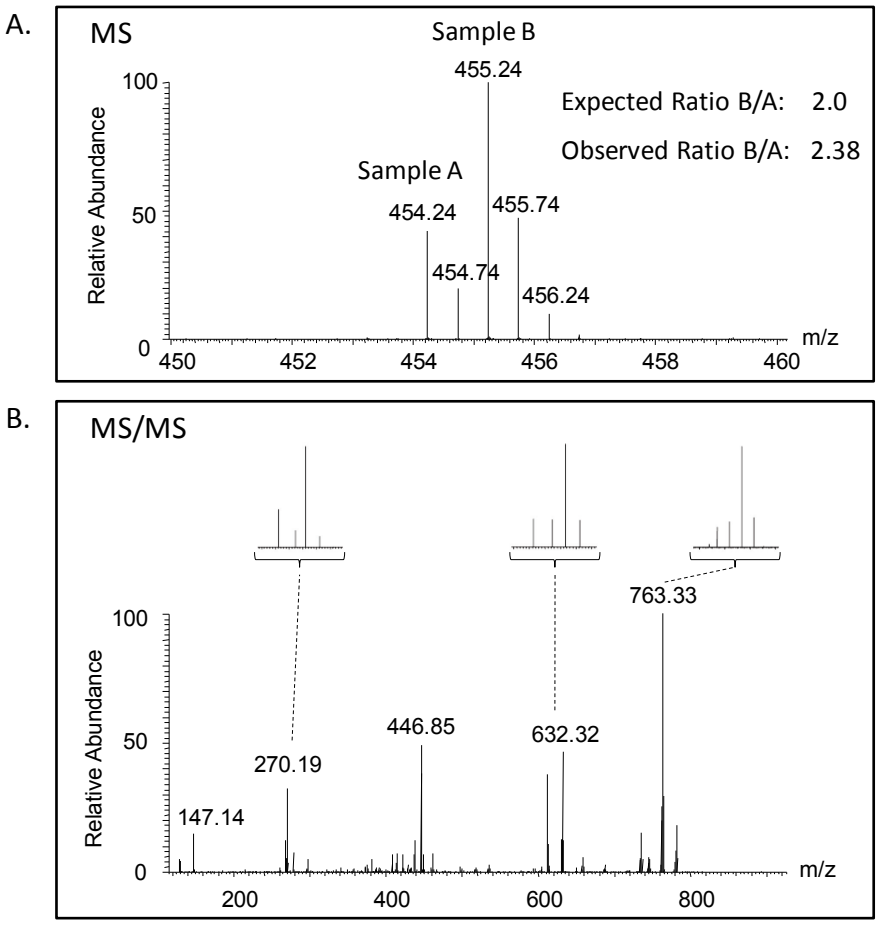

Figure 4. Representative MS and MS/MS spectra demonstrating proof-of-concept
Two aliquots differing in protein abundance by a factor of two were collected from an HNE-treated rat skeletal muscle tissue lysate and processed according to the workflow in Figure 3, with the sample higher in protein content labeled with ^{18}O. **A**. MS spectrum of a $^{16}O/^{18}O$ ion pair producing the ^{18}O isotope signature expected for HNE-modified peptides. Specifically, the signal intensity of the ^{16}O ion (454.24m/z) is about half that of the ^{18}O ion (455.24m/z), which is expected for the 2-to-1 peptide ratio generated between the samples. **B**. MS/MS spectrum resulting from fragmentation of the $^{16}O/^{18}O$ ion pair reveals several fragment ions also labeled with ^{18}O, which can be used, together with the non-labeled ions, to localize the site of carbonylation within the peptide sequence.

reflect an abundance ratio of 2.39:1, which correlates to a 19% error and is on-par with comparative proteomic analyses using other stable isotope labels (Gygi, Rist et al. 1999; Ross, Huang et al. 2004). Notably, the +2 isotope ($2C^{13}$) from the ^{16}O peptide contributes to the M+H signal of the ^{18}O peptide, thus inflating the ratio. The use of isotope deconvolution software, which was not used for this preliminary analysis, will thus likely improve the accuracy of the relative quantitation. Finally, the presence of several fragment ions in the MS/MS spectrum presenting ^{18}O isotope signatures confirm that the peptide is carbonylated and can be used to validate its site(s) of modification (Figure 4B).

The data so-far collected are very preliminary and represent a starting-point for future experiments aimed at ^{18}O-guided relative quantitation of carbonylated peptides. Several issues remain that require further investigation, including the consistent accuracy of quantitation across the entire data analysis, and the utility of this approach for comparative proteomic analysis of endogeneous carbonyl proteomes. However, once an optimal protocol is established, a variety of biologically relevant studies could be conducted, including a two-way comparative proteomic analysis of the carbonyl proteomes in young and old rat skeletal muscle tissue homogenates (Feng, Xie et al. 2008). Alternatively, a quantitative comparison of the carbonyl proteomes between wild-type and GSTA4 knockout adipocytes could lead to greater understanding of how oxidative damage to proteins may contribute to obesity and complications thereof (Grimsrud, Picklo et al. 2007).

Chapter 3 Future Directions II: Tandem stable isotope labeling for targeted multiplexed comparative proteomic analysis of carbonylated peptides

A limitation of the ^{18}O relative quantitation approach is the inability to compare more than two states in a single analysis. This precludes the use of ^{18}O-labeling alone for time-course studies, as may be conducted to characterize changes in the carbonyl proteome associated with various stages of oxidative stress. Alternatively, iTRAQ offers multiplexed relative quantitation of peptides, suitable for comparing as many as eight different samples at once (see Appendix I). Thus, one could envision a multiplexed comparative proteomic analysis of protein carbonylation that uses iTRAQ to label SPH-enriched carbonylated peptides. While attractive, this idea can be improved by incorporating carbonyl-specific ^{18}O-labeling as a way to distinguish the iTRAQ-labeled carbonylated peptides from the iTRAQ-labeled background peptides.

A protocol describing this tandem stable isotope labeling approach for relative quantitation of carbonylated peptides is proposed in Figure 5. In this case, SPH-enriched carbonylated peptides from four different samples are independently labeled with an isotopically unique iTRAQ reagent. The peptides are then combined, labeled with 70% ^{18}O, and analyzed by μLC-LTQ-Orbitrap in PQD mode. ^{18}O isotope signatures distinguish carbonylated peptides in the full-scan MS spectrum from the background, while the relative abundance of iTRAQ reporter-ions (114-117m/z) generated during MS/MS fragmentation indicates the extent to which a given peptide derived from each sample.

The potential of the tandem stable isotope labeling approach for relative quantitation of carbonylated peptides was examined by comparing complex protein mixtures from rat skeletal muscle homogenates treated with varying amounts of HNE. Specifically, four aliquots equal in protein content were treated with either 0, 50, 100, or 500uM HNE, independently digested, and the resulting peptides incubated with SPH. The enriched carbonylated peptides were subsequently processed according to the protocol outlined in Figure 5, with increased iTRAQ reporter-ion mass corresponding to increased HNE-treatment. The full-scan MS spectrum and the MS/MS fragmentation spectra from a representative peptide labeled with both ^{18}O and iTRAQ are shown in Figures 6A and B, respectively. HNE-modification of the peptide on a histidine (His) residue is indicated first by the ^{18}O isotope signature observed for the unfragmented peptide in the full-scan spectrum, and more specifically by a similar isotope signature for the HNE-modified immonium ion of His (ratio of 268-to-270m/z). Finally, the iTRAQ reporter ions indicate very little contribution from the non-treated sample (114), while the remaining HNE-treated samples appear to contribute to the overall peptide signal in the ratio of 1:3:15 (115:116:117m/z), which roughly approximates the expected ratio of 1:2:10.

While the preliminary data presented supports the concept of tandem stable isotope labeling for comparative proteomic analysis of carbonylated peptides, the majority of the data not shown is much more convoluted and points to the need for additional proof-of-principle studies that more precisely examine the quantitative accuracy of this approach.

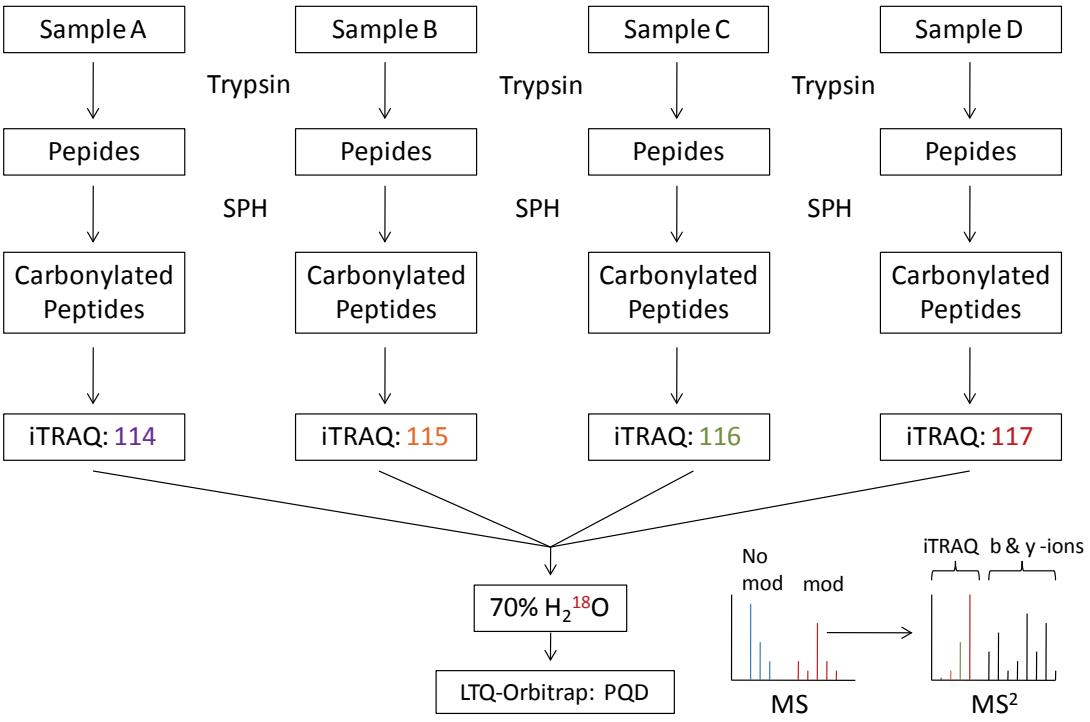

Figure 5. Tandem stable isotope labeling for targeted multiplexed comparative proteomic analysis of carbonylated peptides. SPH enriched carbonylated peptides from four different samples are independently labeled with isotopically distinct iTRAQ reagents and then combined. The resulting peptide mixture is subsequently labeled with a controlled amount of ^{18}O prior to analysis by a high resolution mass spectrometer capable of reliably sampling low m/z ions. Carbonylated peptides containing ^{18}O isotope signatures are differentiated from background peptides in the full scan MS spectra, while the intensities of the sample specific iTRAQ reporter ions generated during MS/MS fragmentation provide a measure of relative quantitation.

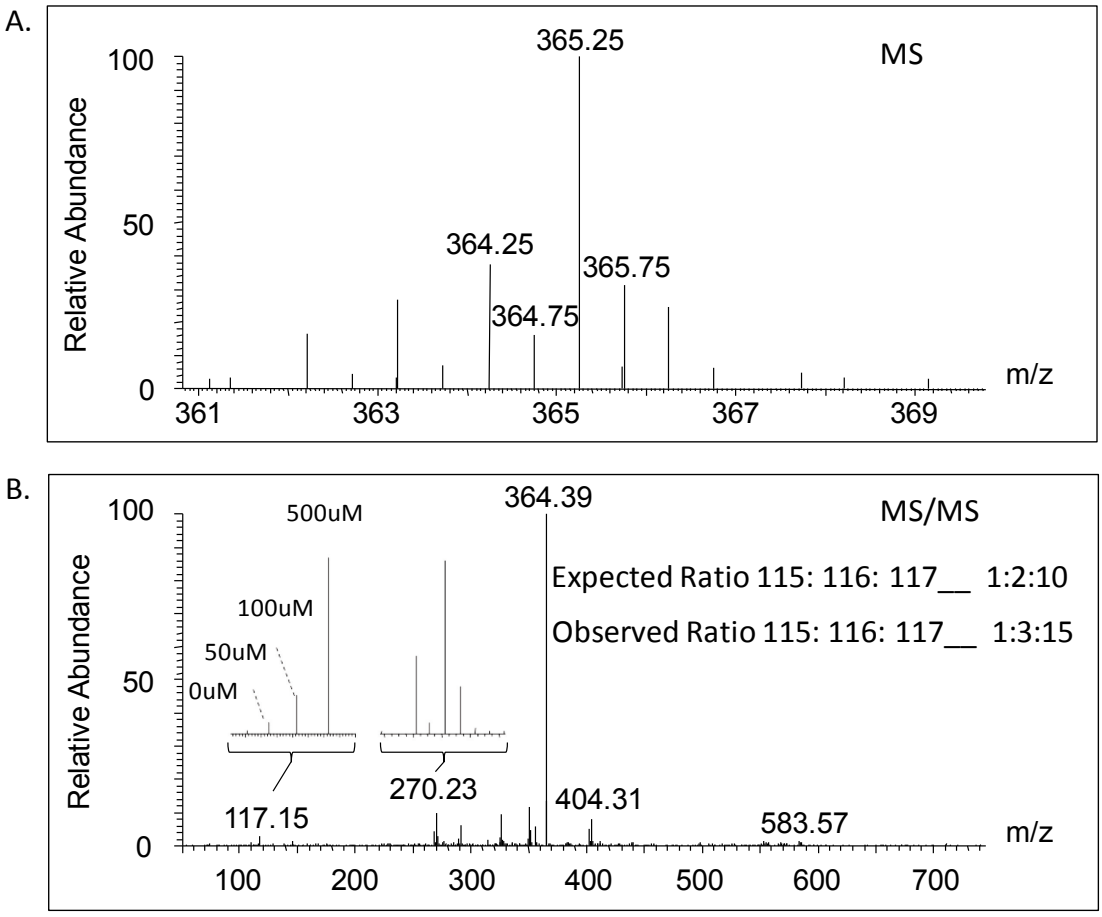

Figure 6. Representative MS and MS/MS spectra demonstrating proof-of-concept
Equal protein aliquots from a rat skeletal muscle lysate were treated with 0, 50, 100, and 500uM HNE respectively, and processed according to the workflow in Figure 5, with the heavier iTRAQ reporter ions corresponding to higher HNE concentrations. **A**. MS spectrum showing a $^{16}O/^{18}O$ ion pair (364.25m/z, 365.25m/z) producing the ^{18}O isotope signature that destinguishes HNE-modified peptides from the background. **B**. MS/MS spectrum produced by fragmentation of the $^{16}O/^{18}O$ ion pair contains iTRAQ reporter ions in the a ratio expected for the mixture of peptides used (1:2:10). That an ion consistent with the m/z for the immonium ion of a HNE-modified histidine residue is also ^{18}O-labeled further indicates that the peptide is HNE-modified.

Indeed, a major assumption of the above experiment is that differential treatment of complex protein mixtures with increasing amounts of HNE linearly correlates with increased protein carbonylation of the same proteins, which may be incorrect. Alternatively, comparing peptide aliquots from the same HNE-treated complex protein mixture circumvents this assumption and should provide a better assessment of the quantitative accuracy provided by the tandem stable isotope labeling method. Ultimately, this labeling method could be used to track age-associated abundance changes of carbonylated proteins in slow and fast twitch skeletal muscle fibers (Feng, Xie et al. 2008). It may also prove valuable for monitoring protein carbonylation in saliva as a function of oral cancer progression (Bahar, Feinmesser et al. 2007).

Closing remarks

The proteomic tools generated during the course of my thesis research, and their application to HNE-treated complex biological protein mixtures, represent important incremental steps towards reaching the end goal of mapping *in vivo* sites of protein carbonylation on a proteomic scale. As the protein carbonylation field is relatively young, akin to where phosphoproteomics was 15 years ago and only now finally maturing, achieving the high sensitivity required for accomplishing this objective understandably remains a formidable challenge, and promises to be the focus of future studies. The complexity of the issue is heightened for protein carbonylation compared to more prominent post-translational modifications such as phosphorylation, as the low endogenous levels of modification require greater sensitivity. Even so, the lessons

learned during the maturation of phosphoproteomics are likely applicable to redox proteomics, and may contribute greatly to solving the sensitivity requirements needed for mapping *in vivo* sites of protein carbonylation. The specific aspects of current phosphoproteomics experiments that could be adopted to improve the detection of endogenously modified proteins by mass spectrometry are as follows:

- Use larger amounts of protein as starting material (~10mg)
  -This will increase the overall levels of the low abundant carbonylated proteins

- Extensively fractionate samples via large scale HPLC or preparative gels and react individual fractions with carbonyl enrichment methods.
  - This will simplify the initial sample while concentrating individual carbonylated peptides to specific fractions.

- Enrich samples with two-orthogonal methods in tandem (i.e. enrich peptides with the SPH reagent and then derivatize them with reagents such as GRP and APC to enhance their signal strength in the mass spectrometer)
  - Note: Such combinations are only possible with the SPH reagent as the other reagents used for enriching carbonylated peptides irreversibly quench the carbonyl group, precluding any subsequent carbonyl-specific labeling

Ultimately, high-throughput mapping of *in vivo* protein carbonylation sites on a proteome-wide scale may require a new generation of mass spectrometers with even greater sensitivity than the current class of instruments. In the meantime, the established methods for enriching carbonylated peptides could be combined with the Oxyblot™

approach so as to map endogenous sites of carbonylation one protein at a time. Although providing lower throughput than desired, this combination, if successful, would represent a significant achievement in the field.

Bibliography

Adam-Vizi, V. and C. Chinopoulos (2006). "Bioenergetics and the formation of mitochondrial reactive oxygen species." Trends Pharmacol Sci **27**(12): 639-45.

Aebersold, R. and M. Mann (2003). "Mass spectrometry-based proteomics." Nature **422**(6928): 198-207.

Ahmad, S. and M. M. Gromiha (2002). "NETASA: neural network based prediction of solvent accessibility." Bioinformatics **18**(6): 819-24.

Ahmed, N., D. Dobler, et al. (2005). "Peptide mapping identifies hotspot site of modification in human serum albumin by methylglyoxal involved in ligand binding and esterase activity." J Biol Chem **280**(7): 5724-32.

Alderton, A. L., C. Faustman, et al. (2003). "Induction of redox instability of bovine myoglobin by adduction with 4-hydroxy-2-nonenal." Biochemistry **42**(15): 4398-405.

Aldini, G., I. Dalle-Donne, et al. (2005). "Covalent modification of actin by 4-hydroxy-trans-2-nonenal (HNE): LC-ESI-MS/MS evidence for Cys374 Michael adduction." J Mass Spectrom **40**(7): 946-54.

Amici, A., R. L. Levine, et al. (1989). "Conversion of amino acid residues in proteins and amino acid homopolymers to carbonyl derivatives by metal-catalyzed oxidation reactions." J Biol Chem **264**(6): 3341-6.

Andreyev, A. Y., Y. E. Kushnareva, et al. (2005). "Mitochondrial metabolism of reactive oxygen species." Biochemistry (Mosc) **70**(2): 200-14.

Asselin, C., B. Bouchard, et al. (2006). "Circulating 4-hydroxynonenal-protein thioether adducts assessed by gas chromatography-mass spectrometry are increased with disease progression and aging in spontaneously hypertensive rats." Free Radic Biol Med **41**(1): 97-105.

Ayyadevara, S., M. R. Engle, et al. (2005). "Lifespan and stress resistance of Caenorhabditis elegans are increased by expression of glutathione transferases capable of metabolizing the lipid peroxidation product 4-hydroxynonenal." Aging Cell **4**(5): 257-71.

Babcock, G. T. and M. Wikstrom (1992). "Oxygen activation and the conservation of energy in cell respiration." Nature **356**(6367): 301-9.

Bahar, G., R. Feinmesser, et al. (2007). "Salivary analysis in oral cancer patients: DNA and protein oxidation, reactive nitrogen species, and antioxidant profile." Cancer **109**(1): 54-9.

Barja, G. and A. Herrero (1998). "Localization at complex I and mechanism of the higher free radical production of brain nonsynaptic mitochondria in the short-lived rat than in the longevous pigeon." J Bioenerg Biomembr **30**(3): 235-43.

Beausoleil, S. A., M. Jedrychowski, et al. (2004). "Large-scale characterization of HeLa cell nuclear phosphoproteins." Proc Natl Acad Sci U S A **101**(33): 12130-5.

Beckman, K. B. and B. N. Ames (1998). "The free radical theory of aging matures." Physiol Rev **78**(2): 547-81.

Benderdour, M., G. Charron, et al. (2003). "Cardiac mitochondrial NADP+-isocitrate dehydrogenase is inactivated through 4-hydroxynonenal adduct formation: an event that precedes hypertrophy development." J Biol Chem **278**(46): 45154-9.

Benedetti, A., M. Comporti, et al. (1980). "Identification of 4-hydroxynonenal as a cytotoxic product originating from the peroxidation of liver microsomal lipids." Biochim Biophys Acta **620**(2): 281-96.

Bennaars-Eiden, A., L. Higgins, et al. (2002). "Covalent modification of epithelial fatty acid-binding protein by 4-hydroxynonenal in vitro and in vivo. Evidence for a role in antioxidant biology." J Biol Chem **277**(52): 50693-702.

Berlett, B. S. and E. R. Stadtman (1997). "Protein oxidation in aging, disease, and oxidative stress." J Biol Chem **272**(33): 20313-6.

Bolgar, M. a. G. S. (1996). "Determination of the Sites of 4-Hydroxy-2-nonenal Adduction to Protein by Electrospray Tandem Mass Spectrometry." Anal Chem **68**: 2325-2330.

Bolgar, M. S. G., S.J. (1996). "Determination of the Sites of 4-Hydroxy-2-nonenal Adduction to Protein by Electrospray Tandem Mass Spectrometry." Anal Chem **68**(14): 2325-2330.

Breusing, N. and T. Grune (2008). "Regulation of proteasome-mediated protein degradation during oxidative stress and aging." Biol Chem **389**(3): 203-9.

Bruns, C. M., I. Hubatsch, et al. (1999). "Human glutathione transferase A4-4 crystal structures and mutagenesis reveal the basis of high catalytic efficiency with toxic lipid peroxidation products." J Mol Biol **288**(3): 427-39.

Bulteau, A. L., L. I. Szweda, et al. (2002). "Age-dependent declines in proteasome activity in the heart." Arch Biochem Biophys **397**(2): 298-304.

Bunyapaiboonsri, T., O. Ramstrom, et al. (2001). "Dynamic deconvolution of a pre-equilibrated dynamic combinatorial library of acetylcholinesterase inhibitors." Chembiochem **2**(6): 438-44.

Butterfield, D. A., T. Reed, et al. (2006). "Elevated protein-bound levels of the lipid peroxidation product, 4-hydroxy-2-nonenal, in brain from persons with mild cognitive impairment." Neurosci Lett **397**(3): 170-3.

Cadenas, E., A. Boveris, et al. (1977). "Production of superoxide radicals and hydrogen peroxide by NADH-ubiquinone reductase and ubiquinol-cytochrome c reductase from beef-heart mitochondria." Arch Biochem Biophys **180**(2): 248-57.

Calingasan, N. Y., K. Uchida, et al. (1999). "Protein-bound acrolein: a novel marker of oxidative stress in Alzheimer's disease." J Neurochem **72**(2): 751-6.

Canuto, R. A., M. Ferro, et al. (1994). "Role of aldehyde metabolizing enzymes in mediating effects of aldehyde products of lipid peroxidation in liver cells." Carcinogenesis **15**(7): 1359-64.

Carbone, D. L., J. A. Doorn, et al. (2005). "Modification of heat shock protein 90 by 4-hydroxynonenal in a rat model of chronic alcoholic liver disease." J Pharmacol Exp Ther **315**(1): 8-15.

Carbone, D. L., J. A. Doorn, et al. (2005). "Cysteine modification by lipid peroxidation products inhibits protein disulfide isomerase." Chem Res Toxicol **18**(8): 1324-31.

Carbone, D. L., J. A. Doorn, et al. (2004). "Inhibition of Hsp72-mediated protein refolding by 4-hydroxy-2-nonenal." Chem Res Toxicol **17**(11): 1459-67.

Castegna, A., M. Aksenov, et al. (2002). "Proteomic identification of oxidatively modified proteins in Alzheimer's disease brain. Part I: creatine kinase BB,

glutamine synthase, and ubiquitin carboxy-terminal hydrolase L-1." Free Radic Biol Med **33**(4): 562-71.

Castegna, A., M. Aksenov, et al. (2002). "Proteomic identification of oxidatively modified proteins in Alzheimer's disease brain. Part II: dihydropyrimidinase-related protein 2, alpha-enolase and heat shock cognate 71." J Neurochem **82**(6): 1524-32.

Catala, A. (2009). "Lipid peroxidation of membrane phospholipids generates hydroxy-alkenals and oxidized phospholipids active in physiological and/or pathological conditions." Chem Phys Lipids **157**(1): 1-11.

Chakravarti, B. and D. N. Chakravarti (2007). "Oxidative modification of proteins: age-related changes." Gerontology **53**(3): 128-39.

Chavez, J., J. Wu, et al. (2006). "New role for an old probe: affinity labeling of oxylipid protein conjugates by N'-aminooxymethylcarbonylhydrazino d-biotin." Anal Chem **78**(19): 6847-54.

Chelius, D. and T. A. Shaler (2003). "Capture of peptides with N-terminal serine and threonine: a sequence-specific chemical method for Peptide mixture simplification." Bioconjug Chem **14**(1): 205-11.

Chen, H. S., T. Rejtar, et al. (2005). "High-speed, high-resolution monolithic capillary LC-MALDI MS using an off-line continuous deposition interface for proteomic analysis." Anal Chem **77**(8): 2323-31.

Chen, Y., J. D. Morrow, et al. (1999). "Formation of reactive cyclopentenone compounds in vivo as products of the isoprostane pathway." J Biol Chem **274**(16): 10863-8.

Chen, Y., W. E. Zackert, et al. (1999). "Evidence for the formation of a novel cyclopentenone isoprostane, 15-A2t-isoprostane (8-iso-prostaglandin A2) in vivo." Biochim Biophys Acta **1436**(3): 550-6.

Chevion, M., E. Berenshtein, et al. (2000). "Human studies related to protein oxidation: protein carbonyl content as a marker of damage." Free Radic Res **33 Suppl**: S99-108.

Chiarpotto, E., F. Biasi, et al. (1995). "Metabolism of 4-hydroxy-2-nonenal and aging." Biochem Biophys Res Commun **207**(2): 477-84.

Choksi, K. B., W. H. Boylston, et al. (2004). "Oxidatively damaged proteins of heart mitochondrial electron transport complexes." Biochim Biophys Acta **1688**(2): 95-101.

Choksi, K. B., J. E. Nuss, et al. (2007). "Age-related increases in oxidatively damaged proteins of mouse kidney mitochondrial electron transport chain complexes." Free Radic Biol Med **43**(10): 1423-38.

Choksi, K. B., J. E. Nuss, et al. (2008). "Age-related alterations in oxidatively damaged proteins of mouse skeletal muscle mitochondrial electron transport chain complexes." Free Radic Biol Med **45**(6): 826-38.

Codreanu, S. G., B. Zhang, et al. (2009). "Global analysis of protein damage by the lipid electrophile 4-hydroxy-2-nonenal." Mol Cell Proteomics **8**(4): 670-80.

Conrad, C. C., J. Choi, et al. (2001). "Identification of protein carbonyls after two-dimensional electrophoresis." Proteomics **1**(7): 829-34.

Dalle-Donne, I., G. Aldini, et al. (2006). "Protein carbonylation, cellular dysfunction, and disease progression." J Cell Mol Med **10**(2): 389-406.

Dalle-Donne, I., D. Giustarini, et al. (2003). "Protein carbonylation in human diseases." Trends Mol Med **9**(4): 169-76.

Dalle-Donne, I., R. Rossi, et al. (2006). "Biomarkers of oxidative damage in human disease." Clin Chem **52**(4): 601-23.

Dalle-Donne, I., A. Scaloni, et al. (2005). "Proteins as biomarkers of oxidative/nitrosative stress in diseases: the contribution of redox proteomics." Mass Spectrom Rev **24**(1): 55-99.

Davies, M. J., S. Fu, et al. (1999). "Stable markers of oxidant damage to proteins and their application in the study of human disease." Free Radic Biol Med **27**(11-12): 1151-63.

Del Corso, A., M. Dal Monte, et al. (1998). "Site-specific inactivation of aldose reductase by 4-hydroxynonenal." Arch Biochem Biophys **350**(2): 245-8.

Dey, S., M. Guha, et al. (2009). "Malarial infection develops mitochondrial pathology and mitochondrial oxidative stress to promote hepatocyte apoptosis." Free Radic Biol Med **46**(2): 271-81.

Domon, B. and R. Aebersold (2006). "Mass spectrometry and protein analysis." Science **312**(5771): 212-7.

Doorn, J. A., T. D. Hurley, et al. (2006). "Inhibition of human mitochondrial aldehyde dehydrogenase by 4-hydroxynon-2-enal and 4-oxonon-2-enal." Chem Res Toxicol **19**(1): 102-10.

Drake, J., R. Petroze, et al. (2004). "4-Hydroxynonenal oxidatively modifies histones: implications for Alzheimer's disease." Neurosci Lett **356**(3): 155-8.

Ellis, E. M. (2007). "Reactive carbonyls and oxidative stress: potential for therapeutic intervention." Pharmacol Ther **115**(1): 13-24.

Eng, J. K., McCormack, A.L. & Yates, J.R. III (1994). "An approach to correlate mass spectral data of peptides with amino acid sequences in a protein database." J Am Soc Mass Spectrom **5**: 976-989.

Engle, M. R., S. P. Singh, et al. (2004). "Physiological role of mGSTA4-4, a glutathione S-transferase metabolizing 4-hydroxynonenal: generation and analysis of mGsta4 null mouse." Toxicol Appl Pharmacol **194**(3): 296-308.

Esterbauer, H., R. J. Schaur, et al. (1991). "Chemistry and biochemistry of 4-hydroxynonenal, malonaldehyde and related aldehydes." Free Radic Biol Med **11**(1): 81-128.

Eugene Kapp, F. S. (2007). "Overview of Tandem Mass Spectrometry (MS/MS) Database Search Algorithms." Curr. Protoc. Protein Sci. **49**: 25.2.1-25.2.19.

Fang, J. and A. Holmgren (2006). "Inhibition of thioredoxin and thioredoxin reductase by 4-hydroxy-2-nonenal in vitro and in vivo." J Am Chem Soc **128**(6): 1879-85.

Farout, L., J. Mary, et al. (2006). "Inactivation of the proteasome by 4-hydroxy-2-nonenal is site specific and dependant on 20S proteasome subtypes." Arch Biochem Biophys **453**(1): 135-42.

Fenaille, F., V. Parisod, et al. (2005). "Carbonylation of milk powder proteins as a consequence of processing conditions." Proteomics **5**(12): 3097-104.

Fenaille, F., J. C. Tabet, et al. (2002). "Immunoaffinity purification and characterization of 4-hydroxy-2-nonenal- and malondialdehyde-modified peptides by electrospray ionization tandem mass spectrometry." Anal Chem **74**(24): 6298-304.

Fenaille, F., J. C. Tabet, et al. (2004). "Identification of 4-hydroxy-2-nonenal-modified peptides within unfractionated digests using matrix-assisted laser desorption/ionization time-of-flight mass spectrometry." Anal Chem **76**(4): 867-73.

Feng, J., H. Xie, et al. (2008). "Quantitative proteomic profiling of muscle type-dependent and age-dependent protein carbonylation in rat skeletal muscle mitochondria." J Gerontol A Biol Sci Med Sci **63**(11): 1137-52.

Fenn, J. B., M. Mann, et al. (1989). "Electrospray ionization for mass spectrometry of large biomolecules." Science **246**(4926): 64-71.

Ferrington, D. A. and R. J. Kapphahn (2004). "Catalytic site-specific inhibition of the 20S proteasome by 4-hydroxynonenal." FEBS Lett **578**(3): 217-23.

Ficarro, S. B., M. L. McCleland, et al. (2002). "Phosphoproteome analysis by mass spectrometry and its application to Saccharomyces cerevisiae." Nat Biotechnol **20**(3): 301-5.

Fridovich, I. (1995). "Superoxide radical and superoxide dismutases." Annu Rev Biochem **64**: 97-112.

Friguet, B. and L. I. Szweda (1997). "Inhibition of the multicatalytic proteinase (proteasome) by 4-hydroxy-2-nonenal cross-linked protein." FEBS Lett **405**(1): 21-5.

Fukui, T., N. Ishizaka, et al. (1997). "p22phox mRNA expression and NADPH oxidase activity are increased in aortas from hypertensive rats." Circ Res **80**(1): 45-51.

Gil, L., W. Siems, et al. (2006). "Age-associated analysis of oxidative stress parameters in human plasma and erythrocytes." Free Radic Res **40**(5): 495-505.

Goldstein, S., D. Meyerstein, et al. (1993). "The Fenton reagents." Free Radic Biol Med **15**(4): 435-45.

Gorg, A., W. Weiss, et al. (2004). "Current two-dimensional electrophoresis technology for proteomics." Proteomics **4**(12): 3665-85.

Griffin, T. J., S. P. Gygi, et al. (2001). "Quantitative proteomic analysis using a MALDI quadrupole time-of-flight mass spectrometer." Anal Chem **73**(5): 978-86.

Griffin, T. J., C. M. Lock, et al. (2003). "Abundance ratio-dependent proteomic analysis by mass spectrometry." Anal Chem **75**(4): 867-74.

Griffin, T. J., H. Xie, et al. (2007). "iTRAQ reagent-based quantitative proteomic analysis on a linear ion trap mass spectrometer." J Proteome Res **6**(11): 4200-9.

Grimsrud, P. A., M. J. Picklo, Sr., et al. (2007). "Carbonylation of adipose proteins in obesity and insulin resistance: identification of adipocyte fatty acid-binding protein as a cellular target of 4-hydroxynonenal." Mol Cell Proteomics **6**(4): 624-37.

Grimsrud, P. A., H. Xie, et al. (2008). "Oxidative stress and covalent modification of protein with bioactive aldehydes." J Biol Chem **283**(32): 21837-41.

Gu, X., W. Zhang, et al. (2007). "Fe2+ catalyzes vitamin E-induced fragmentation of hydroperoxy and hydroxy endoperoxides that generates gamma-hydroxy alkenals." J Am Chem Soc **129**(19): 6088-9.

Gygi, S. P., G. L. Corthals, et al. (2000). "Evaluation of two-dimensional gel electrophoresis-based proteome analysis technology." Proc Natl Acad Sci U S A **97**(17): 9390-5.

Gygi, S. P., B. Rist, et al. (1999). "Quantitative analysis of complex protein mixtures using isotope-coded affinity tags." Nat Biotechnol **17**(10): 994-9.

Hajkova, D., K. C. Rao, et al. (2006). "pH dependency of the carboxyl oxygen exchange reaction catalyzed by lysyl endopeptidase and trypsin." J Proteome Res **5**(7): 1667-73.

Ham, A. J. and D. C. Liebler (1995). "Vitamin E oxidation in rat liver mitochondria." Biochemistry **34**(17): 5754-61.

Han, B., J. F. Stevens, et al. (2007). "Design, synthesis, and application of a hydrazide-functionalized isotope-coded affinity tag for the quantification of oxylipid-protein conjugates." Anal Chem **79**(9): 3342-54.

Hansford, R. G., B. A. Hogue, et al. (1997). "Dependence of H2O2 formation by rat heart mitochondria on substrate availability and donor age." J Bioenerg Biomembr **29**(1): 89-95.

Hardman, M. and A. A. Makarov (2003). "Interfacing the orbitrap mass analyzer to an electrospray ion source." Anal Chem **75**(7): 1699-705.

Harman, D. (1956). "Aging: a theory based on free radical and radiation chemistry." J Gerontol **11**(3): 298-300.

Harman, D. (1972). "The biologic clock: the mitochondria?" J Am Geriatr Soc **20**(4): 145-7.

Harper, M. E., L. Bevilacqua, et al. (2004). "Ageing, oxidative stress, and mitochondrial uncoupling." Acta Physiol Scand **182**(4): 321-31.

Heller, M., H. Mattou, et al. (2003). "Trypsin catalyzed 16O-to-18O exchange for comparative proteomics: tandem mass spectrometry comparison using MALDI-TOF, ESI-QTOF, and ESI-ion trap mass spectrometers." J Am Soc Mass Spectrom **14**(7): 704-18.

Hirst, J., J. Carroll, et al. (2003). "The nuclear encoded subunits of complex I from bovine heart mitochondria." Biochim Biophys Acta **1604**(3): 135-50.

Honzatko, A., J. Brichac, et al. (2005). "Enantioselective metabolism of trans-4-hydroxy-2-nonenal by brain mitochondria." Free Radic Biol Med **39**(7): 913-24.

Hu, Q., R. J. Noll, et al. (2005). "The Orbitrap: a new mass spectrometer." J Mass Spectrom **40**(4): 430-43.

Hubatsch, I., B. Mannervik, et al. (2002). "The cyclopentenone product of lipid peroxidation, 15-A(2t)-isoprostane (8-isoprostaglandin A(2)), is efficiently conjugated with glutathione by human and rat glutathione transferase A4-4." Chem Res Toxicol **15**(9): 1114-8.

Humphries, K. M. and L. I. Szweda (1998). "Selective inactivation of alpha-ketoglutarate dehydrogenase and pyruvate dehydrogenase: reaction of lipoic acid with 4-hydroxy-2-nonenal." Biochemistry **37**(45): 15835-41.

Hunt, D. F., J. R. Yates, 3rd, et al. (1986). "Protein sequencing by tandem mass spectrometry." Proc Natl Acad Sci U S A **83**(17): 6233-7.

Ishii, T., E. Tatsuda, et al. (2003). "Molecular basis of enzyme inactivation by an endogenous electrophile 4-hydroxy-2-nonenal: identification of modification sites in glyceraldehyde-3-phosphate dehydrogenase." Biochemistry **42**(12): 3474-80.

Isom, A. L., S. Barnes, et al. (2004). "Modification of Cytochrome c by 4-hydroxy- 2-nonenal: evidence for histidine, lysine, and arginine-aldehyde adducts." J Am Soc Mass Spectrom **15**(8): 1136-47.

Itakura, K., T. Oya-Ito, et al. (2000). "Detection of lipofuscin-like fluorophore in oxidized human low-density lipoprotein. 4-hydroxy-2-nonenal as a potential source of fluorescent chromophore." FEBS Lett **473**(2): 249-53.

Iwata, S., J. W. Lee, et al. (1998). "Complete structure of the 11-subunit bovine mitochondrial cytochrome bc1 complex." Science **281**(5373): 64-71.

Johnson, K. L. and D. C. Muddiman (2004). "A method for calculating 16O/18O peptide ion ratios for the relative quantification of proteomes." J Am Soc Mass Spectrom **15**(4): 437-45.

JW, H. (2002). "A new linear ion trap mass spectrometer." Rapid Commun. Mass Spectrom. **16**: 512-526.

Kapphahn, R. J., B. M. Giwa, et al. (2006). "Retinal proteins modified by 4-hydroxynonenal: identification of molecular targets." Exp Eye Res **83**(1): 165-75.

Karas, M. and F. Hillenkamp (1988). "Laser desorption ionization of proteins with molecular masses exceeding 10,000 daltons." Anal Chem **60**(20): 2299-301.

Keller, A., A. I. Nesvizhskii, et al. (2002). "Empirical statistical model to estimate the accuracy of peptide identifications made by MS/MS and database search." Anal Chem **74**(20): 5383-92.

Keller, J. N., K. B. Hanni, et al. (2000). "Impaired proteasome function in Alzheimer's disease." J Neurochem **75**(1): 436-9.

Kim, C. H., Y. Zou, et al. (2006). "Proteomic analysis of nitrated and 4-hydroxy-2-nonenal-modified serum proteins during aging." J Gerontol A Biol Sci Med Sci **61**(4): 332-8.

Kim, S. Y., T. B. Kim, et al. (2008). "Regulation of pro-inflammatory responses by lipoxygenases via intracellular reactive oxygen species in vitro and in vivo." Exp Mol Med **40**(4): 461-76.

Klose, J. (1975). "Protein mapping by combined isoelectric focusing and electrophoresis of mouse tissues. A novel approach to testing for induced point mutations in mammals." Humangenetik **26**(3): 231-43.

Kudin, A. P., N. Y. Bimpong-Buta, et al. (2004). "Characterization of superoxide-producing sites in isolated brain mitochondria." J Biol Chem **279**(6): 4127-35.

Kushnareva, Y., A. N. Murphy, et al. (2002). "Complex I-mediated reactive oxygen species generation: modulation by cytochrome c and NAD(P)+ oxidation-reduction state." Biochem J **368**(Pt 2): 545-53.

Kussmaul, L. and J. Hirst (2006). "The mechanism of superoxide production by NADH:ubiquinone oxidoreductase (complex I) from bovine heart mitochondria." Proc Natl Acad Sci U S A **103**(20): 7607-12.

Laakso, J. T., T. L. Teravainen, et al. (2004). "Renal xanthine oxidoreductase activity during development of hypertension in spontaneously hypertensive rats." J Hypertens **22**(7): 1333-40.

Lacy, F., D. A. Gough, et al. (1998). "Role of xanthine oxidase in hydrogen peroxide production." Free Radic Biol Med **25**(6): 720-7.

Lambert, A. J. and M. D. Brand (2004). "Inhibitors of the quinone-binding site allow rapid superoxide production from mitochondrial NADH:ubiquinone oxidoreductase (complex I)." J Biol Chem **279**(38): 39414-20.

Lee, S., N. L. Young, et al. (2006). "Method to site-specifically identify and quantitate carbonyl end products of protein oxidation using oxidation-dependent element coded affinity tags (O-ECAT) and nanoliquid chromatography fourier transform mass spectrometry." J Proteome Res **5**(3): 539-47.

Lee, S. H., T. Oe, et al. (2001). "Vitamin C-induced decomposition of lipid hydroperoxides to endogenous genotoxins." Science **292**(5524): 2083-6.

Lees, A., G. Sen, et al. (2006). "Versatile and efficient synthesis of protein-polysaccharide conjugate vaccines using aminooxy reagents and oxime chemistry." Vaccine **24**(6): 716-29.

Levonen, A. L., A. Landar, et al. (2004). "Cellular mechanisms of redox cell signalling: role of cysteine modification in controlling antioxidant defences in response to electrophilic lipid oxidation products." Biochem J **378**(Pt 2): 373-82.

Levrand, B., Y. Ruff, et al. (2006). "Controlled release of volatile aldehydes and ketones by reversible hydrazone formation--classical" profragrances are getting dynamic." Chem Commun (Camb)(28): 2965-7.

Lin, M. T. and M. F. Beal (2006). "Mitochondrial dysfunction and oxidative stress in neurodegenerative diseases." Nature **443**(7113): 787-95.

Liu, Q., A. K. Raina, et al. (2003). "Hydroxynonenal, toxic carbonyls, and Alzheimer disease." Mol Aspects Med **24**(4-5): 305-13.

Liu, T., W. J. Qian, et al. (2004). "High-throughput comparative proteome analysis using a quantitative cysteinyl-peptide enrichment technology." Anal Chem **76**(18): 5345-53.

Liu, Y., G. Fiskum, et al. (2002). "Generation of reactive oxygen species by the mitochondrial electron transport chain." J Neurochem **80**(5): 780-7.

Loboda, A. V., A. N. Krutchinsky, et al. (2000). "A tandem quadrupole/time-of-flight mass spectrometer with a matrix-assisted laser desorption/ionization source: design and performance." Rapid Commun Mass Spectrom **14**(12): 1047-57.

Louie, J. L., R. J. Kapphahn, et al. (2002). "Proteasome function and protein oxidation in the aged retina." Exp Eye Res **75**(3): 271-84.

Lucas, D. T. and L. I. Szweda (1999). "Declines in mitochondrial respiration during cardiac reperfusion: age-dependent inactivation of alpha-ketoglutarate dehydrogenase." Proc Natl Acad Sci U S A **96**(12): 6689-93.

Makarov, A. (2000). "Electrostatic axially harmonic orbital trapping: a high-performance technique of mass analysis." Anal Chem **72**(6): 1156-62.

Makarov, A., E. Denisov, et al. (2006). "Dynamic range of mass accuracy in LTQ Orbitrap hybrid mass spectrometer." J Am Soc Mass Spectrom **17**(7): 977-82.

Mann, M., R. C. Hendrickson, et al. (2001). "Analysis of proteins and proteomes by mass spectrometry." Annu Rev Biochem **70**: 437-73.

McCord, J. M. and I. Fridovich (1988). "Superoxide dismutase: the first twenty years (1968-1988)." Free Radic Biol Med **5**(5-6): 363-9.

Meany, D. L., H. Xie, et al. (2007). "Identification of carbonylated proteins from enriched rat skeletal muscle mitochondria using affinity chromatography-stable isotope labeling and tandem mass spectrometry." Proteomics **7**(7): 1150-63.

Medzihradszky, K. F., J. M. Campbell, et al. (2000). "The characteristics of peptide collision-induced dissociation using a high-performance MALDI-TOF/TOF tandem mass spectrometer." Anal Chem **72**(3): 552-8.

Mervaala, E. M., Z. J. Cheng, et al. (2001). "Endothelial dysfunction and xanthine oxidoreductase activity in rats with human renin and angiotensinogen genes." Hypertension **37**(2 Part 2): 414-8.

Milne, G. L., E. S. Musiek, et al. (2005). "The cyclopentenone (A2/J2) isoprostanes--unique, highly reactive products of arachidonate peroxidation." Antioxid Redox Signal **7**(1-2): 210-20.

Mirzaei, H., B. Baena, et al. (2008). "Identification of oxidized proteins in rat plasma using avidin chromatography and tandem mass spectrometry." Proteomics **8**(7): 1516-27.

Mirzaei, H. and F. Regnier (2005). "Affinity chromatographic selection of carbonylated proteins followed by identification of oxidation sites using tandem mass spectrometry." Anal Chem **77**(8): 2386-92.

Mirzaei, H. and F. Regnier (2006). "Enrichment of carbonylated peptides using Girard P reagent and strong cation exchange chromatography." Anal Chem **78**(3): 770-8.

Mitchell, A. E., D. Morin, et al. (1995). "Purification, mass spectrometric characterization, and covalent modification of murine glutathione S-transferases." Chem Res Toxicol **8**(8): 1054-62.

Monnier, V. M. (1990). "Nonenzymatic glycosylation, the Maillard reaction and the aging process." J Gerontol **45**(4): B105-11.

Moreau, R., S. H. Heath, et al. (2003). "Age-related increase in 4-hydroxynonenal adduction to rat heart alpha-ketoglutarate dehydrogenase does not cause loss of its catalytic activity." Antioxid Redox Signal **5**(5): 517-27.

Muller, F. L., Y. Liu, et al. (2004). "Complex III releases superoxide to both sides of the inner mitochondrial membrane." J Biol Chem **279**(47): 49064-73.

Murphy, M. P. (2009). "How mitochondria produce reactive oxygen species." Biochem J **417**(1): 1-13.

Nadkarni, D. V. and L. M. Sayre (1995). "Structural definition of early lysine and histidine adduction chemistry of 4-hydroxynonenal." Chem Res Toxicol **8**(2): 284-91.

Nesvizhskii, A. I., O. Vitek, et al. (2007). "Analysis and validation of proteomic data generated by tandem mass spectrometry." Nat Methods **4**(10): 787-97.

Nguyen, R. and I. Huc (2003). "Optimizing the reversibility of hydrazone formation for dynamic combinatorial chemistry." Chem Commun (Camb)(8): 942-3.

Nohl H, J. W. (1980). "The metabolic fate of mitochondrial hydrogen peroxide." Eur J Biochem. **111**(1): 203-210.

Noordermeer, M. A., I. Feussner, et al. (2000). "Oxygenation of (3Z)-alkenals to 4-hydroxy-(2E)-alkenals in plant extracts: a nonenzymatic process." Biochem Biophys Res Commun **277**(1): 112-6.

Okamoto, K., S. Toyokuni, et al. (1994). "Formation of 8-hydroxy-2'-deoxyguanosine and 4-hydroxy-2-nonenal-modified proteins in human renal-cell carcinoma." Int J Cancer **58**(6): 825-9.

Ong, S. E., B. Blagoev, et al. (2002). "Stable isotope labeling by amino acids in cell culture, SILAC, as a simple and accurate approach to expression proteomics." Mol Cell Proteomics **1**(5): 376-86.

Ong, S. E. and M. Mann (2005). "Mass spectrometry-based proteomics turns quantitative." Nat Chem Biol **1**(5): 252-62.

Opii, W. O., V. N. Nukala, et al. (2007). "Proteomic identification of oxidized mitochondrial proteins following experimental traumatic brain injury." J Neurotrauma **24**(5): 772-89.

Orioli, M., G. Aldini, et al. (2005). "LC-ESI-MS/MS determination of 4-hydroxy-trans-2-nonenal Michael adducts with cysteine and histidine-containing peptides as early

markers of oxidative stress in excitable tissues." J Chromatogr B Analyt Technol Biomed Life Sci **827**(1): 109-18.

Ozeki, M., A. Miyagawa-Hayashino, et al. (2005). "Susceptibility of actin to modification by 4-hydroxy-2-nonenal." J Chromatogr B Analyt Technol Biomed Life Sci **827**(1): 119-26.

Pandey, A., A. V. Podtelejnikov, et al. (2000). "Analysis of receptor signaling pathways by mass spectrometry: identification of vav-2 as a substrate of the epidermal and platelet-derived growth factor receptors." Proc Natl Acad Sci U S A **97**(1): 179-84.

Papayannopoulos, I. (1995). "The Interpretation of Collision-Induced Dissocation Tandem Mass Spectra of Pepetides." Mass Spectrometry Reviews **14**: 49-73.

Paravicini, T. M. and R. M. Touyz (2008). "NADPH oxidases, reactive oxygen species, and hypertension: clinical implications and therapeutic possibilities." Diabetes Care **31 Suppl 2**: S170-80.

Park, Y. S., Y. H. Koh, et al. (2003). "Identification of the binding site of methylglyoxal on glutathione peroxidase: methylglyoxal inhibits glutathione peroxidase activity via binding to glutathione binding sites Arg 184 and 185." Free Radic Res **37**(2): 205-11.

Pawlak, K., B. Naumnik, et al. (2004). "Oxidative stress - a link between endothelial injury, coagulation activation, and atherosclerosis in haemodialysis patients." Am J Nephrol **24**(1): 154-61.

Peng, J., J. E. Elias, et al. (2003). "Evaluation of multidimensional chromatography coupled with tandem mass spectrometry (LC/LC-MS/MS) for large-scale protein analysis: the yeast proteome." J Proteome Res **2**(1): 43-50.

Peng, J. and S. P. Gygi (2001). "Proteomics: the move to mixtures." J Mass Spectrom **36**(10): 1083-91.

Petritis, B., W. J. Qian, et al. (2009). "A Simple Procedure for Effective Quenching of Trypsin Activity and Prevention of 18O-Labeling Back-Exchange." J Proteome Res.

Picklo, M. J., T. J. Montine, et al. (2002). "Carbonyl toxicology and Alzheimer's disease." Toxicol Appl Pharmacol **184**(3): 187-97.

Poli, G., R. J. Schaur, et al. (2008). "4-hydroxynonenal: a membrane lipid oxidation product of medicinal interest." Med Res Rev **28**(4): 569-631.

Prokai, L., L. J. Yan, et al. (2007). "Mass spectrometry-based survey of age-associated protein carbonylation in rat brain mitochondria." J Mass Spectrom **42**(12): 1583-9.

Qian, W. J., M. E. Monroe, et al. (2005). "Quantitative proteome analysis of human plasma following in vivo lipopolysaccharide administration using 16O/18O labeling and the accurate mass and time tag approach." Mol Cell Proteomics **4**(5): 700-9.

Rabbani, N. and P. J. Thornalley (2008). "Dicarbonyls linked to damage in the powerhouse: glycation of mitochondrial proteins and oxidative stress." Biochem Soc Trans **36**(Pt 5): 1045-50.

Rajagopalan, S., S. Kurz, et al. (1996). "Angiotensin II-mediated hypertension in the rat increases vascular superoxide production via membrane NADH/NADPH oxidase activation. Contribution to alterations of vasomotor tone." J Clin Invest **97**(8): 1916-23.

Ranish, J. A., E. C. Yi, et al. (2003). "The study of macromolecular complexes by quantitative proteomics." Nat Genet **33**(3): 349-55.

Rauniyar, N., S. M. Stevens, et al. (2009). "Characterization of 4-hydroxy-2-nonenal-modified peptides by liquid chromatography-tandem mass spectrometry using data-dependent acquisition: neutral loss-driven MS3 versus neutral loss-driven electron capture dissociation." Anal Chem **81**(2): 782-9.

Reed, T., M. Perluigi, et al. (2008). "Redox proteomic identification of 4-hydroxy-2-nonenal-modified brain proteins in amnestic mild cognitive impairment: insight into the role of lipid peroxidation in the progression and pathogenesis of Alzheimer's disease." Neurobiol Dis **30**(1): 107-20.

Reed, T. T., W. M. Pierce, et al. (2009). "Proteomic identification of HNE-bound proteins in early Alzheimer disease: Insights into the role of lipid peroxidation in the progression of AD." Brain Res **1274**: 66-76.

Refsgaard, H. H., L. Tsai, et al. (2000). "Modifications of proteins by polyunsaturated fatty acid peroxidation products." Proc Natl Acad Sci U S A **97**(2): 611-6.

Requena, J. R., C. C. Chao, et al. (2001). "Glutamic and aminoadipic semialdehydes are the main carbonyl products of metal-catalyzed oxidation of proteins." Proc Natl Acad Sci U S A **98**(1): 69-74.

Richter, C., J. W. Park, et al. (1988). "Normal oxidative damage to mitochondrial and nuclear DNA is extensive." Proc Natl Acad Sci U S A **85**(17): 6465-7.

Rigoutsos, I. and A. Floratos (1998). "Combinatorial pattern discovery in biological sequences: The TEIRESIAS algorithm." Bioinformatics **14**(1): 55-67.

Roe, M. R. and T. J. Griffin (2006). "Gel-free mass spectrometry-based high throughput proteomics: tools for studying biological response of proteins and proteomes." Proteomics **6**(17): 4678-87.

Roe, M. R., H. Xie, et al. (2007). "Proteomic mapping of 4-hydroxynonenal protein modification sites by solid-phase hydrazide chemistry and mass spectrometry." Anal Chem **79**(10): 3747-56.

Roede, J. R., D. L. Carbone, et al. (2008). "In vitro and in silico characterization of peroxiredoxin 6 modified by 4-hydroxynonenal and 4-oxononenal." Chem Res Toxicol **21**(12): 2289-99.

Ross, P. L., Y. N. Huang, et al. (2004). "Multiplexed protein quantitation in Saccharomyces cerevisiae using amine-reactive isobaric tagging reagents." Mol Cell Proteomics **3**(12): 1154-69.

Sadygov, R. G., D. Cociorva, et al. (2004). "Large-scale database searching using tandem mass spectra: looking up the answer in the back of the book." Nat Methods **1**(3): 195-202.

San Martin, A., P. Du, et al. (2007). "Reactive oxygen species-selective regulation of aortic inflammatory gene expression in Type 2 diabetes." Am J Physiol Heart Circ Physiol **292**(5): H2073-82.

Sayre, L. M., D. Lin, et al. (2006). "Protein adducts generated from products of lipid oxidation: focus on HNE and one." Drug Metab Rev **38**(4): 651-75.

Sazanov, L. A. (2007). "Respiratory complex I: mechanistic and structural insights provided by the crystal structure of the hydrophilic domain." Biochemistry **46**(9): 2275-88.

Schafer, F. Q. and G. R. Buettner (2001). "Redox environment of the cell as viewed through the redox state of the glutathione disulfide/glutathione couple." Free Radic Biol Med **30**(11): 1191-212.

Schneider, C., N. A. Porter, et al. (2004). "Autoxidative transformation of chiral omega6 hydroxy linoleic and arachidonic acids to chiral 4-hydroxy-2E-nonenal." Chem Res Toxicol **17**(7): 937-41.

Schneider, C., N. A. Porter, et al. (2008). "Routes to 4-hydroxynonenal: fundamental issues in the mechanisms of lipid peroxidation." J Biol Chem **283**(23): 15539-43.

Schneider, C., K. A. Tallman, et al. (2001). "Two distinct pathways of formation of 4-hydroxynonenal. Mechanisms of nonenzymatic transformation of the 9- and 13-hydroperoxides of linoleic acid to 4-hydroxyalkenals." J Biol Chem **276**(24): 20831-8.

Schnolzer, M., P. Jedrzejewski, et al. (1996). "Protease-catalyzed incorporation of 18O into peptide fragments and its application for protein sequencing by electrospray and matrix-assisted laser desorption/ionization mass spectrometry." Electrophoresis **17**(5): 945-53.

Schwartz, J. C., M. W. Senko, et al. (2002). "A two-dimensional quadrupole ion trap mass spectrometer." J Am Soc Mass Spectrom **13**(6): 659-69.

Schwartz, J. C., J. P. Syka, et al. (2005). Improving the Fundamentals of Msn on 2D Ion Traps: New Ion Activation and Isolation Techniques. 53rd ASMS Conference on Mass Spectrometry, San Antonio, Texas.

Seo, B. B., M. Marella, et al. (2006). "The single subunit NADH dehydrogenase reduces generation of reactive oxygen species from complex I." FEBS Lett **580**(26): 6105-8.

Sevinsky, J. R., K. J. Brown, et al. (2007). "Minimizing back exchange in 18O/16O quantitative proteomics experiments by incorporation of immobilized trypsin into the initial digestion step." Anal Chem **79**(5): 2158-62.

Shringarpure, R., T. Grune, et al. (2003). "Ubiquitin conjugation is not required for the degradation of oxidized proteins by proteasome." J Biol Chem **278**(1): 311-8.

Shringarpure, R., T. Grune, et al. (2000). "4-Hydroxynonenal-modified amyloid-beta peptide inhibits the proteasome: possible importance in Alzheimer's disease." Cell Mol Life Sci **57**(12): 1802-9.

Siems, W. and T. Grune (2003). "Intracellular metabolism of 4-hydroxynonenal." Mol Aspects Med **24**(4-5): 167-75.

Sies, H. (1991). "Role of reactive oxygen species in biological processes." Klin Wochenschr **69**(21-23): 965-8.

Sies, H. (1997). "Oxidative stress: oxidants and antioxidants." Exp Physiol **82**(2): 291-5.

Sitte, N., M. Huber, et al. (2000). "Proteasome inhibition by lipofuscin/ceroid during postmitotic aging of fibroblasts." FASEB J **14**(11): 1490-8.

Skene, W. G. and J. M. Lehn (2004). "Dynamers: polyacylhydrazone reversible covalent polymers, component exchange, and constitutional diversity." Proc Natl Acad Sci U S A **101**(22): 8270-5.

Sohal, R. S. and R. Weindruch (1996). "Oxidative stress, caloric restriction, and aging." Science **273**(5271): 59-63.

Soreghan, B. A., F. Yang, et al. (2003). "High-throughput proteomic-based identification of oxidatively induced protein carbonylation in mouse brain." Pharm Res **20**(11): 1713-20.

Sorolla, M. A., G. Reverter-Branchat, et al. (2008). "Proteomic and oxidative stress analysis in human brain samples of Huntington disease." Free Radic Biol Med **45**(5): 667-78.

St-Pierre, J., J. A. Buckingham, et al. (2002). "Topology of superoxide production from different sites in the mitochondrial electron transport chain." J Biol Chem **277**(47): 44784-90.

Stadtman, E. R. and B. S. Berlett (1991). "Fenton chemistry. Amino acid oxidation." J Biol Chem **266**(26): 17201-11.

Stadtman, E. R. and R. L. Levine (2003). "Free radical-mediated oxidation of free amino acids and amino acid residues in proteins." Amino Acids **25**(3-4): 207-18.

Stadtman, E. R. and C. N. Oliver (1991). "Metal-catalyzed oxidation of proteins. Physiological consequences." J Biol Chem **266**(4): 2005-8.

Steen, H., B. Kuster, et al. (2002). "Tyrosine phosphorylation mapping of the epidermal growth factor receptor signaling pathway." J Biol Chem **277**(2): 1031-9.

Sultana, R. and D. A. Butterfield (2004). "Oxidatively modified GST and MRP1 in Alzheimer's disease brain: implications for accumulation of reactive lipid peroxidation products." Neurochem Res **29**(12): 2215-20.

Sun, G. and V. E. Anderson (2005). "A strategy for distinguishing modified peptides based on post-digestion 18O labeling and mass spectrometry." Rapid Commun Mass Spectrom **19**(19): 2849-56.

Suzuki, H., F. A. DeLano, et al. (1998). "Xanthine oxidase activity associated with arterial blood pressure in spontaneously hypertensive rats." Proc Natl Acad Sci U S A **95**(8): 4754-9.

Tainer, J. A., E. D. Getzoff, et al. (1983). "Structure and mechanism of copper, zinc superoxide dismutase." Nature **306**(5940): 284-7.

Tanaka, S. (1982). "[Current topics in functioning tumors of the thymus]." Rinsho Kyobu Geka **2**(1): 151-3.

Temple, A., T. Y. Yen, et al. (2006). "Identification of specific protein carbonylation sites in model oxidations of human serum albumin." J Am Soc Mass Spectrom **17**(8): 1172-80.

Thomas, S. N., B. A. Soreghan, et al. (2005). "Reduced neuronal expression of synaptic transmission modulator HNK-1/neural cell adhesion molecule as a potential consequence of amyloid beta-mediated oxidative stress: a proteomic approach." J Neurochem **92**(4): 705-17.

Thornalley, P. J. (1999). "The clinical significance of glycation." Clin. Lab. **45**: 263-273.

Thornalley, P. J., S. Battah, et al. (2003). "Quantitative screening of advanced glycation endproducts in cellular and extracellular proteins by tandem mass spectrometry." Biochem J **375**(Pt 3): 581-92.

Trifunovic, A. and N. G. Larsson (2008). "Mitochondrial dysfunction as a cause of ageing." J Intern Med **263**(2): 167-78.

Trumpower, B. L. (1990). "The protonmotive Q cycle. Energy transduction by coupling of proton translocation to electron transfer by the cytochrome bc1 complex." J Biol Chem **265**(20): 11409-12.

Turrens, J. F. (2003). "Mitochondrial formation of reactive oxygen species." J Physiol **552**(Pt 2): 335-44.

Turrens, J. F., A. Alexandre, et al. (1985). "Ubisemiquinone is the electron donor for superoxide formation by complex III of heart mitochondria." Arch Biochem Biophys **237**(2): 408-14.

Uchida, K. (2003). "Histidine and lysine as targets of oxidative modification." Amino Acids **25**(3-4): 249-57.

Uchida, K., K. Itakura, et al. (1995). "Characterization of epitopes recognized by 4-hydroxy-2-nonenal specific antibodies." Arch Biochem Biophys **324**(2): 241-8.

Uchida, K., M. Shiraishi, et al. (1999). "Activation of stress signaling pathways by the end product of lipid peroxidation. 4-hydroxy-2-nonenal is a potential inducer of intracellular peroxide production." J Biol Chem **274**(4): 2234-42.

Uchida, K. and E. R. Stadtman (1992). "Modification of histidine residues in proteins by reaction with 4-hydroxynonenal." Proc Natl Acad Sci U S A **89**(10): 4544-8.

Uchida, K. and E. R. Stadtman (1992). "Selective cleavage of thioether linkage in proteins modified with 4-hydroxynonenal." Proc Natl Acad Sci U S A **89**(12): 5611-5.

Uchida, K. and E. R. Stadtman (1993). "Covalent attachment of 4-hydroxynonenal to glyceraldehyde-3-phosphate dehydrogenase. A possible involvement of intra- and intermolecular cross-linking reaction." J Biol Chem **268**(9): 6388-93.

Virdis, A., M. F. Neves, et al. (2004). "Role of NAD(P)H oxidase on vascular alterations in angiotensin II-infused mice." J Hypertens **22**(3): 535-42.

Votyakova, T. V. and I. J. Reynolds (2001). "DeltaPsi(m)-Dependent and -independent production of reactive oxygen species by rat brain mitochondria." J Neurochem **79**(2): 266-77.

Wei, J., J. Sun, et al. (2005). "Global proteome discovery using an online three-dimensional LC-MS/MS." J Proteome Res **4**(3): 801-8.

Wolf-Yadlin, A., S. Hautaniemi, et al. (2007). "Multiple reaction monitoring for robust quantitative proteomic analysis of cellular signaling networks." Proc Natl Acad Sci U S A **104**(14): 5860-5.

Wonisch, W., M. Hayn, et al. (1997). "Increased stress parameter synthesis in the yeast Saccharomyces cerevisiae after treatment with 4-hydroxy-2-nonenal." FEBS Lett **405**(1): 11-5.

Wonisch, W., S. D. Kohlwein, et al. (1998). "Treatment of the budding yeast Saccharomyces cerevisiae with the lipid peroxidation product 4-HNE provokes a temporary cell cycle arrest in G1 phase." Free Radic Biol Med **25**(6): 682-7.

Yao, X., A. Freas, et al. (2001). "Proteolytic 18O labeling for comparative proteomics: model studies with two serotypes of adenovirus." Anal Chem **73**(13): 2836-42.

Yarian, C. S., I. Rebrin, et al. (2005). "Aconitase and ATP synthase are targets of malondialdehyde modification and undergo an age-related decrease in activity in mouse heart mitochondria." Biochem Biophys Res Commun **330**(1): 151-6.

Yates, J. R., 3rd (2004). "Mass spectral analysis in proteomics." Annu Rev Biophys Biomol Struct **33**: 297-316.

Yates, J. R., D. Cociorva, et al. (2006). "Performance of a linear ion trap-Orbitrap hybrid for peptide analysis." Anal Chem **78**(2): 493-500.

Yates, J. R., C. I. Ruse, et al. (2009). "Proteomics by mass spectrometry: approaches, advances, and applications." Annu Rev Biomed Eng **11**: 49-79.

Yi, E. C., X. J. Li, et al. (2005). "Increased quantitative proteome coverage with (13)C/(12)C-based, acid-cleavable isotope-coded affinity tag reagent and modified data acquisition scheme." Proteomics **5**(2): 380-7.

Yoo, B. S. and F. E. Regnier (2004). "Proteomic analysis of carbonylated proteins in two-dimensional gel electrophoresis using avidin-fluorescein affinity staining." Electrophoresis **25**(9): 1334-41.

Yoritaka, A., N. Hattori, et al. (1996). "Immunohistochemical detection of 4-hydroxynonenal protein adducts in Parkinson disease." Proc Natl Acad Sci U S A **93**(7): 2696-701.

Yuan, Q., X. Zhu, et al. (2007). "Chemical nature of stochastic generation of protein-based carbonyls: metal-catalyzed oxidation versus modification by products of lipid oxidation." Chem Res Toxicol **20**(1): 129-39.

Zelko, I. N., T. J. Mariani, et al. (2002). "Superoxide dismutase multigene family: a comparison of the CuZn-SOD (SOD1), Mn-SOD (SOD2), and EC-SOD (SOD3) gene structures, evolution, and expression." Free Radic Biol Med **33**(3): 337-49.

Zhang, Q., J. M. Ames, et al. (2009). "A perspective on the Maillard reaction and the analysis of protein glycation by mass spectrometry: probing the pathogenesis of chronic disease." J Proteome Res **8**(2): 754-69.

Zhang, W., M. Sun, et al. (2006). "Preparative singlet oxygenation of linoleate provides doubly allylic dihydroperoxides: putative intermediates in the generation of biologically active aldehydes in vivo." J Org Chem **71**(15): 5607-15.

Zhang, Y., A. Wolf-Yadlin, et al. (2005). "Time-resolved mass spectrometry of tyrosine phosphorylation sites in the epidermal growth factor receptor signaling network reveals dynamic modules." Mol Cell Proteomics **4**(9): 1240-50.

Appendix I

Introduction to Mass Spectrometry in Proteomics

Portions of this appendix are taken from Proteomics, Mikel R. Roe and Timothy J. Griffin, **Gel-free mass spectrometry-based high throughput proteomics: Tools for studying biological response of proteins and proteomes,** vol.6, 4678-4687, copyright 2006 with permission from Wiley InterScience.

Introduction

Mass spectrometry (MS) is a powerful analytical tool for characterizing the primary structure of proteins. Its combination of dynamic range, sensitivity, and resolving power render MS particularly well suited for characterizing complex proteomes (Mann, Hendrickson et al. 2001). Essentially functioning as a molecular balance, MS identifies proteins in samples by matching experimentally measured masses with theoretical masses of proteins. More specifically, mass spectrometers are limited to the analysis of charged analytes, measuring the ratio of a protein's mass-to-charge from which its mass is easily extrapolated.

Anatomy of a mass spectrometer

In general, mass spectrometers contain three separate components: an ion source, a mass analyzer, and a detector (figure 1). Analytes entering mass spectrometers are first ionized so as to enable their subsequent manipulation in the mass analyzer, and ultimately their detection by the detector. Once ionized, analytes pass through the mass analyzer where they are selectively filtered based on their mass-to-charge ratio, and finally sent to an electron multiplier detector. Thus, the intensity of each analyte entering the mass analyzer is measured, and ultimately plotted against its mass-to-charge ratio.

In proteomics the two primary ionization techniques used are matrix assisted laser desporption ionization (MALDI), and electrospray ionization (ESI) (figure 1) (Karas and Hillenkamp 1988; Fenn, Mann et al. 1989). For MALDI, proteins are mixed with an

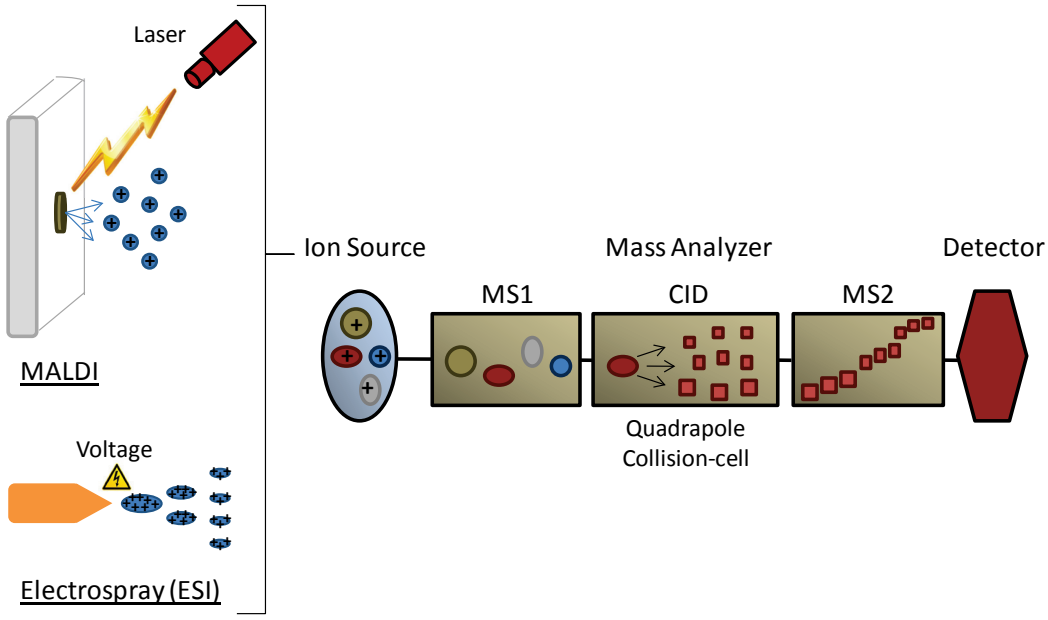

Figure 1. Basic diagram of mass spectrometers used in tandem mass spectrometry

The general compartments of a mass spectrometer are the ion source, the mass analyzer, and the ion detector. The MALDI (matrix assisted laser desorption ionization) ion source uses a laser to vaporize peptides from a metal plate where they are co-crystalized with an acidic matrix. The ESI (electrospray) source ionizes peptides in solution by exciting the sample solvent to the point that it loses cohesion and evaporates to form a fine aerosol. Once ionized, peptides are sent to the mass analyzer which measures their mass-to-charge ratio, selects individual ions to be fragmented by collision induced dissociation (CID) in the collision-cell, and measures the m/z of the resulting fragment ions. The intensity of ions before and after CID fragmentation is measured by the ion detector.

acidic matrix, dried on a metal plate, and then ionized by sublimation using a nitrogen laser(Karas and Hillenkamp 1988). The matrix is critical to the success of this technique, as it functions to improve ionization and vaporization of proteins while also preventing their destruction by the laser. MALDI ion sources are most commonly combined with time-of-flight (TOF) mass analyzers (described later) as their pulsed delivery of ions works well with the mechanism by which TOF analyzers operate. Indeed, MALDI-TOF mass spectrometers are typically the preferred instruments for identifying proteins within gel-spots extracted from 2-DE gels(Aebersold and Mann 2003).

Whereas MALDI operates on proteins in solid-phase, ESI ionizes proteins in solution (Fenn, Mann et al. 1989). Specifically, solvents carrying protein analytes are exposed to high voltage (2-6 kV) as they elute from a separation column so as to generate enough electrostatic-repulsion to overcome the solvent surface tension and force the liquid to aerosolize. Several subsequent cycles of solvent evaporation and fission of droplets releases protons and some analyte until small droplets containing a single analyte and a few protons remain. The resulting droplets of ionized analytes are continuously streamed into the mass spectrometer, and the detected mass-to-charge ratios are plotted against ion intensity. During this process, protons are freely added to the analyte, such that larger analytes typically accumulate greater protons. This is in stark contrast to MALDI where analytes generally carry a single proton. As a solution-phase ionization technique, ESI seamlessly combines with microscale liquid chromatography fractionation to provide greater coverage of proteins than is achieved by MS alone (Yates, Ruse et al. 2009). ESI

sources have been combined with a wide range of mass analyzers and are generally preferred for profiling proteomes of complex mixtures (Aebersold and Mann 2003).

While a number of mass analyzers have been developed since the dawning of the mass spectrometry proteomic era, each with its own benefits and limitations, I will only comment on those utilized in my thesis research (Domon and Aebersold 2006). The time-of-flight (TOF) mass analyzer alluded to above converts the time required for ions to travel through a flight-tube under vacuum into a mass-to-charge ratio. The TOF analyzers offer a combination of good mass accuracy, resolution, and dynamic range but are largely limited to MALDI ion sources, which has traditionally limited their throughput (Aebersold and Mann 2003; Domon and Aebersold 2006). Conversely, linear ion traps (LIT) are comprised of a set of quadrapole rods that isolate ions by manipulating the radio frequency within the trap (JW 2002; Schwartz, Senko et al. 2002). While the rapid accumulation and detection of ions renders the LIT a sensitive high-throughput instrument, it suffers from low mass accuracy and low resolving power (Domon and Aebersold 2006). Alternatively, orbitrap mass analyzers measure the frequency by which ions orbit about a central electrode within a 3D-trap, which is then converted to a mass-to-charge ratio (Makarov 2000; Hardman and Makarov 2003; Hu, Noll et al. 2005). Orbitraps are highly advanced mass analyzers capable of sensitive high-throughput analysis, with excellent mass accuracy, resolution, and dynamic range (Hu, Noll et al. 2005; Makarov, Denisov et al. 2006; Yates, Ruse et al. 2009).

The mass spectrometers employed for proteomics research usually incorporate multiple mass analyzers in series so as to gain the greatest depth of information possible from samples being analyzed (table 1). This is especially important for protein identification by tandem mass spectrometry where iterative mass measurements are required (see below). These instruments either use the same type of mass analyzer in succession, as in MALDI-TOF/TOF, or combine various mass analyzers as seen for quadrapole-TOF (Q-TOFs) and LIT-Orbitraps (Loboda, Krutchinsky et al. 2000; Medzihradszky, Campbell et al. 2000; Makarov, Denisov et al. 2006). The latter group of instruments effectively combines the strengths of the different mass analyzers employed to provide highly versatile hybrid mass spectrometers. For example, LIT-Orbitraps utilize the high mass accuracy and mass resolution of the Orbitrap to measure tryptic peptide masses, while the LIT provides a rapid but less accurate measurement of the subsequent peptide fragment ions (Makarov, Denisov et al. 2006). This combination enables high throughput, high mass accuracy proteomic analysis of complex mixtures, and is a significant advancement in the field of biological mass spectrometry (Yates, Cociorva et al. 2006).

Tandem mass spectrometry

Tandem mass spectrometry (MS/MS) analysis of enzymatically cleaved proteins has proven invaluable for characterizing the proteomes of complex biological mixtures (Yates 2004). By interrogating the amino acid composition of peptides, the MS/MS approach offers the unambiguous identification of proteins, and enables the detection and localization of post-translational modifications that may be present (Pandey,

Table 1. Composition and analytical qualities of select mass spectrometers

Instrument	Ion Source	MS1	MS2	Sensitivity	Throughput	Mass Accuracy	Resolving Power
Qstar-XL	MALDI	Quadrapole	TOF	Good	Good	Good	Good
ABI 4800	MALDI	TOF	TOF	High	Good	Good	High
LTQ	ESI	LIT	_	Good	High	Low	Low
LTQ-Orbitrap	ESI	LIT	Orbitrap	High	High	High	High

Podtelejnikov et al. 2000; Peng and Gygi 2001; Ficarro, McCleland et al. 2002; Steen, Kuster et al. 2002; Roe and Griffin 2006). When combined with front-end sample fractionation, such as microscale liquid chromatography (μLC), MS/MS is capable of identifying thousands of unique proteins in a single analysis (Wei, Sun et al. 2005). Indeed, this proteomic platform (μLC -MS/MS) has enabled the systematic characterization of a wide array of complex proteomes(Mann, Hendrickson et al. 2001).

Known as a 'bottom-up' proteomic approach, μLC-MS/MS identifies proteins by sequencing their constituent peptides (Yates, Ruse et al. 2009). Specifically, complex mixtures of proteins are digested to peptides (usually using the hydrolytic enzyme trypsin), separated based upon hydrophobicity by μLC, and the eluted peptides introduced into the mass spectrometer (figure 2). In the most common format, the peptides eluting from the μLC column are directly introduced into the mass spectrometer via online ESI, although more recently offline spotting of peptides onto sample targets and use of MALDI instruments capable of relatively high throughput MS/MS analysis has been described (Griffin, Gygi et al. 2001; Chen, Rejtar et al. 2005). Once ionized, the tryptic peptides are detected over a wide m/z range, and then single peptide species are isolated within the mass spectrometer, usually via a quadrapole mass filter and subjected to fragmentation by collision-induced-dissociation (CID) (figure 1 and 2) (Hunt, Yates et al. 1986). The resulting peptide fragment ions are produced by random cleavage of the

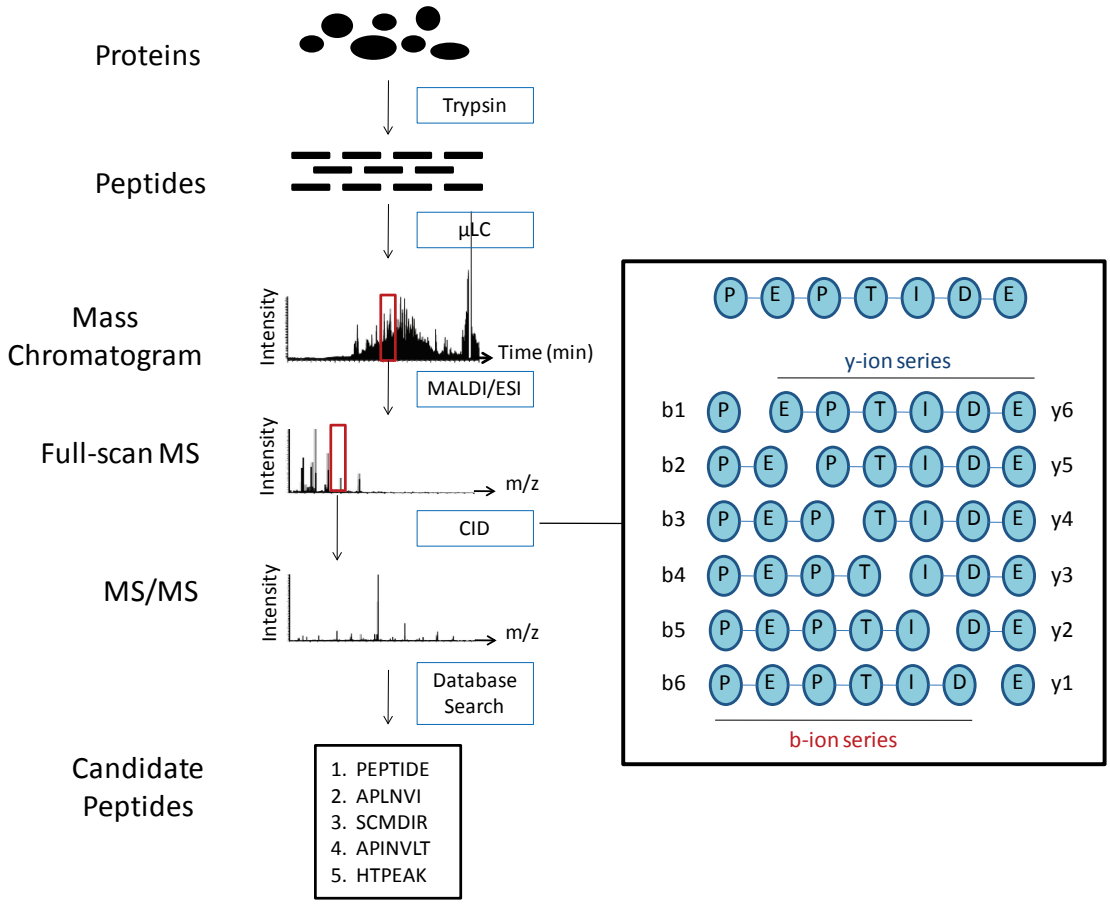

Figure 2. General workflow of the liquid-chromatograpy tandem mass spectrometry experiment. Peptides isolated from protein digests are separated by reverse-phase microscale liquid chromatograpy (µLC) and sequentially analyzed by mass spectrometry to generate a mass chromatogram. Throughout the solvent gradient, peptides eluted into the mass spectrometer are detected and selected for CID, generating both a MS and MS/MS spectrum for each fragmented peptide. CID fragmentation randomly cleaves peptide bonds within the peptide backbone, generating a latter of overlapping fragment ions that contain either the amino (b-ions) or carboxy (y-ions) terminus of the peptide. The resulting MS/MS spectra are searched against a proteomic database, which generates a list of candidate peptide sequences that best match the spectra.

peptide backbone, and subsequently detected in a second mass spectrum. This routine is repeated continuously and automatically over the gradient profile of the μLC, resulting in the acquisition of hundreds to thousands of MS/MS fragmentation spectra. The final step in this process is the identification of the proteins from the starting mixture by automated protein sequence database searching of the MS/MS fragmentation spectra (Sadygov, Cociorva et al. 2004; Nesvizhskii, Vitek et al. 2007).

Fragmentation of peptides by CID within the collision-cell produces a variety of fragment ions (Papayannopoulos 1995). Each peptide is usually cleaved only once at a random peptide bond, generating a latter of overlapping fragment ions that extend from both the amino (b-ions) and carboxy (y-ions) terminus of the peptide, and incrementally increase in mass, one amino acid at a time (figure 2). Thus, the sequence of amino acids that form the tryptic peptide can be reconstructed simply by subtracting the masses of fragment ions derived from the amino or carboxy termini, and often a combination of the two.

In addition to these larger ions, internal fragmentation of individual amino acid residues by cleavage of both the peptide and carbon-carbon bond produces small mass fragments known as immonium ions (Papayannopoulos 1995). These ions are unique to each amino acid and their presence in MS/MS spectra help reveal the composition of the peptide under investigation. Where detection of low mass ions is routine for TOF mass analyzers, LITs are inherently poor as they are unable to detect ions in the lower 1/3 of the m/z range for a given MS/MS fragmentation pattern (1/3 rule) (Mann, Hendrickson et

al. 2001). However, the recent development of pulsed-Q-dissociation (PQD) as an alternative to traditional CID overcomes this limitation, thus enabling the consistent detection of immonium and other low mass ions by LIT mass analyzers (Griffin, Xie et al. 2007)).

Post-translational modifications (PTMs) on peptides are also susceptible to cleavage by CID fragmentation (Beausoleil, Jedrychowski et al. 2004). This type of cleavage is known as neutral-loss since the cleaved PTM is usually uncharged and thus undetectable by MS. Conversely, the resulting charged fragment ion represents the full tryptic peptide in its unmodified form, and often suppresses the signal of b and y-ions in the MS/MS spectra. To address this issue a second round of fragmentation on the neutral-loss peak may be conducted (MS/MS/MS) so as to generate a meaningful mass spectrum from which the amino acid sequence of the peptide can be determined. The utility of this approach has been previously demonstrated with phosphorylated and carbonylated peptides (Beausoleil, Jedrychowski et al. 2004; Rauniyar, Stevens et al. 2009).

Manual interpretation of MS/MS spectra is anything but routine, and as result, high throughput proteomics experiments rely heavily on database search engines for determining peptide sequences (Eugene Kapp 2007). Unlike manual interpretation, or *de novo* sequencing, which involves the tedious process of sequencing peptides one amino acid at a time, these search engines seek to identify the whole sequence at once by matching experimentally generated MS/MS spectra to theoretical spectra extrapolated

from a cDNA library (Eugene Kapp 2007). The resulting candidate matches are prioritized based on their similarity with the experimental spectrum, and the top match further statistically scrutinized for accuracy (Keller, Nesvizhskii et al. 2002; Sadygov, Cociorva et al. 2004). In addition, database search engines are amenable for identifying peptides carrying user-defined PTMs. However, the PTM(s) of interest as well as the expected amino acid targets must be specified prior to the search. A number of both commercial and open-source proteomic database search algorithms are available with Sequest, Mascot, and Xtandem the most commonly used (Eugene Kapp 2007).

Comparative proteomics by relative quantitation of peptides using tandem mass spectrometry

While proteomic profiling alone has value for cataloguing the proteins of a given sample, it is of little use to investigators interested in characterizing quantitative proteomic changes that occur in response to various biological insults and throughout progression of diseases. However, by combining tandem mass spectrometry with stable isotope labeling the relative abundance of individual peptides can be reliably measured across multiple samples (Ong and Mann 2005; Roe and Griffin 2006). In this comparative proteomic analysis, the peptides from one sample are labeled with a "light" isotope tag while those from a second sample are labeled with a chemically identical tag containing "heavy" isotopes. After labeling, the samples are combined and the resulting pooled peptides separated by microscale liquid chromatography. Although the peptides common to both samples are differentially labeled with "light" and "heavy" isotopic tags, they retain the same chemical properties and thus behave similarly during purification and separation

procedures. As a result, peptides common to each sample co-elute into the mass spectrometer and appear as isotopic peak pairs, separated by the mass difference of the "light" and "heavy" tags. To calculate the relative abundance of peptide pairs, either the mass spectral peak heights, or the peak areas, are compared. This allows for the measurement of subtle changes (<twofold) in abundance between samples (Griffin, Lock et al. 2003). Although a number of stable isotope labeling reagents are currently available, I will limit discussion to only the two used during the course of my thesis research (Gygi, Rist et al. 1999; Yao, Freas et al. 2001; Ong, Blagoev et al. 2002; Ross, Huang et al. 2004).

The enzymatic labeling of peptides with heavy oxygen (^{18}O) is one proven method for comparative proteomic studies. Originally described by Fenselau and colleagues, this technique uses proteases to specifically catalyze the oxygen-exchange of the two carboxyl oxygen atoms at the carboxy terminus of proteolyzed peptides with oxygen atoms from the surrounding water molecules (figure 3) (Yao, Freas et al. 2001). For comparative proteomic analysis, this reaction is conducted in the presence of light ($H_2{}^{16}O$) water for one sample and heavy ($H_2{}^{18}O$) water for the other. The resulting peptide pairs differ in mass by 4 Da and are thus easily distinguished in the full-scan mass spectrum. Here, the signal intensities of the individual peptides within the peptide pair are compared to determine relative abundance.

Figure 3. ^{18}O and iTRAQ stable isotope labeling strategies for the relative quantitation of peptides. **A**. Relative quantitation of peptides by ^{18}O-labeling. Peptides from two samples are incubated in light ($H_2{}^{16}O$) or heavy ($H_2{}^{18}O$) water, respectively, into which a protease, such as trypsin, has been added. The protease incorporates two oxygens from the solvent into the peptide c-terminal carboxylate, so as to generate a pool of ^{18}O and ^{16}O containing peptides. The samples are combined and analyzed by μLC-MS/MS. Peptides common to both samples appear together in the full-scan mass spectra and are separated by 4 mass units. The signal intensities of their respective ions are used to measure their relative abundance in each sample. Finally, the MS/MS spectra collected following CID fragmentation is used to determine the sequence of the peptide being quantified. **B**. Relative quantitation of peptides by iTRAQ-labeling. Peptides from four, and as many as eight samples are independently labeled with isotopically distinct iTRAQ reagents, which are comprised of ionizable reporter groups that differ in mass, and non-ionizable balance groups that compensate for their respective reporter groups to ensure all iTRAQ reagents have the same mass. Once labeled, the peptide samples are combined and analyzed together by μLC-MS/MS. While peptides common to all samples co-elute into the mass spectrometer, their shared mass renders them indistinguishable in the MS spectrum, appearing instead as a single ion. However, during CID, iTRAQ reagents fragment to generate low-mass reporter ions whose signal intensities are compared to measure peptide abundances within samples relative to each other. The b and y-ions are preserved during this process and are used to determine the amino acid sequence of the peptide.

A.

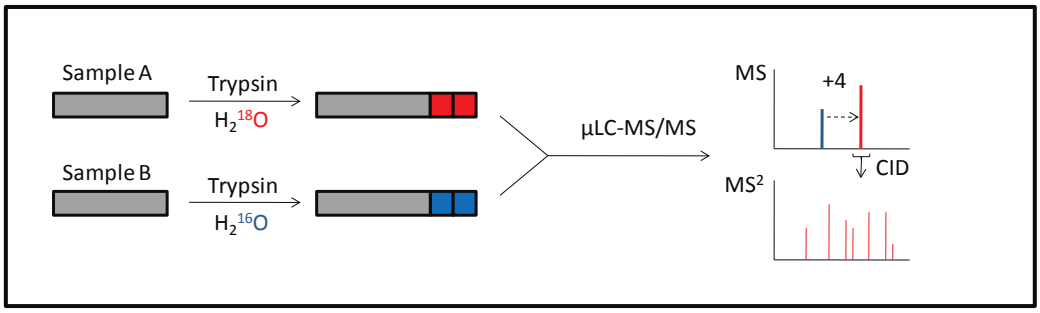
Sample A
Trypsin
$H_2{}^{18}O$
Sample B
Trypsin
$H_2{}^{16}O$
µLC-MS/MS
MS
+4
CID
MS^2

B.

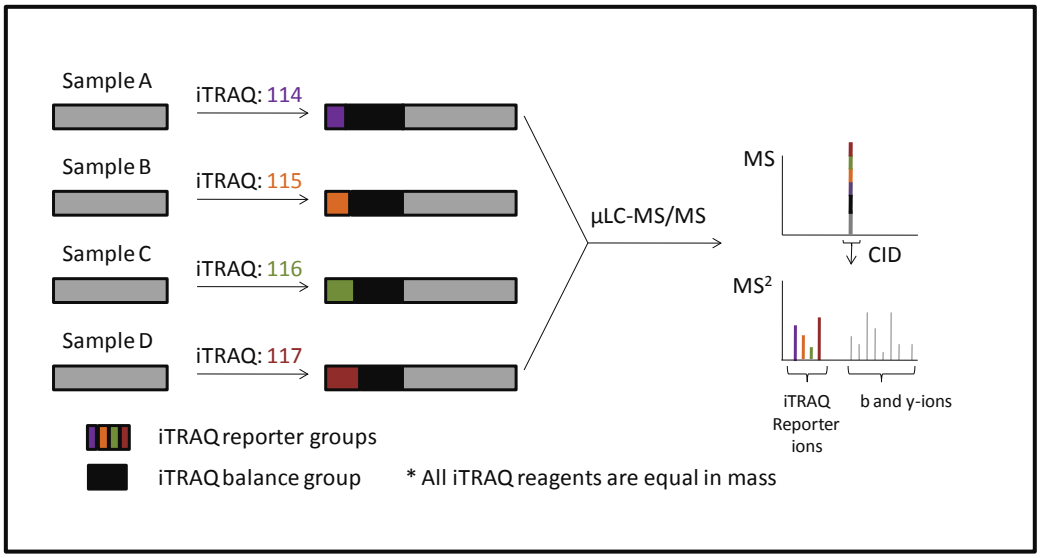
Sample A
iTRAQ: 114
Sample B
iTRAQ: 115
Sample C
iTRAQ: 116
Sample D
iTRAQ: 117
µLC-MS/MS
MS
CID
MS^2
iTRAQ Reporter ions
b and y-ions
iTRAQ reporter groups
iTRAQ balance group
* All iTRAQ reagents are equal in mass

Alternatively, the amine reactive stable isotope reagent iTRAQ (isobaric Tag for Relative and Absolute Quantitation) labels the amino terminus as well as the side-chain amine of lysine residues within peptides (Ross, Huang et al. 2004). In this approach, as many as 8 peptide samples are independently labeled with isotopically unique iTRAQ reagents and combined prior to analysis by μLC-MS/MS. Since all iTRAQ reagents are designed to be isobaric and thus identical in mass, peptides common across all samples appear as a single peak in the MS spectrum. However, cleavage of the iTRAQ reagents during MS/MS fragmentation produces a series of reporter ions (114 -119, and 121 Da), with each reagent contributing a unique ion. Thus, comparison of the reporter ion signals in MS/MS spectra provides relative quantitation of peptides between various samples. The ability to conduct multiplexed comparative proteomic analysis is largely unique to iTRAQ reagents, and is the primary reason for their popularity. However, the low mass of the reporter ions initially limited the use of iTRAQ reagents to TOF/TOF and triple-quadrapole mass spectrometers (Ross, Huang et al. 2004; Zhang, Wolf-Yadlin et al. 2005; Wolf-Yadlin, Hautaniemi et al. 2007). Only recently, with the advent of PQD, have linear ion trap mass spectrometers been shown to be amenable to analysis of iTRAQ labeled peptides (Griffin, Xie et al. 2007).

Appendix II

Copyright permission for material in

Chapters 1 and 2, and Appendix I

From:	Rights DE <RIGHTS-and-LICENCES@wiley-vch.de>
To:	roexx016@umn.edu <roexx016@umn.edu>
Date:	Thu, 29 Oct 2009 07:35:23 +0000
Subject:	AW: AW: AW: AW: Copyright permission for PhD thesis

Dear Mikel,

Thank you for your email.

For print use and use in the password-protected service:

- We hereby grant permission for the requested use expected that due credit is given to the original source.
- For material published before 2007 additionally: Please note that the (co-)author's permission is also required.

If material appears within our work with credit to another source, authorisation from that source must be obtained.

Credit must include the following components:

- Books: Author(s)/ Editor(s) Name(s): Title of the Book. Page(s). Publication
year. Copyright Wiley-VCH Verlag GmbH & Co. KGaA. Reproduced with permission.
- Journals: Author(s) Name(s): Title of the Article. Name of the Journal.
Publication year. Volume. Page(s). Copyright Wiley-VCH Verlag GmbH & Co. KGaA.
Reproduced with permission.

With kind regards

Bettina
****
Bettina Loycke
Senior Rights Manager
Wiley-VCH Verlag GmbH & Co. KGaA
Boschstr. 12
69469 Weinheim
Germany

AMERICAN CHEMICAL SOCIETY LICENSE
TERMS AND CONDITIONS

Oct 09, 2009

This is a License Agreement between Mikel R Roe ("You") and American Chemical Society ("American Chemical Society") provided by Copyright Clearance Center ("CCC"). The license consists of your order details, the terms and conditions provided by American Chemical Society, and the payment terms and conditions.

All payments must be made in full to CCC. For payment instructions, please see information listed at the bottom of this form.

License Number	2252561103212
License Date	Aug 19, 2009
Licensed content publisher	American Chemical Society
Licensed content publication	Analytical Chemistry
Licensed content title	Proteomic Mapping of 4-Hydroxynonenal Protein Modification Sites by Solid-Phase Hydrazide Chemistry and Mass Spectrometry
Licensed content author	Mikel R. Roe et al.
Licensed content date	May 1, 2007
Volume number	79
Issue number	10
Type of Use	Thesis/Dissertation
Requestor type	Not specified
Format	Print
Portion	Full article
Author of this ACS article	Yes
Order reference number	
Title of the thesis / dissertation	Improving the detection of carbonylated peptides by mass spectrometry via solid-phase hydrazide enrichment and selective 18O-labeling
Expected completion date	Sep 2009
Estimated size(pages)	203
Billing Type	Invoice
Billing Address Customer reference info	11102 Aberdeen St. NE Unit B Blaine, MN 55449 United States

Total .00 USD
Terms and Conditions

Submission to a Dissertation Distributor: If you plan to submit your thesis to UMI or to another dissertation distributor, you should not include the unpublished ACS paper in your thesis if the thesis will be disseminated electronically, until ACS has published your paper. After publication of the paper by ACS, you may release the entire thesis (**not the individual ACS article by itself**) for electronic dissemination through the distributor; ACS's copyright credit line should be printed on the first page of the ACS paper.